Optimizing deep brain stimulation using electrophysiological markers and electrical field steering

Dissertation

zur Erlangung des Grades eines
Doktors der Naturwissenschaften

der Mathematisch-Naturwissenschaftlichen Fakultät
und
der Medizinischen Fakultät
der Eberhard-Karls-Universität Tübingen

vorgelegt von

Maximilian Scherer
aus Freiburg am Breisgau, Deutschland

März 2021

Tag der mündlichen Prüfung 22.09.2021

Dekan der Medizinischen Fakultät: Prof Dr. Thilo Stehle

1. Berichtserstatter: Prof Dr. Alireza Gharabaghi
2. Berichtserstatter: Prof. Dr. Christoph Braun

Prüfungskommission: Prof Dr. Alireza Gharabaghi
Prof. Dr. Christoph Braun
Prof. Dr. Anna Levina
Prof. Dr. Andreas Bartels

Erklärung / Declaration:

Ich erkläre, dass ich die zur Promotion eingereichte Arbeit mit dem Titel:

"Optimizing deep brain stimulation using electrophysiological markers and electrical field steering"

selbständig verfasst, nur die angegebenen Quellen und Hilfsmittel benutzt und wörtlich oder inhaltlich übernommene Stellen als solche gekennzeichnet habe. Ich versichere an Eides statt, dass diese Angaben wahr sind und dass ich nichts verschwiegen habe. Mir ist bekannt, dass die falsche Abgabe einer Versicherung an Eides statt mit Freiheitsstrafe bis zu drei Jahren oder mit Geldstrafe bestraft wird.

I hereby declare that I have produced the work entitled "Optimizing deep brain stimulation using electrophysiological markers and electrical field steering", submitted for the award of a doctorate, on my own (without external help), have used only the sources and aids indicated and have marked passages included from other works, whether verbatim or in content, as such. I swear upon oath that these statements are true and that I have not concealed anything. I am aware that making a false declaration under oath is punishable by a term of imprisonment of up to three years or by a fine

Tübingen, den ....
Datum / Date Unterschrift / Signature

Contents

Table of Abbreviations and Definitions

Abbreviations

ANT	Anterior thalamus
AP	Action potential
CA2+	Calcium Ions
CCC	Cortico-cortical coupling
CMC	Cortico-muscular coupling
DBS	Deep brain stimulation
EEG	Electroencephalogram
EMG	Electromyogram
GPi	Globus pallidus pars interna
IPG	implantable pulse generator
PD	Parkinson's disease
STN	Subthalamic nucleus
VTA	Volume of tissue activated

Definitions

Theta band	4-7 Hz
Alpha band	8 - 12 Hz
Beta band	13 - 32 Hz
Low gamma band	33 - 48 Hz

Abstract

Deep brain stimulation (DBS) is an effective treatment for a wide variety of neurological disorders. The efficacy of the treatment strongly depends on the exact location of the DBS-lead within the brain and the programming of the stimulation. In this work, methods and markers are presented which may be applied to improve both, the positioning and the programming of DBS-leads.

Special consideration was given to ensure that any identified potential marker was not only a general effect of the stimulation itself, but actually a marker of clinical benefit. One method for achieving this goal was to investigate whether a qualitative change in clinical improvement was reflected in a qualitative change regarding an electrophysiological marker candidate. A second method to identify markers specific for clinical improvement was to separate the available data into patients responding to the treatment and patients not responding to the treatment. Therefore, potential marker candidates had to be present in the responder data, but absent in the non-responder data. Generally, marker candidates were discarded when they were strongly confounded by other effects like movement.

DBS programming was not only optimized by providing more reliably sources of information during the programming process, but also by evaluating the effect of steering the electrical field. To this end, the clinical utility of segment DBS-lead contacts was compared to ring DBS-lead contacts.

Refining of the implantation procedure itself was explored when a novel method to implant the DBS-leads into patients with Parkinson's disease was investigated. This method allowed for the inclusion of electrophysiological information to the implantation process without the need to a priori record electrophysiological information with either a micro- or macro-electrode.

1 Introduction

Deep brain stimulation (DBS) is a potential treatment option for a number of different neurological disorders, among these are Parkinson's disease (PD) and epilepsy (Groiss et al. 2009; Zangiabadi et al. 2019). DBS is commonly suggested as a second line therapy, especially after a neurological condition becomes medically refractory (Nuttin et al. 2014) as medical treatment (usually the first line therapy) does not require the patient to undergo (multiple) surgeries. Although the mechanisms by which DBS works are not fully explored, it is assumed that these are different from pharmaceutical treatment. This assumption is in line with the observation of effective DBS in patients who do not respond to medical treatment (anymore) (Nuttin et al. 2014).

In order to treat a patient with DBS, DBS-leads need to be implanted into a disease specific target structure. An implantable pulse generator (IPG) is connected to the DBS leads which is usually implanted at the left or right side of the chest. This pulse generator sends electrical pulses to the electrode. The current may return either to the casing of the pulse generator (monopolar stimulation) or to another contact of the DBS-lead (bipolar stimulation). While the current is injected into the tissue, an electric field is generated (Hodgkin and Huxley 1952). This artificial field can affect neuronal populations, although a minimal electrical pulse strength is required to trigger any effect on neuronal or other cells (Holsheimer et al. 2000). Commonly, the electrical field is only of sufficient strength in close proximity to active contacts of the implanted DBS-lead, therefore only neurons close to said active contact of the DBS-lead get stimulated. As the electrical pulses from the pulse generator create an electrical field near the active contact of the DBS-lead, voltage gated ion channels in the proximity to the DBS-lead contact are opened. Opening these channels causes an influx of CA2+ which triggers two action potentials (AP) (McIntyre and R. W. Anderson 2016). One action potential travels downwards the axon (into the orthodromic direction) and another travels upwards (into the antidromic direction) (McIntyre and R. W. Anderson 2016; Herrington, Cheng, and Eskandar 2015; Yi and Grill 2018). Applying these high frequency pulses is hypothesized to cause effectively an information lesion (Grill, Snyder, and Miocinovic 2004). Yet, it is not fully understood how the concept of stimulation triggered APs causes said information lesion. There are multiple theories how these two ideas may be connected. One theory is that the DBS induced antidromically trav-

eling APs cancel out all natural orthodromically traveling pulses thereby blocking the communication towards the targeted structure (García et al. 2013). Another theory is that DBS indeed causes artificial antidromically traveling APs to cancel out some, but not all, natural APs, effectively performing the function of a high pass filter (T. R. Anderson et al. 2006; McIntyre and R. W. Anderson 2016). There is also the theory that DBS causes synaptic depression. While axons themselves are capable of following stimulation frequencies of 100Hz (Andres M. Lozano et al. 2019), axon terminals may exhaust their neurotransmitter pool leading to synaptic depression during high frequency DBS (Rosenbaum et al. 2014; Llinás, Leznik, and Urbano 2002). In line with this theory, it has been shown that high frequency DBS applied to the STN appears to mostly silences the targeted structure (Milosevic, Kalia, et al. 2018). Furthermore, DBS has been described to have not only effects on local neuronal populations, but also on structurally connected neuronal populations (McIntyre and Hahn 2010).

Historically, the idea to apply electrical stimulation in order to induce neuronal responses has been investigated as of the early 19th century (Rolando 1809). In these initial experiments, electrical stimulation was applied to evoke muscle responses (Sironi 2011). In 1874 the first report of applying electrical stimulation to an awake human was published (Bartholow 1874). After electrical stimulation was the first time clinically evaluated in 1938 by Ugo Cerletti (Sironi 2011), in the 1950s the application of electrical stimulation was investigated for the purpose of pain control (Sironi 2011). In these early works, electrical stimulation was mostly applied to patients to identify structures as targets for lesions (Sironi 2011). From observations made during these procedures, DBS developed as a treatment option. Yet, chronic depth stimulation as a treatment was first proposed in 1963 (Bekhtereva et al. 1963).

In the years since the conception of DBS as a chronic treatment for neurological disorders, DBS-leads have become much more sophisticated. Commonly, modern DBS-leads offer four individual contacts which can be used to apply stimulation. These contacts are usually used to steer the stimulation along the implantation trajectory. The latest generation of DBS-leads expands upon the concept of electrical field steering. Some of the ring formed contacts in these DBS-leads are segmented into three individual segments (Steigerwald, Matthies, and Volkmann 2019). This is illustrated in fig. 1. Applying electrical current only to some of the segments of a ring allows for stimulation

to be steered on a plane orthogonal to the implantation trajectory.

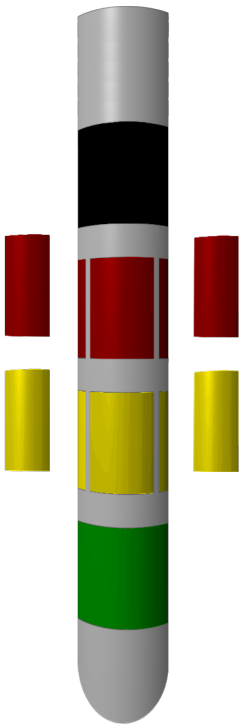

Figure 1: Schematic illustration of a modern DBS-lead's tip. There are contacts on four different height levels on the DBS lead, these are encoded by different colors. When implanted e.g. into the STN, the green contact corresponds to the most ventral contact, whereas the black contact corresponds to the most dorsal contact.

The contacts on the yellow and red levels are split into three equally sized segments. This split is specific to the latest generation of DBS-leads. Previously, only four ring contacts were integrated into each DBS-lead.

Individual contacts or their respective segments can be identified as either the source or the sink of the electrical pulses generated from the pulse generator. In case no sink is defined, the housing of the IPG acts as a sink.

Yet, not only the source and sink of the electrical current flow around the DBS-lead can be programmed, but the properties of the DBS pulses themselves. Commonly, the stimulation frequency, current amplitude or voltage, and pulse width can be programmed. When merely programming the stimulation contacts and the amplitude (assuming standard parameters for the remaining configurable elements) several test runs are necessary to find an ideal stimulation configuration. Yet, the time necessary to evaluate the effect of DBS on the symptoms of neurological disorders is subject to a strong variation of the symptom in question and the patient to be treated. DBS related effects on tremor can usually be seen within a couple of seconds (McIntyre and R. W. Anderson 2016) whereas multiple weeks may be necessary to evaluate the effect of DBS on epilepsy related seizures through the use of a seizure diary (R. S. Fisher et al. 2012). Therefore, it may be concluded that markers based on clinical outcome are often not ideal to investigate the effectiveness of DBS. Furthermore, while clinical markers have to be mostly subjectively evaluated, electrophysiological markers may be evaluated objectively.

In order to maximize the benefit of DBS as a treatment, correct stimulation configuration is vital (Volkmann, Moro, and Pahwa 2006). Yet, as previously discussed, clinical markers are not ideal to assess neither the implantation location, nor the stimulation

configuration. An example of such a marker can be found in patients with Parkinson's disease, namely an exaggerated beta band activity in the basal ganglia. This beta peak is considered to be pathological (P. Brown 2006; Hammond, Bergman, and Peter Brown 2007; Pollok et al. 2012). The suppression of this electrophysiological marker has been reported to correlate with clinical benefit related to DBS (Little and Peter Brown 2014; Weinberger et al. 2006; Ray et al. 2008; Kühn, Kupsch, et al. 2006). This electrophysiological marker is commonly used to guide the implantation procedure, supplementing imaging information (Zaidel et al. 2010). The position of said pathological beta activity is commonly explored via micro-electrodes. No comparative marker has been discovered in patients with epilepsy so far, thereby forcing the implantation procedure to be solely imaging based (Cukiert and Lehtimäki 2017). Consequently, in case electrophysiological information is not or cannot be used to supplement imaging information, any error in said imaging information (i.e. synchronization inaccuracies) cannot be detected.

Yet, clinical and electrophysiological markers are not only needed to determine the ideal positioning of the DBS-lead during DBS-lead implantation, but also during DBS programming. Exemplary, the programming of the DBS-lead for maximal clinical effectiveness in patients with epilepsy may take up to several months. As no electrophysiological marker is available to determine the effectiveness of the stimulation, the effectiveness of a certain DBS program can only be evaluated based on clinical markers. Therefore, epilepsy patients are programmed with a specific setting and told to keep a seizure diary (R. S. Fisher et al. 2012). In case the seizure count remains too high (a reduction of at least 50% is expected (Orosz et al. 2014; Järvenpää et al. 2018; Karoly et al. 2019)) the DBS programming is adjusted. A single evaluation cycle may take up to several weeks as seizure count varies between patients and across time (mostly due to external factors like stress (Temkin and Davis 1984)).

1.1 Investigated conditions

In the scope of this work, the effects of DBS on patients with epilepsy and Parkinson's disease were investigated. The following paragraph explains the history and aims of the application of DBS in said conditions.

Epilepsy

Epilepsy is a neurological condition which affects approximately 1% of the global population, across all ages (Kwan and Brodie 2000). In patients with temporal lobe epilepsy, seizures originate in the temporal lobe. This type of epilepsy is the most common type of epilepsy in adults (Téllez-Zenteno and Hernández-Ronquillo 2012). The exact mechanisms of ictogenic activity and their link to prolonged seizures are not fully explored (Jacob et al. 2019), yet epilepsy is considered a disorder of hypersynchronization (Penfield and Jasper 1954). First line of treatment to counter this neurological disorder are antiepileptic drugs. These work primarily through the enhancement of inhibitory neurotransmitters and the attenuation of excitatory neurotransmitters (Löscher et al. 2013; Vajda and Eadie 2014). In case the pharmacological treatment loses efficacy over time, or is not effective in the first place (applies to 30% of all patients), DBS may be considered as an alternative treatment (R. Fisher et al. 2010; Laxpati, Kasoff, and Gross 2014; Lim et al. 2007; Salanova et al. 2015; Sitnikov, Grigoryan, and Mishnyakova 2018). In order to treat an epilepsy patient with DBS, a DBS-lead needs to be implanted. A common target region for implantation is the anterior part of the thalamus (ANT). High frequency DBS as a treatment for epilepsy has been most prominently investigated in the SANTE study (R. Fisher et al. 2010). This study revealed a median seizure reduction rate of 40% several months after the implantation (double blinded phase), yet there is a wide variation in the clinical efficacy of ANT-DBS (Bouwens van der Vlis et al. 2019). By which means ANT-DBS effectively causes a reduction in ictogenic activity is still not fully explored (R. Fisher et al. 2010). Yet, it has been observed that effective ANT-DBS is connected to a decrease in activity within the hippocampus (Yu et al. 2018), in a single case this has been localized within the delta and theta bands (Zumsteg, Andres M. Lozano, and Wennberg 2006).

Parkinson's disease

Parkinson's disease (PD) affects approximately 1% of the global population over the age of 60 (Lau and Breteler 2006), yet incidence increases exponentially between 55 and 79 years of age (Driver et al. 2009). A hallmark of Parkinson's disease is a degeneration of dopaminergic neurons in the nigrostriatal pathway (Riederer and Wuketich 1976). Parkinson's disease has effects on both motor and non-motor functions in affected pa-

tients (Sveinbjornsdottir 2016). Commonly observed motor symptoms related to this pathological change are tremor, rigidity, and postural instability (Jankovic 2008). As with epilepsy, the initial treatment for patients with Parkinson's disease is pharmaceutical, a combination of levodopa and supplementary drugs (Katzenschlager and Lees 2002; Salat and Tolosa 2013). Over time, clinical efficacy of this treatment diminishes which in turn necessitates higher doses of medication. Yet, at certain levels the antiparkinsonian medication is known to cause side-effects like levodopa-induced dyskinesias (Thanvi and Lo 2004). After the condition is classified as refractory (epilepsy) or in case medication is insufficient to suppress symptoms (Parkinson's disease), DBS is usually suggested to the patient as an alternative treatment option (Benabid et al. 1994; Limousin et al. 1995). Common implantation targets in patients with Parkinson's disease are the subthalamic nucleus (STN) and the globus pallidus pars interna (GPi) (Dallapiazza et al. 2018). In the studies investigated in the scope of this work, only patients implanted into the STN were investigated.

1.2 Effectiveness of DBS in these conditions

Epilepsy

The effectiveness of DBS in patients with epilepsy varies strongly (Bouwens van der Vlis et al. 2019). This is likely due to the fact that epilepsy is not a neurological disorder with a singular well-defined area of origin, as in e.g., Parkinson's disease. Seizure onset zones need to be identified via diagnostic tools (Elahian et al. 2017). The ANT has been identified as an effective DBS implantation target for those patients with temporal lobe epilepsy (R. Fisher et al. 2010). Furthermore, the role of ANT-DBS in the treatment of epilepsy is not fully explored (R. Fisher et al. 2010). Currently the exact cause of ictogenic activity (Blauwblomme, Jiruska, and Huberfeld 2014) is also not fully explored. Yet, seizure onsets do not necessarily have to occur at only a single area within the brain. Multiple seizure onset zones have been reported in some patients with epilepsy. Another reason for the strong variation of ANT-DBS effectiveness may be the metric applied to evaluated the effectiveness of ANT-DBS. As previously explained, the effectiveness is often evaluated via seizure diaries (R. S. Fisher et al. 2012). This approach has a number of drawbacks: 1) It is fully dependent on the quality of the patients cooperation. This approach necessitates that the patient

himself/herself can classify his/her own seizures reliably into different classes (e.g., strong seizures, mild seizures), furthermore does this approach necessitate that the patient reports all seizures that occurred to them (2). 3) This approach is likely strongly affected by confounding factors such as the personal stress level (Temkin and Davis 1984).

Due to these factors, there is a large variation regarding the effectiveness of ANT-DBS for patients with epilepsy. The mean seizure reduction rates of post-SANTE studies were between 11.5% and 70.51% (Bouwens van der Vlis et al. 2019).

Parkinson's disease

DBS as a treatment for patients with Parkinson's disease is comparatively more advanced. The implantation procedure in patients with Parkinson's disease is commonly guided by imaging information which is supplemented by electrophysiological information (Brunenberg et al. 2011; Hutchison et al. 1998). The precise localization within the targeted structure depends on the primary symptoms (Hariz 2002; Andres M Lozano et al. 2010; Nickl et al. 2019). Yet, imprecise lead positioning is a major cause for ineffective DBS in patients with Parkinson's disease (Rolston et al. 2016). The primary motor symptoms associated with Parkinson's disease, tremor and rigidity, can be evaluated much faster and more reliably compared to the seizure count in patients with epilepsy. While the effects of DBS on tremor can be observed within seconds (McIntyre and R. W. Anderson 2016), the effects of DBS on rigidity are usually observed within a minute or two (Levin et al. 2009). Motor symptoms associated with Parkinson's disease are mitigated by approximately 40-70% in the medication-off and stimulation-on condition a year after the implantation (Shahidi et al. 2017; Tsai et al. 2013; Zibetti et al. 2011).

1.3 Hypothesis and aims

The goal of this work was to optimize the application of DBS in patients with epilepsy and Parkinson's disease. This goal was to be achieved by providing additional information for DBS positioning and programming.

Optimizing ANT-DBS in patients with epilepsy

There are no known electrophysiological markers which may be used to guide either the implantation into the ANT, or to guide the programming of implanted DBS-leads (Son et al. 2016; Sweeney-Reed et al. 2016). The presented work focused on the investigation of electrophysiological markers for the post-operative programming of DBS-leads.

It has previously been shown that ANT-DBS is associated with a decrease in electrical activity over a broad frequency spectrum within the hippocampal formation (Yu et al. 2018). In line with this study, a case report showed reduction of hippocampal activity in the theta and delta range (Zumsteg, Andres M. Lozano, and Wennberg 2006). Therefore, we hypothesized that clinical effects of ANT-DBS may be related to these findings. Yet, these findings could have also been explained by the mere effects of ANT-DBS which do not necessarily have to be linked to the clinical efficacy of the treatment. To this end, we investigated patients with temporal lobe epilepsy and patients whose epilepsy did not (exclusively) originate in the temporal lobe.

In this investigation, all patients had been implanted into the ANT. The patients with temporal lobe epilepsy were classified as responders based on their respective seizure reduction rates. The patients with other forms of epilepsy were classified as non-responders, due to substantially lower/no seizure reduction rates. This was in line with the results from SANTE (R. Fisher et al. 2010) and other studies (Salanova et al. 2015; Osorio et al. 2007). We assumed that effects linked to the clinical efficacy of ANT-DBS should be strongest in the patients with temporal lobe epilepsy and mostly absent in the patients with other forms of epilepsy; as only patients with temporal lobe epilepsy benefited from the treatment. This contrast allowed us to distinguish between the effects of ANT-DBS related to clinical efficacy and the effects of ANT-DBS not related to clinical efficacy.

Identification of such an electrophysiological marker would be most useful for the programming of DBS-leads in patients with epilepsy. This identification would (potentially), substantially decrease the evaluation periods for individual settings (from several months/years down to minutes/hours) and thereby, significantly increase the benefit of ANT-DBS for patients with temporal lobe epilepsy.

Optimizing STN-DBS in patients with Parkinson's disease

In this work, we aimed at improving the identification of the target structure during implantation, investigate potential benefits & drawback of steered stimulation, and explore non-invasive markers for clinically effective STN-DBS in patients with Parkinson's disease.

The dopaminergic degeneration of the nigrostriatal pathway in patients with Parkinson's disease commonly coincides with a beta band activity increase within the STN (P. Brown 2006). This activity within the range of 20-40 Hz can be used to identify the target structure (STN) along the implantation trajectory (Hutchison et al. 1998). By default, micro-electrodes are used to acquire this supplementary information (Amirnovin et al. 2006; Bour et al. 2010; Schlaier et al. 2013). Yet, we hypothesized that this approach should also be applicable when using the permanently implantable DBS-lead. To this end, the implantation trajectory was mapped using both, micro-electrodes and DBS-leads. We hypothesized that the electrophysiologically determined position of the STN should be the same, independent of the approach applied to identify it. Furthermore, the reliability of both approaches was also investigated and compared.

In order to optimize the programming of DBS in patients with Parkinson's disease, we employed two approaches. In the first approach, we investigated ring DBS-lead contact and segment DBS-lead contact stimulation. The latter allowed for steering of the stimulation on a plane orthogonal to the implantation trajectory. We hypothesized that steered stimulation may potentially result in a better outcome for the patient. Although larger therapeutic windows using segment stimulation (compared to ring stimulation) had been reported previously, these results can be explained by DBS-lead positioning. If indeed no significant clinical benefit between segment stimulation and ring stimulation was to be found, this would affect the degrees of freedom for DBS programming. This finding would decrease the number of potential stimulation contacts down from eight to four. By reducing the number of programming candidates, stimulation programming is indirectly optimized as it will not only be faster, but also less prone to accidental suboptimal programming.

In the second approach, we sought a reliable electrophysiological marker which could be used to supplement information from clinical markers. To this end, the behavioral response to STN-DBS was compared to the presence/absence of electroencephalo-

graphic/electromyographic (EEG/EMG) markers. Furthermore, clinically effective and ineffective STN-DBS programs were compared to delineate STN-DBS effects which contribute towards clinical benefit and those who do not. We expected the beta band to play a major role in this due to the prominence of sub-cortical, pathological beta band activity (P. Brown 2006) in patients with Parkinson's disease.

2 Included studies

This section describes the studies included in this work.

2.1 Desynchronization of temporal lobe theta band activity during effective anterior thalamus deep brain stimulation in epilepsy

This study delineated clinically beneficial and clinically indifferent effects of ANT-DBS. Therefore, we investigated how the effects of ANT-DBS differed between patients with epilepsy who did benefit from the treatment and those who did no benefit from the treatment. Based on this comparison, an electrophysiological marker candidate was derived which could potentially guide the DBS-lead implantation and the subsequent programming in the future. As the acquisition of subcortical data was not feasible in this study, only cortical data was acquired. Treatment benefit was determined based on seizure diaries. The implanted DBS-leads were programmed according to the results of the SANTE study (R. Fisher et al. 2010). Subsequently, patients kept their seizure diaries for several months. The post-operative evaluation period lasted from the 2nd month after implantation until the 5th month after implantation. The month directly after implantation was not eligible for the inclusion into the study due to the possible presence of micro-lesion effects (Granziera et al. 2008). Clinical benefit was quantified based on the average seizure count during this evaluation period divided by the pre-implantation seizure count.

The analysis revealed that patients, who benefited from the treatment, showed a pronounced reduction of theta band activity measured at the temporal lobe EEG channels. Modulations of theta band activity can be observed in the hippocampal formation and the cortex during a variety of tasks, among them behavior during wakefulness (Arnolds et al. 1980), spatial navigation (Kahana et al. 1999), and working memory (Raghavachari et al. 2001) (among others (Cantero et al. 2003)). When investigating individual subjects, a lasting ANT-DBS induced reduction of theta band activity in the temporal lobe channels was only observed in patients who responded positively to the treatment. Comparing the seizure onset zones with the response rates revealed that patients whose seizure onset zone was within the temporal lobe benefited

from the treatment whereas patients with other seizure onset zones did not benefit. This finding was in line with the results reported in the SANTE study which found ANT-DBS to be most effective in patients with temporal lobe epilepsy (R. Fisher et al. 2010). In summary, we observed that patients responding to ANT-DBS were mostly temporal lobe epilepsy patients and that the reduction in seizure count correlated with the reduction in theta band power measured from EEG above the temporal lobe.

The classification of epilepsy as a disorder of hypersynchronization during epileptiform activity is supported by the fact that patients with epilepsy appear to have hypersynchronized cortical theta band activity compared to healthy controls (Adebimpe et al. 2015; Miyauchi et al. 1991; Quraan et al. 2013). Furthermore, ANT-DBS has recently been shown to cause a reduction in broad band (Yu et al. 2018), more precise theta band activity (Zumsteg, Andres M. Lozano, and Wennberg 2006). The presented study adds to these findings that the observed reduction in theta band activity does appear to be not merely a general effect of ANT-DBS, but critical for its clinical efficacy.

Previously, there have been no electrophysiological markers to determine the correctness of lead-placement in ANT-DBS patients, or to program the stimulation effectively (Son et al. 2016; Sweeney-Reed et al. 2016). We suggest that further investigation of the discovered link between clinical efficacy of ANT-DBS and theta band power reduction measured at the temporal lobe EEG channels, may yield such a marker. Furthermore, the proposed marker candidate may be measured non-invasively, thereby offering greatly increased accessibility. This is especially important for DBS-lead programming as at the time of programming, subcortical data is commonly inaccessible.

2.2 Online Mapping With the Deep Brain Stimulation Lead: A Novel Targeting Tool in Parkinson's Disease

Goal of this study was to investigate whether the DBS-lead implantation trajectory in patients with Parkinson's disease could be mapped using the permanently implantable DBS-lead. To this end, we investigated how well electrophysiological markers recorded via micro-electrodes align with electrophysiological markers recorded from macro-electrodes/DBS-leads. This study included data from 39 patients with Parkinson's disease. Micro electrode based identification of the ideal DBS-lead placement site was investi-

gated via manual online evaluation of neuronal spiking activity. The target structure was identified through analysis of single neuron firing patterns (Milosevic, Kalia, et al. 2018; Hutchison et al. 1998). Macro-electrode-based identification of the ideal DBS-lead placement site was investigated via the absence/presence of pathological beta band peaks commonly observed in the STN of patients with Parkinson's disease (P. Brown 2006; Kühn, Kempf, et al. 2008). The resulting positions for DBS-lead placement from both approaches were compared and found to converge.

Theoretically DBS-leads may be implanted solely based on imaging information (Brunenberg et al. 2011) which is acquired prior to the DBS-lead implantation. Although this information is supplemented by intra-operative imaging information, the information provided is limited. Supplementary electrophysiological guiding of the implantation may be applied to increase the precision of DBS-lead placement (Hariz 2002; Lee, Crammond, and Richardson 2018). When applying electrophysiological measurements, the information generated via this approach is fused with the imaging information. Although micro-electrodes are considered the gold standard (Burchiel et al. 2013; Shahlaie, Larson, and Starr 2011; Sokal et al. 2015) for supplementary electrophysiological information, this approach is of limited usability due to the dependence on a substantial amount of expertise. The approach presented here may add supplementary electrophysiological information without the need for a specialist trained in the manual online analysis of single neuron spiking activity. Therefore, the presented approach may easily be applied to increase the precision of DBS-lead placement compared to purely imaging based implantation procedures (Bour et al. 2010; C. S. Lozano et al. 2018; Montgomery Jr 2012).

2.3 Comparing the therapeutic window of omnidirectional and directional subthalamic deep brain stimulation in Parkinsons disease

Goal of this study was to determine whether steering of STN-DBS in patients Parkinson's disease orthogonal to the implantation trajectory increases the clinical benefit. Data from 17 patients with Parkinson's disease were included in this study. The data were acquired over the course of two days. OFF stimulation and multiple stimulation

intensities were evaluated in each patient, ranging from 0.5 mA to 2.5 mA (incremental steps of 0.2 mA). For each stimulation condition (including OFF), the patients were at rest for 30 s followed by 60 s of passive arm movement.

The analysis of the collected data revealed that with increasing stimulation intensity the clinical benefit increased too until it plateaued at specific stimulation intensities (varying values for different contacts & patients). Rigidity could be suppressed in 90% of the patients already at 1.1 mA.

Segment DBS-lead contacts were introduced with the latest generation of DBS-leads. The effectivity of said segment DBS-lead contacts is subject of ongoing research efforts (Steigerwald, Matthies, and Volkmann 2019; Amon and Alesch 2017; Tinkhauser et al. 2018). In this study, the therapeutic threshold of DBS was comparable, irregardless of whether DBS was applied from the best segment DBS-lead contact or the reference ring DBS-lead contact. This is in line with the reports from (Contarino et al. 2014; Dembek et al. 2017), but opposes results presented by (Pollo et al. 2014; Bruno et al. 2020). The side-effect threshold from the best segment DBS-lead contact was also not larger than the side-effect threshold of the reference ring DBS-lead contact. This is in line with the observations from (Bruno et al. 2020), yet contradicts the findings from (Dembek et al. 2017). Therefore, in this investigation the size of the therapeutic window was largely unchanged when comparing the best segment DBS-lead contact and the reference ring DBS-lead contact. (Pollo et al. 2014; Dembek et al. 2017; Bruno et al. 2020) reported a significantly larger therapeutic window size due to either a lower therapeutic threshold or a larger side-effect threshold. The report from (Contarino et al. 2014) showed that generalization of these findings is not a simple task, this is emphasized by the finding of Contarino and colleagues ((Contarino et al. 2014)) who report a larger therapeutic window size in only 3 out of 8 patients. Due to the strong dependence of these findings on the quality of DBS-lead positioning (which is varying), some variability in regards to these findings is to be expected. Following this line of thought, steering the stimulation is unlikely to improve the therapeutic window size when the DBS-lead is already well placed within the STN.

On another note, we observed that DBS applied from smaller electrode contact areas (as with segment DBS-lead contacts for steering) needs to overcome higher impedances during electrical stimulation. The observed increase in impedance is necessitated by

the inverse relationship between impedance and capacitance (which is in turn affected by surface area) (Irwin and Nelms 2020). An increase in impedance causes an increase in power consumption (in case the electrical field strength is supposed to not diminish (Butson, Maks, and McIntyre 2006)) which in turn drains the battery faster. This is a major point of concern considering that battery replacement surgeries are not without danger to the patient. Infection of the implantable pulse generator (IPG) site is a major adverse effect described during DBS-surgery (Themistocleous et al. 2011) which increases in likelihood with repeated replacements (Pepper et al. 2013).

2.4 State-dependent decoupling of interhemispheric motor networks with effective deep brain stimulation in Parkinson's disease

The goal of this study was to investigate the electrophysiological differences between clinically effective and ineffective DBS in patients with Parkinson's disease. The data analyzed in this study was identical to the data analyzed in the previous study (see section 2.3). Contrary to the previous study, data from different contacts were pooled, regardless of contact type (ring DBS-lead contact/segment DBS-lead contact) as majorly the difference between effective and ineffective stimulation was investigated.

Analysis of this study showed that clinical benefit did indeed increase with increasing stimulation intensity. This was in line with the previous study (see section 2.3). EEG power decreased across all frequency ranges. Motor-cortical and non-motor-cortical activity decreased in an almost sigmoidal shape. The analysis of the recorded EMG activity showed that EMG activity decreased in an rather linear fashion, but only during movement. The movement related beta band modulation increased for effective stimulation compared to ineffective/suboptimal stimulation. Furthermore, we observed that effective stimulation exclusively was also linked to a decrease in same frequency coupling measured between the left and the right motor cortex. This result persisted independent of the presence or absence of passive movement. Additionally, effective stimulation exclusively was related to an increase in ipsilateral cortico-muscular coherence, which was observed exclusively during movement. Comparing ring DBS-lead contacts and segment DBS-lead contacts showed that the DBS induced cortical

desynchronization was much more pronounced when stimulation was applied via a ring DBS-lead contact compared to a segment DBS-lead contact.

These results are in line with previous findings on the modulation of cortical activity (Heinrichs-Graham et al. 2014), coupling of cortical activity (Silberstein et al. 2005; Weiss et al. 2015) and cortical muscular coupling (Salenius et al. 2002; Sridharan et al. 2019) either induced by STN-DBS or comparing patients with Parkinson's disease to healthy controls. In this study, we investigated which of these effects merely correlated with the presence of STN-DBS or were actually markers of clinically effective STN-DBS. In line with previous studies, we observed an decreased in motor cortical CCC (Silberstein et al. 2005; Weiss et al. 2015) and increase in movement related beta band modulation range (Heinrichs-Graham et al. 2014). Furthermore, we also observed an increase in ipsilateral CMC while beta band CMC has been reportedly decreased in patients with Parkinson's disease compared to healthy controls (Salenius et al. 2002). Both, improvements in CCC and CMC were observed to significantly change with increasing stimulation intensity while DBS was not fully effective. After stimulation was fully effective, no further significant change observed for both CCC and CMC. This finding implies a build up pattern for the DBS induced motor cortical CCC reduction and the ipsilateral CMC increase. Furthermore, this build up pattern is apparently supplemented by an stimulation intensity dependent threshold after which no further significant change can be observed (and no further clinical improvement). Both metrics normalize towards observations commonly made in healthy subjects (Salenius et al. 2002; Sridharan et al. 2019) during this build up phase.

Pathologically increased levels of beta activity within the basal-ganglia are the hallmark of patients with Parkinson's disease (Kühn, Trottenberg, et al. 2005), from an electrophysiological point of view. This information is commonly used to guide the implantation process (Kühn, Trottenberg, et al. 2005; Zaidel et al. 2010), either via microelectrodes (Hutchison et al. 1998) (usually considered the gold standard, yet difficult to execute), or via macroelectrodes (Milosevic, Scherer, et al. 2020). Subcortical beta activity has been a prime marker candidate for the investigation of adaptive DBS systems (Little and Peter Brown 2020), yet this marker is commonly strongly confounded by movement (Johnson et al. 2016). The same issue is present in case cortical beta activity is used to inform the adaptive DBS process. To this end, cortico-cortical

synchronization of the motor cortices might be an interesting marker candidate as this marker strongly reflects the effectiveness of STN-DBS and (maybe even more important in this regard) is not affected by passive movement (unlike beta power).

3 Discussion

3.1 Importance of optimal DBS-lead programming and the impact of biomarkers

The clinical efficacy of DBS as a treatment for neurological disorders strongly depends on the correct DBS-lead positioning and IPG programming (Okun et al. 2005). The latest generation of DSB-leads further increased the flexibility of stimulation by splitting the two middle ring DBS-lead contacts into three distinct segments. Therefore, in order to properly configure a DBS-lead to a patient, most commonly the amplitude and the source contact of the stimulation need to be determined. Although frequency and pulse width are also configurable, these parameters are modified less often. Even when probing DBS in intensity changes of 0.5 mA, 96 different parameter combinations are available per hemisphere. In case DBS intensity is probed in 0.2 mA steps, the number of possible parameter combinations for DBS configuration increases to 240 per hemisphere. Tens of thousands of parameter combinations are possible when all parameters are modified (Erwin B Montgomery 2020). This translates to very long programming times for patients with Parkinson's disease. While the effects of DBS on tremor can be evaluated within approximately 15 s (McIntyre and R. W. Anderson 2016), at least 60 s are required to estimate the effects of DBS on rigidity (Levin et al. 2009). This in turn translates to 2 h of evaluation in case of tremor and 8 h of evaluation in case of rigidity (for both hemispheres). These calculations assume that the treated symptom remains constant during the examination period. For patients with epilepsy, this translates to unrealistic programming times as the evaluation of a single configuration setting may take multiple weeks. Even when assuming that one month would be sufficient, proper configuration of the DBS-leads would take 20+ years (assuming seizure count is perfectly stable and only modified by DBS).

The goal of this work was to potentially minimize the number of potential stimulation configurations and to support the identification of clinically effective DBS programming. To this end, we compared the effect of directionally-steered vs. non-steered stimulation and searched for markers, which may inform about the effectiveness of DBS in both patients with Parkinson's disease and patients with epilepsy.

3.2 Utility of discovered biomarkers for effective ANT-DBS in patients with epilepsy

In the scope of the work presented in this thesis, we investigated markers for effective deep brain stimulation in patients with epilepsy. Although it had previously been shown that ANT-DBS is related to a number of electrophysiological effects (Silberstein et al. 2005; Weiss et al. 2015), it was unclear whether these effects were merely related to the presence of DBS or also to clinical benefit. ANT-DBS has previously been shown to cause a reduction of subcortical activity in the hippocampal formation (Yu et al. 2018), more specifically in the theta band (Zumsteg, Andres M. Lozano, and Wennberg 2006). We observed a similar effect on cortical theta band activity, recorded above the temporal area, most prominent in the theta band. In contrast to previous studies, we showed that this effect was specific to responders, as we contrasted responding and non-responding patients. Therefore, the cortically measurable reduction of theta band activity induced by ANT-DBS is a marker which may be used to assess the effectiveness of ANT-DBS without the need for a seizure diary. The use of an electrophysiological marker indicating the effectiveness of ANT-DBS would not only tremendously reduce the time required for DBS programming in patients with epilepsy. Such a marker may also be used to inform the implantation procedure itself via test-stimulation during surgery in order to optimize DBS-lead positioning. Furthermore, the information extracted from the proposed biomarker is likely much more stable and objective than information extracted from a patient seizure diary.

3.3 Utility of the investigated approach for intra-operative STN identification in patients with Parkinson's disease

DBS-lead implantation in Parkinson's disease may be assisted by supplementary electrophysiological information. Previously, this required trained personnel to online assess the properties of single neuron spiking activity. Without the availability of trained personnel, DBS-leads are often implanted based on imaging information only (Brunenberg et al. 2011). The latter approach has obvious drawbacks, e.g., this process does not fully account for a potential brain-shift (Halpern et al. 2008) which may occur after the skull has been opened. The presented approach of using the DBS-lead, not a micro-

electrode, for semi-automated mapping of the DBS lead implantation trajectory may be applied to acquire electrophysiological information without the need for specifically trained personnel. The accuracy of micro-electrode guided implantations and DBS-lead guided implantations were compared and found similar. Yet, the DBS-lead based approach necessitates the existence of pathologically high beta activity within the STN which has not been observed in all patients with Parkinson's disease (Tinkhauser et al. 2018; Milosevic, Scherer, et al. 2020; Kühn, Tsui, et al. 2009). The micro-electrode guided approach may have an edge in these cases as the micro-electrode approach does not only look for neuronal group activity, but also single unit spiking activity, the amplitude of neuronal background noise, and other markers (Weinberger et al. 2006; Hutchison et al. 1998; Abosch et al. 2002).

3.4 Utility of biomarkers for effective STN-DBS in patients with Parkinson's disease

Although DBS programming in patients with Parkinson's disease is much quicker compared to DBS programming in patients with epilepsy, the process needs to be improved. Especially when considering that DBS programming is not a one-time procedure as the parameters need to be adjusted to the progression of the neurological disorder (Swann et al. 2018). DBS-leads implanted into patients with Parkinson's disease are commonly programmed based solely on information provided by clinical markers, like visually confirmed absence of tremor (Wagle Shukla et al. 2017). This evaluation may very well be supplemented by electrophysiological information. While the STN-DBS induced desynchronization of cortical motor area beta band activity is stronger during effective levels of STN-DBS compared to ineffective levels of STN-DBS, this electrophysiological marker is likely not viable for the evaluation of the effectiveness of STN-DBS. Cortical desynchronization is also induced by active and passive movement of limbs which confounds the evaluation of STN-DBS induced reduction of cortical activity (as shown in the included study). EMG is also not a viable marker to determine the effectiveness of STN-DBS. Although, there was a general trend that EMG power decreased with increasing stimulation intensity (similar to the clinical benefit), yet these results were only reliable on a group level. The reason for this limitation was not only a high inter subject variation, but also the need for large amounts of data to estimate a reliable

trend. Cortico-cortical same frequency coupling between the two motor cortices in the beta band may be a reliable marker candidate to objectively assess the effectivity of STN-DBS. Our results showed that this marker is present for the contrast of effective vs ineffective stimulation, but it is not present for the contrast between rest and movement. The observed modulation of cortico-cortical coupling between the motor cortices is in line with previous findings reported in (Silberstein et al. 2005; Weiss et al. 2015). Changes in cortico-muscular coupling are also likely not a valid candidate to assess the effectiveness of STN-DBS in patients with Parkinson's disease. Although we observed an increase in ipsilateral cortico-muscular coupling between the motor cortex and the corresponding biceps, this marker was also strongly influenced by the presence/absence of movement. In short, based on our observations, only cortico-cortical coupling may be a viable marker to objectively estimate the effectiveness of STN-DBS in patients with Parkinson's disease. Cortical power, muscular power, and cortico-muscular coupling were shown to be strongly affected by movement. This potential marker may inform adaptive DBS strategies which currently receive an increased research interest (Piña-Fuentes et al. 2017; Beudel and P. Brown 2016). Common problem among many of these adaptive approaches is that the marker chosen for the activation/inactivation of DBS is also modulated by movement (Johnson et al. 2016). This in turn may lead to an inadvertent activation/inactivation of the DBS implant. As cortico-cortical beta band coupling of the motor cortices has been shown to be exempt from modulation by movement, this marker may provide a viable alternative to advance the concept of adaptive DBS. Yet, investigation into other possible confounding factors is warranted.

3.5 Advantages and disadvantages of electrical field steering

While electrophysiological markers are one way to optimize DBS programming, reducing the number of stimulation configuration candidates is another. To this end, we compared directionally-steered and non-steered stimulation. In contrast to previous studies (Bruno et al. 2020; Contarino et al. 2014; Dembek et al. 2017; Pollo et al. 2014; Steigerwald, Müller, et al. 2016), we did not find an increased therapeutic window size (rigidity reduction), when applying stimulation via the best segment DBS-lead contact compared to the reference ring DBS-lead contact. Previous studies have shown either decreased therapeutic thresholds (Pollo et al. 2014; Bruno et al. 2020) or increased side-

effect thresholds (Dembek et al. 2017). This suggested that segmented stimulation is potentially superior to ring stimulation. Although the findings of the presented study differ, they do not suggest that ring stimulation is per se superior. When stimulation is steered into a certain direction by using segmented contacts instead of ring contacts, only the position of the electrical field shifts. Assuming the field strength was adapted for the higher impedance, all attributes of the electrical field, but the position, remain equal. Therefore, it is unlikely that either stimulation type is generally superior; rather the position of the field is more important. Yet, as segment DBS-lead contacts have a higher impedance than ring DBS-lead contacts (as per our observations), the power consumption is increased (in case of equally strong electrical fields (Butson, Maks, and McIntyre 2006)) causing an increased battery drain. As infection of the IPG site is one of the major adverse effects during DBS surgery (Themistocleous et al. 2011) (especially for repeated replacement (Pepper et al. 2013)), the presented findings advice caution when applying segment DBS-lead stimulation.

3.6 Future outlook

The use of electrophysiological information during the implantation of DBS-leads in patients with Parkinson's disease is common and advised (Hariz 2002; Lee, Crammond, and Richardson 2018), yet electrophysiological information is not used to optimize the stimulation programming yet. Moreover, electrophysiological information is not yet used in patients with epilepsy to guide the implantation or for DBS programming (Son et al. 2016; Sweeney-Reed et al. 2016). The identified electrophysiological markers (coupling of cortico-coritcal beta band activity in patients with Parkinson's disease and temporal lobe theta band power in patients with temporal lobe epilepsy) may provide additional information which may be utilized to refine DBS-lead placement and programming in these patients.

Furthermore, we think the proposed markers may be of great interest to the field of adaptive DBS. The identified markers may be used to determine when short-term DBS is necessary to achieve effects similar to chronic stimulation. A prospective change from chronic to adaptive, short-term DBS may not only reduce the number and/or severity of side-effects commonly reported from DBS patients, but may also help to increase battery life time.

4 References

References

Groiss, S. J. et al. (Nov. 2009). "Deep Brain Stimulation in Parkinson's Disease". In: *Ther Adv Neurol Disord* 2.6, pp. 20–28.

Zangiabadi, Nasser et al. (June 6, 2019). "Deep Brain Stimulation and Drug-Resistant Epilepsy: A Review of the Literature". In: *Front Neurol* 10.

Nuttin, Bart et al. (Sept. 2014). "Consensus on guidelines for stereotactic neurosurgery for psychiatric disorders". In: *J Neurol Neurosurg Psychiatry* 85.9, pp. 1003–1008.

Hodgkin, A. L. and A. F. Huxley (Aug. 28, 1952). "A quantitative description of membrane current and its application to conduction and excitation in nerve". In: *J Physiol* 117.4, pp. 500–544.

Holsheimer, J. et al. (Dec. 2000). "Identification of the target neuronal elements in electrical deep brain stimulation". In: *Eur J Neurosci* 12.12, pp. 4573–4577.

McIntyre, Cameron C. and Ross W. Anderson (Oct. 2016). "Deep Brain Stimulation Mechanisms: The Control of Network Activity via Neurochemistry Modulation". In: *J Neurochem* 139 (Suppl 1), pp. 338–345.

Herrington, Todd M., Jennifer J. Cheng, and Emad N. Eskandar (Oct. 28, 2015). "Mechanisms of deep brain stimulation". In: *Journal of Neurophysiology* 115.1. Publisher: American Physiological Society, pp. 19–38.

Yi, Guosheng and Warren M. Grill (July 2018). "Frequency-dependent antidromic activation in thalamocortical relay neurons: effects of synaptic inputs". In: *J. Neural Eng.* 15.5. Publisher: IOP Publishing, p. 056001.

Grill, Warren M., Andrea N. Snyder, and Svjetlana Miocinovic (May 19, 2004). "Deep brain stimulation creates an informational lesion of the stimulated nucleus". In: *NeuroReport* 15.7, pp. 1137–1140.

García, Míriam R. et al. (Sept. 16, 2013). "A Slow Axon Antidromic Blockade Hypothesis for Tremor Reduction via Deep Brain Stimulation". In: *PLOS ONE* 8.9. Publisher: Public Library of Science, e73456.

Anderson, Trent R. et al. (Jan. 18, 2006). "Selective Attenuation of Afferent Synaptic Transmission as a Mechanism of Thalamic Deep Brain Stimulation-Induced Tremor

Arrest". In: *J. Neurosci.* 26.3. Publisher: Society for Neuroscience Section: Neurobiology of Disease, pp. 841–850.

Lozano, Andres M. et al. (Mar. 2019). "Deep brain stimulation: current challenges and future directions". In: *Nature Reviews Neurology* 15.3. Number: 3 Publisher: Nature Publishing Group, pp. 148–160.

Rosenbaum, Robert et al. (Feb. 2014). "Axonal and synaptic failure suppress the transfer of firing rate oscillations, synchrony and information during high frequency deep brain stimulation". In: *Neurobiol Dis* 62, pp. 86–99.

Llinás, Rodolfo R., Elena Leznik, and Francisco J. Urbano (Jan. 8, 2002). "Temporal binding via cortical coincidence detection of specific and nonspecific thalamocortical inputs: A voltage-dependent dye-imaging study in mouse brain slices". In: *PNAS* 99.1. Publisher: National Academy of Sciences Section: Biological Sciences, pp. 449–454.

Milosevic, Luka, Suneil K. Kalia, et al. (Jan. 1, 2018). "Neuronal inhibition and synaptic plasticity of basal ganglia neurons in Parkinson's disease". In: *Brain* 141.1. Publisher: Oxford Academic, pp. 177–190.

McIntyre, Cameron C. and Philip J. Hahn (June 1, 2010). "Network perspectives on the mechanisms of deep brain stimulation". In: *Neurobiology of Disease*. Frontiers in Brain Stimulation 38.3, pp. 329–337.

Rolando, Luigi (1809). *Saggio sopra la vera struttura del cervello dell'uomo e degl'animali e sopra le funzioni del sistema nervoso di Luigi Rolando.*. Issue: 2. nella stamperia da SSRM privilegiata.

Sironi, Vittorio A. (Aug. 18, 2011). "Origin and Evolution of Deep Brain Stimulation". In: *Front Integr Neurosci* 5.

Bartholow, Roberts (1874). "ART. I.–Experimental Investigations into the Functions of the Human Brain." In: *The American Journal of the Medical Sciences (1827-1924)* 134. Publisher: American Periodicals Series II, p. 305.

Bekhtereva, N. P. et al. (1963). "[Utilization of multiple electrodes implanted in the subcortical structure of the human brain for the treatment of hyperkinesis]". In: *Zh Nevropatol Psikhiatr Im S S Korsakova* 63, pp. 3–8.

Steigerwald, Frank, Cordula Matthies, and Jens Volkmann (Jan. 2019). "Directional Deep Brain Stimulation". In: *Neurotherapeutics* 16.1, pp. 100–104.

Fisher, Robert S. et al. (July 1, 2012). “Seizure diaries for clinical research and practice: Limitations and future prospects”. In: *Epilepsy Behav* 24.3. Publisher: Elsevier, pp. 304–310.

Volkmann, Jens, Elena Moro, and Rajesh Pahwa (2006). “Basic algorithms for the programming of deep brain stimulation in Parkinson’s disease”. In: *Movement Disorders* 21 (S14). _eprint: https://movementdisorders.onlinelibrary.wiley.com/doi/pdf/10.1002/mds.2096 S284–S289.

Brown, P. (2006). “Bad oscillations in Parkinsons disease”. In: *Parkinsons Disease and Related Disorders*. Ed. by P. Riederer et al. Journal of Neural Transmission. Supplementa. Vienna: Springer, pp. 27–30.

Hammond, Constance, Hagai Bergman, and Peter Brown (July 1, 2007). “Pathological synchronization in Parkinson’s disease: networks, models and treatments”. In: *Trends in Neurosciences* 30.7. Publisher: Elsevier, pp. 357–364.

Pollok, B et al. (July 1, 2012). “Motor-cortical oscillations in early stages of Parkinson’s disease”. In: *J Physiol* 590 (Pt 13), pp. 3203–3212.

Little, Simon and Peter Brown (Jan. 1, 2014). “The functional role of beta oscillations in Parkinson’s disease”. In: *Parkinsonism & Related Disorders*. Proceedings of XX World Congress on Parkinson’s Disease and Related Disorders 20, S44–S48.

Weinberger, Moran et al. (Dec. 1, 2006). “Beta Oscillatory Activity in the Subthalamic Nucleus and Its Relation to Dopaminergic Response in Parkinson’s Disease”. In: *Journal of Neurophysiology* 96.6. Publisher: American Physiological Society, pp. 3248–3256.

Ray, NJ et al. (2008). “Local field potential beta activity in the subthalamic nucleus of patients with Parkinson’s disease is associated with improvements in bradykinesia after dopamine and deep brain stimulation”. In: *Experimental neurology* 213.1. Publisher: Elsevier, pp. 108–113.

Kühn, Andrea A., Andreas Kupsch, et al. (2006). “Reduction in subthalamic 835 Hz oscillatory activity correlates with clinical improvement in Parkinson’s disease”. In: *European Journal of Neuroscience* 23.7. _eprint: https://onlinelibrary.wiley.com/doi/pdf/10.1111/j.1460-9568.2006.04717.x, pp. 1956–1960.

Zaidel, Adam et al. (July 1, 2010). “Subthalamic span of oscillations predicts deep brain stimulation efficacy for patients with Parkinsons disease”. In: *Brain* 133.7. Publisher: Oxford Academic, pp. 2007–2021.

Cukiert, Arthur and Kai Lehtimäki (2017). “Deep brain stimulation targeting in refractory epilepsy”. In: *Epilepsia* 58 (S1), pp. 80–84.

Orosz, Iren et al. (2014). “Vagus nerve stimulation for drug-resistant epilepsy: A European long-term study up to 24 months in 347 children”. In: *Epilepsia* 55.10. _eprint: https://onlinelibrary.wiley.com/doi/pdf/10.1111/epi.12762, pp. 1576–1584.

Järvenpää, Soila et al. (Nov. 1, 2018). “Reversible psychiatric adverse effects related to deep brain stimulation of the anterior thalamus in patients with refractory epilepsy”. In: *Epilepsy & Behavior* 88, pp. 373–379.

Karoly, Philippa J et al. (2019). “When can we trust responders? Serious concerns when using 50% response rate to assess clinical trials”. In: *Epilepsia* 60.9. Publisher: Wiley Online Library, e99–e103.

Temkin, Nancy R. and Gay R. Davis (1984). “Stress as a Risk Factor for Seizures Among Adults with Epilepsy”. In: *Epilepsia* 25.4. _eprint: https://onlinelibrary.wiley.com/doi/pdf/10.1111/j.1528-1157.1984.tb03442.x, pp. 450–456.

Kwan, Patrick and Martin J. Brodie (Feb. 3, 2000). “Early Identification of Refractory Epilepsy”. In: *New England Journal of Medicine* 342.5, pp. 314–319.

Téllez-Zenteno, Jose F. and Lizbeth Hernández-Ronquillo (2012). “A Review of the Epidemiology of Temporal Lobe Epilepsy”. In: *Epilepsy Res Treat* 2012.

Jacob, Theju et al. (Jan. 16, 2019). “A Proposed Mechanism for Spontaneous Transitions between Interictal and Ictal Activity”. In: *J. Neurosci.* 39.3. Publisher: Society for Neuroscience Section: Research Articles, pp. 557–575.

Penfield, Wilder and Herbert Jasper (1954). *Epilepsy and the functional anatomy of the human brain*. Epilepsy and the functional anatomy of the human brain. Oxford, England: Little, Brown & Co. xv, 896.

Löscher, Wolfgang et al. (Sept. 2013). “New avenues for anti-epileptic drug discovery and development”. In: *Nature Reviews Drug Discovery* 12, p. 757.

Vajda, Frank J.E. and Mervyn J. Eadie (2014). “The clinical pharmacology of traditional antiepileptic drugs”. In: *Epileptic Disorders* 16.4, pp. 395–408.

Fisher, Robert et al. (May 2010). “Electrical stimulation of the anterior nucleus of thalamus for treatment of refractory epilepsy: Deep Brain Stimulation of Anterior Thalamus for Epilepsy”. In: *Epilepsia* 51.5, pp. 899–908.

Laxpati, Nealen G., Willard S. Kasoff, and Robert E. Gross (July 2014). “Deep Brain Stimulation for the Treatment of Epilepsy: Circuits, Targets, and Trials”. In: *Neurotherapeutics* 11.3, pp. 508–526.

Lim, Siew-Na et al. (2007). “Electrical Stimulation of the Anterior Nucleus of the Thalamus for Intractable Epilepsy: A Long-term Follow-up Study”. In: *Epilepsia* 48.2, pp. 342–347.

Salanova, Vicenta et al. (Mar. 10, 2015). “Long-term efficacy and safety of thalamic stimulation for drug-resistant partial epilepsy”. In: *Neurology* 84.10, pp. 1017–1025.

Sitnikov, A. R., Yu A. Grigoryan, and L. P. Mishnyakova (July 19, 2018). “Bilateral stereotactic lesions and chronic stimulation of the anterior thalamic nuclei for treatment of pharmacoresistant epilepsy”. In: *Surg Neurol Int* 9.

Bouwens van der Vlis, Tim A. M. et al. (June 1, 2019). “Deep brain stimulation of the anterior nucleus of the thalamus for drug-resistant epilepsy”. In: *Neurosurg Rev* 42.2, pp. 287–296.

Yu, Tao et al. (2018). “High-frequency stimulation of anterior nucleus of thalamus desynchronizes epileptic network in humans”. In: *Brain* 141.9, pp. 2631–2643.

Zumsteg, Dominik, Andres M. Lozano, and Richard A. Wennberg (2006). “Mesial Temporal Inhibition in a Patient with Deep Brain Stimulation of the Anterior Thalamus for Epilepsy”. In: *Epilepsia* 47.11, pp. 1958–1962.

Lau, Lonneke ML de and Monique MB Breteler (June 1, 2006). “Epidemiology of Parkinson’s disease”. In: *The Lancet Neurology* 5.6. Publisher: Elsevier, pp. 525–535.

Driver, Jane A. et al. (Feb. 3, 2009). “Incidence and remaining lifetime risk of Parkinson disease in advanced age”. In: *Neurology* 72.5, pp. 432–438.

Riederer, P. and St. Wuketich (Sept. 1, 1976). “Time course of nigrostriatal degeneration in parkinson’s disease”. In: *J. Neural Transmission* 38.3, pp. 277–301.

Sveinbjornsdottir, Sigurlaug (2016). “The clinical symptoms of Parkinson’s disease”. In: *Journal of Neurochemistry* 139 (S1). _eprint: https://onlinelibrary.wiley.com/doi/pdf/10.1111/jn pp. 318–324.

Jankovic, J. (Apr. 1, 2008). "Parkinsons disease: clinical features and diagnosis". In: *Journal of Neurology, Neurosurgery & Psychiatry* 79.4. Publisher: BMJ Publishing Group Ltd Section: Review, pp. 368–376.

Katzenschlager, Regina and Andrew J. Lees (Sept. 1, 2002). "Treatment of Parkinson's disease: levodopa as the first choice". In: *J Neurol* 249.2, pp. ii19–ii24.

Salat, David and Eduardo Tolosa (Jan. 1, 2013). "Levodopa in the Treatment of Parkinson's Disease: Current Status and New Developments". In: *Journal of Parkinson's Disease* 3.3. Publisher: IOS Press, pp. 255–269.

Thanvi, B and T Lo (Aug. 2004). "Long term motor complications of levodopa: clinical features, mechanisms, and management strategies". In: *Postgrad Med J* 80.946, pp. 452–458.

Benabid, A. L. et al. (1994). "Acute and Long-Term Effects of Subthalamic Nucleus Stimulation in Parkinson's Disease". In: *SFN* 62.1. Publisher: Karger Publishers, pp. 76–84.

Limousin, P. et al. (Jan. 14, 1995). "Effect on parkinsonian signs and symptoms of bilateral subthalamic nucleus stimulation". In: *The Lancet* 345.8942. Publisher: Elsevier, pp. 91–95.

Dallapiazza, Robert F. et al. (2018). "Considerations for Patient and Target Selection in Deep Brain Stimulation Surgery for Parkinsons Disease". In: *Parkinsons Disease: Pathogenesis and Clinical Aspects*. Ed. by Thomas B. Stoker and Julia C. Greenland. Brisbane (AU): Codon Publications.

Elahian, Bahareh et al. (Oct. 2017). "Identifying seizure onset zone from electrocorticographic recordings: A machine learning approach based on phase locking value". In: *Seizure* 51, pp. 35–42.

Blauwblomme, Thomas, Premysl Jiruska, and Gilles Huberfeld (Jan. 1, 2014). "Chapter Seven - Mechanisms of Ictogenesis". In: *International Review of Neurobiology*. Ed. by Premysl Jiruska, Marco de Curtis, and John G. R. Jefferys. Vol. 114. Modern Concepts of Focal Epileptic Networks. Academic Press, pp. 155–185.

Brunenberg, Ellen JL et al. (2011). "Magnetic resonance imaging techniques for visualization of the subthalamic nucleus: a review". In: *Journal of neurosurgery* 115.5. Publisher: American Association of Neurological Surgeons, pp. 971–984.

Hutchison, W. D. et al. (1998). "Neurophysiological identification of the subthalamic nucleus in surgery for Parkinson's disease". In: *Annals of Neurology* 44.4, pp. 622–628.

Hariz, Marwan I (2002). "Complications of deep brain stimulation surgery". In: *Movement disorders: official journal of the Movement Disorder Society* 17 (S3). Publisher: Wiley Online Library, S162–S166.

Lozano, Andres M et al. (2010). "Basal ganglia physiology and deep brain stimulation". In: *Movement disorders* 25 (S1). Publisher: Wiley Online Library, S71–S75.

Nickl, Robert C et al. (2019). "Rescuing suboptimal outcomes of subthalamic deep brain stimulation in Parkinson disease by surgical lead revision". In: *Neurosurgery* 85.2. Publisher: Oxford University Press, E314–E321.

Rolston, John D et al. (2016). "An unexpectedly high rate of revisions and removals in deep brain stimulation surgery: analysis of multiple databases". In: *Parkinsonism & related disorders* 33. Publisher: Elsevier, pp. 72–77.

Levin, Johannes et al. (2009). "Objective measurement of muscle rigidity in parkinsonian patients treated with subthalamic stimulation". In: *Movement Disorders* 24.1, pp. 57–63.

Shahidi, Gholam Ali et al. (2017). "Outcome of subthalamic nucleus deep brain stimulation on long-term motor function of patients with advanced Parkinson disease". In: *Iranian Journal of Neurology* 16.3. Publisher: Tehran University of Medical Sciences, p. 107.

Tsai, Sheng-Tzung et al. (2013). "Long-term outcome of young onset Parkinson's disease after subthalamic stimulationA cross-sectional study". In: *Clinical neurology and neurosurgery* 115.10. Publisher: Elsevier, pp. 2082–2087.

Zibetti, Maurizio et al. (2011). "Beyond nine years of continuous subthalamic nucleus deep brain stimulation in Parkinson's disease". In: *Movement Disorders* 26.13. Publisher: Wiley Online Library, pp. 2327–2334.

Son, Byung-chul et al. (2016). "Relationship between Postoperative EEG Driving Response and Lead Location in Deep Brain Stimulation of the Anterior Nucleus of the Thalamus for Refractory Epilepsy". In: *SFN* 94.5, pp. 336–341.

Sweeney-Reed, Catherine M. et al. (Oct. 1, 2016). “Thalamic interictal epileptiform discharges in deep brainăstimulated epilepsy patients”. In: *J Neurol* 263.10, pp. 2120–2126.

Osorio, Ivan et al. (2007). “High Frequency Thalamic Stimulation for Inoperable Mesial Temporal Epilepsy”. In: *Epilepsia* 48.8, pp. 1561–1571.

Amirnovin, Ramin et al. (2006). “Experience with microelectrode guided subthalamic nucleus deep brain stimulation”. In: *Operative Neurosurgery* 58 (suppl_1). Publisher: Oxford University Press, ONS–96.

Bour, Lo J. et al. (Dec. 1, 2010). “Long-term experience with intraoperative microrecording during DBS neurosurgery in STN and GPi”. In: *Acta Neurochir* 152.12, pp. 2069–2077.

Schlaier, Juergen Ralf et al. (Feb. 1, 2013). “The influence of intraoperative microelectrode recordings and clinical testing on the location of final stimulation sites in deep brain stimulation for Parkinsons disease”. In: *Acta Neurochir* 155.2, pp. 357–366.

Granziera, C. et al. (Mar. 1, 2008). “Sub-acute delayed failure of subthalamic DBS in Parkinson’s disease: The role of micro-lesion effect”. In: *Parkinsonism & Related Disorders* 14.2, pp. 109–113.

Arnolds, D. E. et al. (Nov. 1980). “The spectral properties of hippocampal EEG related to behaviour in man”. In: *Electroencephalogr Clin Neurophysiol* 50.3, pp. 324–328.

Kahana, Michael J. et al. (June 1999). “Human theta oscillations exhibit task dependence during virtual maze navigation”. In: *Nature* 399.6738. Number: 6738 Publisher: Nature Publishing Group, pp. 781–784.

Raghavachari, S. et al. (May 1, 2001). “Gating of human theta oscillations by a working memory task”. In: *J Neurosci* 21.9, pp. 3175–3183.

Cantero, Jose L. et al. (Nov. 26, 2003). “Sleep-Dependent Oscillations in the Human Hippocampus and Neocortex”. In: *J. Neurosci.* 23.34. Publisher: Society for Neuroscience Section: Behavioral/Systems/Cognitive, pp. 10897–10903.

Adebimpe, Azeez et al. (Jan. 1, 2015). “EEG resting state analysis of cortical sources in patients with benign epilepsy with centrotemporal spikes”. In: *NeuroImage: Clinical* 9, pp. 275–282.

Miyauchi, Toshiro et al. (1991). “Computerized Analysis of EEG Background Activity in Epileptic Patients”. In: *Epilepsia* 32.6, pp. 870–881.

Quraan, Maher A. et al. (July 26, 2013). "Altered Resting State Brain Dynamics in Temporal Lobe Epilepsy Can Be Observed in Spectral Power, Functional Connectivity and Graph Theory Metrics". In: *PLOS ONE* 8.7, e68609.

Kühn, Andrea A., Florian Kempf, et al. (June 11, 2008). "High-Frequency Stimulation of the Subthalamic Nucleus Suppresses Oscillatory Activity in Patients with Parkinson's Disease in Parallel with Improvement in Motor Performance". In: *J Neurosci* 28.24, pp. 6165–6173.

Lee, Philip S, Donald J Crammond, and R Mark Richardson (2018). "Deep brain stimulation of the subthalamic nucleus and globus pallidus for Parkinson's disease". In: *Current Concepts in Movement Disorder Management*. Vol. 33. Karger Publishers, pp. 207–221.

Burchiel, Kim J. et al. (Aug. 1, 2013). "Accuracy of deep brain stimulation electrode placement using intraoperative computed tomography without microelectrode recording: Clinical article". In: *Journal of Neurosurgery* 119.2. Publisher: American Association of Neurological Surgeons Section: Journal of Neurosurgery, pp. 301–306.

Shahlaie, Kiarash, Paul S. Larson, and Philip A. Starr (Mar. 1, 2011). "Intraoperative Computed Tomography for Deep Brain Stimulation Surgery: Technique and Accuracy Assessment". In: *Oper Neurosurg (Hagerstown)* 68 (suppl_1). Publisher: Oxford Academic, ons114–ons124.

Sokal, P. et al. (Mar. 1, 2015). "Intraoperative CT verification of electrode localization in DBS surgery in Parkinson's disease". In: *Interdisciplinary Neurosurgery* 2.1, pp. 6–9.

Lozano, Christopher S et al. (2018). "Imaging alone versus microelectrode recordingguided targeting of the STN in patients with Parkinsons disease". In: *Journal of neurosurgery* 130.6. Publisher: American Association of Neurological Surgeons, pp. 1847–1852.

Montgomery Jr, Erwin B (2012). "Microelectrode targeting of the subthalamic nucleus for deep brain stimulation surgery". In: *Movement disorders* 27.11. Publisher: Wiley Online Library, pp. 1387–1391.

Amon, A. and F. Alesch (Sept. 1, 2017). "Systems for deep brain stimulation: review of technical features". In: *J Neural Transm* 124.9, pp. 1083–1091.

Tinkhauser, Gerd et al. (2018). "Directional local field potentials: A tool to optimize deep brain stimulation". In: *Movement Disorders* 33.1, pp. 159–164.

Contarino, M. Fiorella et al. (Sept. 23, 2014). "Directional steering". In: *Neurology* 83.13, p. 1163.

Dembek, Till A. et al. (2017). "Directional DBS increases side-effect thresholdsA prospective, double-blind trial". In: *Movement Disorders* 32.10. _eprint: https://movementdisorders.onlinelibrary.wiley.com/doi/pdf/10.1002/mds.27093, pp. 1380–1388.

Pollo, Claudio et al. (2014). "Directional deep brain stimulation: an intraoperative double-blind pilot study". In: *Brain* 137.7, pp. 2015–2026.

Bruno, Sabine et al. (July 15, 2020). "Directional Deep Brain Stimulation of the Thalamic Ventral Intermediate Area for Essential Tremor Increases Therapeutic Window". In: *Neuromodulation: Technology at the Neural Interface* n/a (n/a). _eprint: https://onlinelibrary.wiley.com/doi/pdf/10.1111/ner.13234.

Irwin, J David and R Mark Nelms (2020). *Basic engineering circuit analysis*. Wiley.

Butson, Christopher R., Christopher B. Maks, and Cameron C. McIntyre (Feb. 1, 2006). "Sources and effects of electrode impedance during deep brain stimulation". In: *Clinical Neurophysiology* 117.2, pp. 447–454.

Themistocleous, Marios S. et al. (Mar. 23, 2011). "Infected internal pulse generator: Treatment without removal". In: *Surg Neurol Int* 2.

Pepper, Joshua et al. (2013). "The Risk of Hardware Infection in Deep Brain Stimulation Surgery Is Greater at Impulse Generator Replacement than at the Primary Procedure". In: *SFN* 91.1. Publisher: Karger Publishers, pp. 56–65.

Heinrichs-Graham, Elizabeth et al. (Oct. 1, 2014). "Neuromagnetic Evidence of Abnormal Movement-Related Beta Desynchronization in Parkinson's Disease". In: *Cereb Cortex* 24.10. Publisher: Oxford Academic, pp. 2669–2678.

Silberstein, Paul et al. (June 1, 2005). "Cortico-cortical coupling in Parkinson's disease and its modulation by therapy". In: *Brain* 128.6. Publisher: Oxford Academic, pp. 1277–1291.

Weiss, Daniel et al. (Mar. 1, 2015). "Subthalamic stimulation modulates cortical motor network activity and synchronization in Parkinsons disease". In: *Brain* 138.3. Publisher: Oxford Academic, pp. 679–693.

Salenius, Stephan et al. (Mar. 1, 2002). “Defective cortical drive to muscle in Parkinsons disease and its improvement with levodopa”. In: *Brain* 125.3. Publisher: Oxford Academic, pp. 491–500.

Sridharan, Kousik Sarathy et al. (June 3, 2019). “Electromagnetic mapping of the effects of deep brain stimulation and dopaminergic medication on movement-related cortical activity and corticomuscular coherence in Parkinsons disease”. In: *bioRxiv*. Publisher: Cold Spring Harbor Laboratory Section: New Results, p. 657882.

Kühn, Andrea A., Thomas Trottenberg, et al. (July 2005). “The relationship between local field potential and neuronal discharge in the subthalamic nucleus of patients with Parkinson’s disease”. In: *Exp Neurol* 194.1, pp. 212–220.

Milosevic, Luka, Maximilian Scherer, et al. (2020). “Online Mapping With the Deep Brain Stimulation Lead: A Novel Targeting Tool in Parkinson’s Disease”. In: *Movement Disorders* 35.9. _eprint: https://movementdisorders.onlinelibrary.wiley.com/doi/pdf/10.100 pp. 1574–1586.

Little, Simon and Peter Brown (2020). “Debugging Adaptive Deep Brain Stimulation for Parkinson’s Disease”. In: *Movement Disorders* 35.4. _eprint: https://movement-disorders.onlinelibrary.wiley.com/doi/pdf/10.1002/mds.27996, pp. 555–561.

Johnson, Luke A. et al. (Dec. 2016). “Closed-Loop Deep Brain Stimulation Effects on Parkinsonian Motor Symptoms in a Non-Human Primate - Is Beta Enough?” In: *Brain Stimul* 9.6, pp. 892–896.

Okun, Michael S. et al. (Aug. 1, 2005). “Management of Referred Deep Brain Stimulation Failures: A Retrospective Analysis From 2 Movement Disorders Centers”. In: *Archives of Neurology* 62.8, pp. 1250–1255.

Erwin B Montgomery, Jr (2020). *Deep Brain Stimulation Programming: Mechanisms, Principles and Practice*. Publication Title: Deep Brain Stimulation Programming. Oxford University Press.

Halpern, Casey H. et al. (2008). “Brain Shift during Deep Brain Stimulation Surgery for Parkinsons Disease”. In: *SFN* 86.1. Publisher: Karger Publishers, pp. 37–43.

Kühn, Andrea A., Alexander Tsui, et al. (Feb. 2009). “Pathological synchronisation in the subthalamic nucleus of patients with Parkinson’s disease relates to both bradykinesia and rigidity”. In: *Exp. Neurol.* 215.2, pp. 380–387.

Abosch, Aviva et al. (2002). "Movement-related neurons of the subthalamic nucleus in patients with Parkinson disease". In: *Journal of neurosurgery* 97.5. Publisher: Journal of Neurosurgery Publishing Group, pp. 1167–1172.

Swann, Nicole C. et al. (Aug. 2018). "Adaptive deep brain stimulation for Parkinsons disease using motor cortex sensing". In: *J Neural Eng* 15.4, p. 046006.

Wagle Shukla, Aparna et al. (2017). "DBS programming: an evolving approach for patients with Parkinsons disease". In: *Parkinsons Disease* 2017. Publisher: Hindawi.

Piña-Fuentes, Dan et al. (Aug. 2017). "Adaptive DBS in a Parkinsons Patient with Chronically Implanted DBS: A Proof of Principle". In: *Mov Disord* 32.8, pp. 1253–1254.

Beudel, M. and P. Brown (Jan. 1, 2016). "Adaptive deep brain stimulation in Parkinson's disease". In: *Parkinsonism & Related Disorders*. Proceedings of XXI World Congress on Parkinson's Disease and Related Disorders, December 6-9, 2015, Milan, Italy 22, S123–S126.

Steigerwald, Frank, Lorenz Müller, et al. (2016). "Directional deep brain stimulation of the subthalamic nucleus: A pilot study using a novel neurostimulation device". In: *Movement Disorders* 31.8. _eprint: https://movementdisorders.onlinelibrary.wiley.com/doi/pdf/10.1002/mds.26669, pp. 1240–1243.

5 List of appended manuscripts and contributions

1. Desynchronization of temporal lobe theta band activity during effective anterior thalamus deep brain stimulation in epilepsy
   Published in NeuroImage 2020 Sep 01
   Contributions:
   Maximilian Scherer: 1A, 2A, 2B, 3A
   Luka Milosevic: 1A, 2C, 3A
   Robert Guggenberger: 2C, 3B
   Volker Maus: 1B, 1C, 3B
   Georgios Naros: 1C, 3B
   Florian Grimm: 1C, 3B
   Iancu Bucurenciu: 1C, 3B
   Bernhard J. Steinhoff: 1B, 3B
   Yvonne G. Weber: 1C, 3B
   Holger Lerche: 1B, 3B
   Daniel Weiss: 1B, 3B
   Sabine Rona: 1B, 1C, 3B
   Alireza Gharabaghi: 1A, 1B, 1C, 3A, 3B

2. Online Mapping With the Deep Brain Stimulation Lead: A Novel Targeting Tool in Parkinson's Disease
   Published in Movement Disorders 2020 May 18
   Constributions:
   Luka Milosevic: 1A, 1B, 1C, 2A, 2B, 3A
   Maximilian Scherer: 1A, 1B, 1C, 2A, 2B, 3B
   Idil Cebi: 1B, 1C, 3B
   Robert Guggenberger: 2A, 2C, 3B
   Kathrin Machetanz: 1B, 1C, 3B
   Georgios Naros: 1B, 1C, 3B
   Daniel Weiss: 1B, 2C, 3B
   Alireza Gharabaghi: 1A, 1B, 1C, 2C, 3B

3. Desynchronization of temporal lobe theta band activity during effective anterior thalamus deep brain stimulation in epilepsy
   In preparation
   Contributions:
   Maximilian Scherer: 1A, 1B, 1C, 2A, 2B, 3A
   Luka Milosevic: 1A, 1B, 1C, 2A, 2C, 3B
   Patrick Bookjans: 1B, 1C, 3B
   Bastian Brunett: 1B, 1C, 3B
   Idil Hanci: 1B, 1C, 3B
   Robert Guggenberger: 1A, 2C, 3B
   Daniel Weiss: 1B, 1C, 3B
   Alireza Gharabaghi: 1A, 1B, 2C, 3A

4. State-dependent decoupling of interhemispheric motor networks with effective deep brain stimulation in Parkinson's disease
   In preparation
   Contributions:
   Maximilian Scherer: 1A, 1B, 1C, 2A, 2B, 3A
   Luka Milosevic: 1B, 1C, 2A, 2C, 3A
   Patrick Bookjans: 1B, 1C, 3B
   Bastian Brunett: 1B, 1C, 3B
   Idil Hanci: 1B, 1C, 3B
   Robert Guggenberger: 2C, 3B
   Daniel Weiss: 1B, 1C, 3B
   Alireza Gharabaghi: 1A, 1B, 2C, 3A

Individual contributions:

1. Research project: A. Conception, B. Organization, C. Execution.
2. Data and statistical analysis: A. Design, B. Execution, C. Review and Critique.
3. Manuscript: A. Writing of the first draft, B. Review and Critique.

NeuroImage 218 (2020) 116967

Contents lists available at ScienceDirect

NeuroImage

journal homepage: www.elsevier.com/locate/neuroimage

Desynchronization of temporal lobe theta-band activity during effective anterior thalamus deep brain stimulation in epilepsy

Maximillian Scherer [a], Luka Milosevic [a], Robert Guggenberger [a], Volker Maus [a], Georgios Naros [a], Florian Grimm [a], Iancu Bucurenciu [b], Bernhard J. Steinhoff [b], Yvonne G. Weber [c,e], Holger Lerche [c], Daniel Weiss [d], Sabine Rona [e], Alireza Gharabaghi [a,*]

[a] Division of Functional and Restorative Neurosurgery, Department of Neurosurgery, And Tübingen NeuroCampus, University of Tübingen, 72076, Tübingen, Germany
[b] Kork Epilepsy Center, Kehl-Kork, Germany
[c] Department of Neurology and Epileptology, Hertie Institute for Clinical Brain Research, University of Tübingen, Tübingen, Germany
[d] Department for Neurodegenerative Diseases, Hertie Institute for Clinical Brain Research, And German Centre of Neurodegenerative Diseases (DZNE), University Tübingen, Tübingen, Germany
[e] Epilepsy Unit, Department of Neurosurgery, University of Tübingen, Tübingen, Germany

ARTICLE INFO

Keywords:
Anterior nucleus of the thalamus
Deep brain stimulation
Electroencephalography
Epilepsy
Biomarker

ABSTRACT

Background: Bilateral cyclic high frequency deep brain stimulation (DBS) of the anterior nucleus of the thalamus (ANT) reduces the seizure count in a subset of patients with epilepsy. Detecting stimulation-induced alterations of pathological brain networks may help to unravel the underlying physiological mechanisms related to effective stimulation delivery and optimize target engagement.

Methods: We acquired 64-channel electroencephalography during ten ANT-DBS cycles (145 Hz, 90 μs, 3–5 V) of 1-min ON followed by 5-min OFF stimulation to detect changes in cortical activity related to seizure reduction. The study included 14 subjects (three responders, four non-responders, and seven healthy controls). Mixed-model ANOVA tests were used to compare differences in cortical activity between subgroups both ON and OFF stimulation, while investigating frequency-specific effects for the seizure onset zones.

Results: ANT-DBS had a widespread desynchronization effect on cortical theta and alpha band activity in responders, but not in non-responders. Time domain analysis showed that the stimulation induced reduction in theta-band activity was temporally linked to the stimulation period. Moreover, stimulation induced theta-band desynchronization in the temporal lobe channels correlated significantly with the therapeutic response. Responders to ANT-DBS and healthy-controls had an overall lower level of theta-band activity compared to non-responders.

Conclusion: This study demonstrated that temporal lobe channel theta-band desynchronization may be a predictive physiological hallmark of therapeutic response to ANT-DBS and may be used to improve the functional precision of this intervention by verifying implantation sites, calibrating stimulation contacts, and possibly identifying treatment responders prior to implantation.

1. Introduction

Epilepsy is a well-described neurological condition which affects individuals of all ages and approximately 1% of the global population (Kwan and Brodie, 2000). Seizures originating in the temporal lobe(s) are most common in adults (Téllez-Zenteno and Hernández-Ronquillo, 2012). While antiepileptic drugs, which primarily work through the enhancement of inhibitory neurotransmission and attenuation of excitatory transmission (Löscher et al., 2013; Vajda and Eadie, 2014) can be efficacious, up to 30% of patients continue to experience recurrent seizures despite optimal medical therapy (Halpern et al., 2008; Kwan and Brodie, 2000). For these patients, bilateral deep brain stimulation (DBS) of the thalamic anterior nuclei (ANT) is a therapeutic option (Fisher et al., 2010; Laxpati et al., 2014; Lim et al., 2007; Salanova et al., 2015; Sitnikov et al., 2018). The clinical efficacy of ANT-DBS was systematically evaluated in the "Stimulation of the Anterior Nucleus of the Thalamus for

* Corresponding author. Division of Functional and Restorative Neurosurgery, University of Tübingen, Otfried-Mueller-Str.45, 72076, Tübingen, Germany.
E-mail address: alireza.gharabaghi@uni-tuebingen.de (A. Gharabaghi).

https://doi.org/10.1016/j.neuroimage.2020.116967
Received 7 November 2019; Received in revised form 4 May 2020; Accepted 13 May 2020
Available online 20 May 2020

Epilepsy" (SANTE) study and revealed median seizure reduction rates of 40.4% in the in the double-blinded phase 3–4 months after surgery (Fisher et al., 2010). Moreover, it was determined that treatment efficacy was greatest in patients with seizures originating in one or both temporal regions. During the unblinded phase, the authors reported that patients experienced a median seizure reduction rate of 56%, and that 54% of the patient population had seizure reductions of at least 50% (at 2 years postoperatively). However, there is still a lack of a reliable functional marker for therapy response (Son et al., 2016; Sweeney-Reed et al., 2016). While the therapeutic potential of ANT-DBS is promising, the efficacy is widely variable. As such, further efforts are warranted in order to understand the variability in clinical benefit, and in order to define functional markers/readouts. Furthermore, the therapeutic mechanisms of ANT-DBS are not well-understood (Fisher and Velasco, 2014). The selection of ANT as a target for DBS was justified by its central connectivity and possible role in propagation of epileptiform activity (Wyckhuys et al., 2009). Several studies in rat models have shown that bilateral high-frequency stimulation or lesions of the ANT reduced seizure frequency (Child and Benarroch, 2013; Hamani et al., 2004; Mirski et al., 1997; Takebayashi et al., 2007). As such, it was hypothesized that ANT stimulation or lesions may work to suppress the amplification, propagation, and/or synchronization of seizure activity (Takebayashi et al., 2007). Animal studies at the cellular/microcircuit level have suggested that ANT stimulation may work to restore the balance between excitatory and inhibitory neurotransmission, with findings of increased levels of GABA in the hippocampus in response to ANT-DBS (Child and Benarroch, 2013; Liu et al., 2012; Shi et al., 2015). At the subcortical network level, one study in humans with multiple intracerebral depth electrodes has demonstrated that high-frequency ANT stimulation decreased electrical activity over a broad frequency range, and reduced interictal spikes in the hippocampus (Yu et al., 2018), while a single case study demonstrated that ANT-DBS reduced the power of hippocampal delta and theta activity (Zumsteg et al., 2006). However, the synergistic use of human brain mapping techniques and ANT-DBS is scares.

Detecting stimulation-induced alterations of pathological brain networks may unravel the underlying physiological mechanisms related to effective stimulation delivery and optimize target engagement. To the best of our knowledge, this is the first study to assess network/macrocircuit effects of ANT-DBS at the level of cortical oscillatory networks related to epilepsy and therapy response. The study of the cortical mechanisms of ANT-DBS in this context may help to explain the variability in therapeutic efficacy, to refine patient selection criteria, and to define functional therapeutic markers which can guide electrode placements and the calibration of stimulation parameters.

2. Methods

2.1. Patients

This study included n = 14 individuals, seven of whom were patients who had undergone ANT-DBS surgeries ($n_{patients} = 7$) and an additional seven who were healthy control subjects ($n_{controls} = 7$); all provided written informed consent. All patients had a prolonged history of epilepsy and were refractory to conventional pharmacological therapy. Patient demographics are presented in Table 1. All patients had undergone bilateral, image-guided implantations of Medtronic 3389 leads (Medtronic, MN, USA) into the ANT using an extra-ventricular trajectory (Fig. 1; postoperative images for all patients are available in supplementary material). Stimulation parameters followed the SANTE protocol (145 Hz, 90 μs and 3–5 V; Fisher et al., 2010). Patients kept a seizure diary before and after surgery counting the number of seizures they experienced. The clinical benefit was quantified by counting the number of seizures they experienced from the beginning of the second month postoperatively (when the stimulation was turned on) to the end of the fifth month (four-month period) in comparison to the mean preoperative status. The first postoperative month was excluded due to the possibility of micro-lesion effects (Lane et al., 2017).

Table 1
Patient demographics.

ID	Age	EEG Seizure onset foci	Seizure history (years)	Avg. seizures/ month (before DBS)	Median seizure reduction rate in % (4 months)	Maximum likelihood estimation
1	51	Right temporo-parieto-occipital	Childhood	28	5.5	non-responder
2	22	Multifocal Left > Right	5	13	8	non-responder
3	45	Left temporal	10	7	71	responder
4	48	Bitemporal, independent	5	80	42	responder
5	26	Multifocal Left > Right	16	174	25	non-responder
6[a]	31	Bitemporal, independent	4	15	77	responder
7	25	Right > Left temporo-parieto-occipital	17	57	−3.5	non-responder

[a] Patient with bilateral periventricular heterotopia.

Out of the seven subjects of this study, two could clearly be identified as responders (seizure reduction rates: 77% and 71%) and three as non-responders (5.5%, 8% and −3.5%). The two remaining subjects (seizure reduction rates: 42% and 25%) were classified based on whether they are more likely to belong to the responder (mean seizure reduction rate = 74%) or the non-responder (mean seizure reduction rate = 3.33%) clusters within our cohort, i.e. by a maximum likelihood approach. Assuming a Gaussian distribution with uniform variance for responder and non-responder populations, it was determined that the patient with a seizure reduction rate of 42% was a responder and the patient with a seizure reduction rate of 25% was a non-responder.

In total, three patients were classified as responders (nresponders = 3) and four as non-responders (nnon-responders = 4). Two of the responders presented with bilateral mesial temporal lobe epilepsy and the third responder presented with temporal lobe type seizures due to bilateral periventricular heterotopia, whereas the non-responders all presented with extratemporal or multifocal seizure origins. Some of the patients were part of the European registration study (Lehtimäki et al., 2018). This study was approved by the ethics committee of the Medical Faculty Tübingen.

2.2. Data acquisition

64-channel resting-state electroencephalography (EEG) data were collected from each subject via two synchronized BrainAmp DC Amplifiers (Brain Products, Munich, Germany) and sampled at ≥1000 Hz. The EEG electrodes were placed according to the extended 10–20 system. For the duration of the examination, the subjects and patients alike were instructed to lay flat, but awake, on a bed with their eyes closed. The experimenter a) periodically confirmed wakefulness during the experiment and b) asked the patients after the measurements whether they had fallen asleep, which was denied by all of them. Furthermore, the qualified examiner was always present and verified that none of the patients experienced a seizure during the recording sessions. In patients, recordings encompassed 10 stimulation trials at 140 Hz, 90 μs and 3–5 V. Each trial consisted of a period of 5-min OFF stimulation, followed by 1-min ON stimulation. This paradigm (stimulation parameters and periodic stimulation delivery) is based on the chronic stimulation delivery paradigm of the SANTE study. Stimulation was always delivered bipolarly using the two dorsal-most electrode contacts. In controls, only resting-

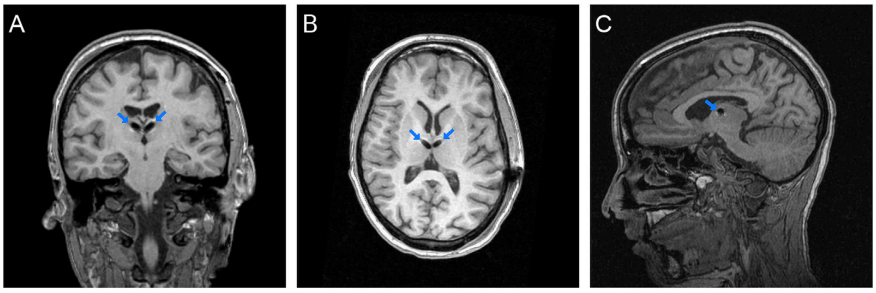

Fig. 1. Postoperative MRI images from a representative patient. Representative coronal (A), axial (B), and sagittal (C) MRI images from a single patient demonstrating lead placement (highlighted by arrows).

state data were acquired.

2.3. Pre-processing

The EEG data were visually inspected for large scale artifacts (e.g. movement artifacts). Bad channels were removed from the analysis. The data were low-pass filtered (45 Hz) for anti-aliasing using a finite-impulse-response filter with a high suppression factor. The ripple pass-band suppression was chosen as 10e-5 and the stopband suppression as 10e-7. Subsequently, the data were down-sampled to 100 Hz, common average re-referenced and cut into 40-s epochs. ON data were taken from the central 40s of a stimulation period, while OFF (resting-state) data were selected as the period from 50 to 10 s prior to stimulation onset. Each epoch consisted of 4000 samples. Visual inspection was applied to detect bad epochs (i.e. corrupt channels or moved EEG cables). These were excluded from any further analysis. Each epoch was high-pass filtered (2 Hz) to remove movement artifacts. Afterwards, a power spectrum density was calculated using Welch's method with a Hamming window, 1 Hz bins, 50% overlap, and 1s segment size. To analyze frequency-specific power in each block, the bins of each frequency band were summed up. The analyzed frequency bands included the theta (4–7 Hz), alpha (8–12 Hz), beta (13–32 Hz) and low gamma (33–45 Hz) bands. Furthermore, the power was calculated for smaller 2 Hz-wide sub-bands, starting from 4 to 6 Hz, 5–7 Hz and so on, up to 10–12 Hz (as theta and alpha were identified as frequency bands of interest during later steps of the analysis).

2.4. Effects of stimulation and responsiveness on cortical activity

Since this study was exploratory, the first objective was to identify the presence of any effects related to the response-type (responder, non-responder), stimulation-condition (ON, OFF), and the interaction of these factors. Thus, the two-way ANOVA model represents the most statistically appropriate method, in which we furthermore used a rather conservative multiple comparisons correction (Bonferroni-Holm method). Beyond the initial exploratory results, the subsequent analyses were discovery-driven, and performed in a systematic manner.

More specifically, a mixed-model two-way ANOVA was used to identify frequency bands of interest on the patient group level in the theta, alpha, beta and lower gamma frequency-bands, and subsequently to identify sub-bands of interest. Frequency bands were identified as being of interest if the ANOVA revealed a significant effect within a particular frequency band, after multiple comparison correction (Bonferroni-Holm). The two fixed factors (main effects) of the ANOVA-model were stimulation-condition (ON/OFF; within subject factor) and response-type (responder/non-responder; between-subjects factor), and subject-ID was included as a random factor (as each subject was measured repeatedly and a general offset between subjects was expected; random-intercept per subject). The gradient of the main effects determined their respective effect (increasing/decreasing). The interaction between the two fixed factors was also modeled in the ANOVA. The stimulation-condition main effect was used to model the measured change in cortical power (i.e. synchronization or desynchronization) when DBS was ON compared to OFF, irrespective of response-type. The response-type main effect was used to model the difference in cortical power between responders and non-responders, irrespective of the stimulation-condition. The interaction effect was used to model a conditional change in cortical activity depending on both main effects (for example a larger effect size of stimulation-condition in responders compared to a smaller effect size in non-responders). Information regarding interpretation of ANOVA results is summarized in supplementary fig. 1.

In the two-way ANOVA, the presence of an interaction effect between stimulation-condition and response-type may be the result of (1) a cortical power change in responders (but not non-responders) due to a change in the stimulation-condition, (2) a cortical power change in non-responders (but not responders) due to a change in the stimulation-condition, (3) a difference in cortical power during stimulation ON (but not OFF) due to differences between responders and non-responders (4) a difference in cortical power during stimulation OFF (but not ON) due to differences between responders and non-responders. Since the mixed-model two-way ANOVA only determines the presence or absence of an interaction effect, subsequent one-way ANOVAs were performed in order to determine potential causes of this interaction. As such, four subsequent mixed-model one-way ANOVA analyses were computed to determine (i) the main effect of stimulation-condition in responders only, (ii) the main effect of stimulation-condition in non-responders only, (iii) the main effect of response-type during stimulation ON, and (iv) the main effect of response-type during stimulation OFF. For all ANOVA analyses, in order to compensate for the type-1 error inflation, multiple comparison corrections were applied to correct the significance threshold using the Bonferroni-Holm method with a hypothesis count of 63, which was derived based on the number of non-overlapping frequency bands investigated (the theta and alpha sub-bands 4–6 Hz; 5–7 Hz; 6–8 Hz; 7–9 Hz; 8–10 Hz; 9–11 Hz; 10–12 Hz; and broad-band beta (13–32 Hz) and gamma (33–45 Hz), which were also assessed in preliminary analyses, i.e. 9 in total) and the number of brain regions (temporal left, temporal right, frontal left, frontal right, parietal left, parietal right, occipital; i.e. 7 in total).

2.5. Stimulation and seizure reduction

After determining frequency bands of interest by using the aforementioned ANOVA analyses, we investigated whether stimulation-induced changes of these frequencies were of clinical relevance. For this purpose, we defined cortical regions of interest based on the seizure-onset zones of the patients, i.e., effects on the temporal lobe channels (FT7, T7, TP7, FT8, T8, TP8) and widespread areas were investigated. Since Pearson's definition assumes a linear relationship, the Spearman correlation coefficient was used for this estimation as it does not assume a specific shape of the investigated relationship. The correlation analyses

(Fig. 3) indeed confirmed that decreases in theta activity correlated with seizure reductions (this finding is expanded upon in the results section, but mentioned here since it informed the subsequent analyses).

2.6. Theta activity differences in temporal lobe channels

In regions where spatio-spectrally localized clinical relevance was found (from above correlations), the DBS induced cortical-activity changes were investigated further. At the group level, cortical-activity was investigated for five individual groups; responders and non-responders in both stimulation ON and stimulation OFF, and healthy controls. Since multiple measurements were utilized for each patient (i.e. data from 10 trials for each patient, from multiple EEG channels), one-way ANOVA analyses were performed to compare activity between these groups, using subject-id and channel-id as random factors. At the single subject level, the same was done, except using only channel-id as a random factor. Subjects (subject-id) were modeled as a random factor due to multiple measurements within subjects; the same reasoning applies to EEG channels (channel-id) within regions since neighboring EEG channels carry mutual information.

2.7. Time-domain analysis of identified effects in single subjects

In order to investigate the temporal relationship between the onset of DBS and the incurred changes in cortical activity, the complete recording sessions were filtered in accordance to spatio-spectral regions of interest. The complete recording sessions were windowed (1s window size; 10 ms step width) and each segment was transformed into the frequency domain using Welch's method (Hanning window, 0.5 s fast Fourier transform window size, and 50% overlap). Afterwards, the amount of relative theta-activity was calculated by dividing the sum of the theta-band bins (4–6 Hz) by the sum of all frequency bins (2–45 Hz). In order to reduce temporal smearing, post-process smoothing was limited to a rolling mean filter with a window width of 1000 samples.

3. Results

3.1. Effects of stimulation and responsiveness on cortical activity

Stimulation induced a significant desynchronization in the temporal lobe channels area in responders only. The mixed-model two-way ANOVA revealed significant main effects of response-type on cortical activity in the theta-band (i.e. there were significant differences in cortical activity between responders and non-responders, regardless of whether stimulation was ON or OFF). The theta-band power was overall lower (desynchronized; negative gradient) in responders compared to non-responders, without spatial specificity. There were no significant effects of stimulation when responders and non-responders were pooled together. Furthermore, the two-way ANOVA analyses also revealed significant interaction effects between stimulation-condition and response-type, which were significant in the alpha-band after multiple comparison correction (meaning that changes of cortical activity were dependent on both stimulation-condition and response-type simultaneously.

This observation implicates that either the effect of stimulation on cortical activity was dependent on whether the individual was a responder and non-responder, or that the cortical differences between responders and non-responders were dependent upon whether stimulation was ON or OFF. In order to discern which of these phenomena was true, and to investigate these effects in greater detail, subsequent one-way ANOVA analyses were performed for the theta and alpha frequency bands (frequency bands of interest based on the two-way ANOVA results). The subsequent one-way ANOVA analyses were done for 2 Hz wide sub-bands of the theta and alpha frequency bands.

With regards to the effects of stimulation-condition, the one-way ANOVA analyses did not reveal significant main effects of stimulation in the non-responders' sub-group (i.e. cortical activity did not change when stimulation was changed from OFF to ON in non-responders; Fig. 2A). However, the one-way ANOVA analyses did reveal significant main effects of stimulation-condition in responders, which were present without spatial specificity in the theta and alpha bands (Fig. 2A). The negative gradient is suggestive of a desynchronization of activity in these frequency bands (i.e. cortical theta and alpha-band activity were desynchronized when stimulation was changed from OFF to ON in responders). Taken together, these analyses reveal ANT-DBS desynchronized theta and alpha-band activity in responders, but had no effect on cortical activity in non-responders; these differences between responders and non-responders were the reason for the interaction effect in the previous two-way ANOVA analyses.

With regard to the effects of response-type, the one-way ANOVA analyses revealed significant main effects of response-type both when stimulation was ON and when it was OFF, localized to the theta-frequency band (Fig. 2B). Taken together, these analyses suggest that there was an overall lower level the theta-band activity in responders compared to non-responders both when stimulation was ON and OFF; which validates the significant main effect of response-type in the previous two-way ANOVA analyses. Detailed statistical figures for one-way ANOVAs are available in Fig. 2.

3.2. Stimulation and seizure reduction

Seizure reduction correlated with DBS induced activity reduction in the theta-band only. As were interested in determining whether the stimulation-induced desynchronization of cortical activity might be associated with seizure reduction. For this purpose, we correlated the strongest desynchronization of cortical activity in seizure onset zones with seizure reduction. Using the previous one-way ANOVA analyses, it was quantitatively determined that the 4–6 Hz and 10–12 Hz sub-bands were the theta and alpha sub-bands most strongly modulated in the temporal lobe channels. Same applied to the 5–7 Hz and 10–12 Hz frequency sub-bands in the rest of the cortex. To select the respective sub-bands, the EEG channels with the greatest power change were selected and then pooled into a) the temporal area channels only and b) all channels (i.e. widespread). Theta is henceforth defined as 4–6 Hz for temporal lobe channels. A significant correlation was found between seizure reduction and reduction of 4–6 Hz theta-band activity for the temporal lobe channels only ($r = 0.82$; $p = 0.023$; Fig. 3).

3.3. Theta activity differences in temporal lobe channels

Group and single subject level evaluations revealed significantly greater levels of theta band activity in non-responders (during stimulation ON and OFF) compared to both responders and healthy controls (i.e. temporal lobe channel theta activity was greater for non-responders compared to responders and healthy controls). Temporal lobe theta activity did not differ between responders and healthy controls. Furthermore, the difference in temporal lobe channels theta band activity between stimulation ON and stimulation OFF was significant for responders, whereas this difference was not significant for non-responders. Detailed statistical figures are available in Fig. 4 for the group level and for the individual subject level in Fig. 5.

Subsequently, the stimulation-induced effects (ON vs. OFF) on temporal lobe channels theta activity were also investigated at the single-subject level. These analyses revealed that indeed, temporal lobe channels theta activity was in general greater for non-responders compared to responders and healthy controls, and that temporal lobe channels theta activity was consistently reduced during stimulation ON in responders, but not in non-responders.

3.4. Time-domain analysis of identified effects in single subjects

We furthermore investigated whether the reduction of temporal lobe channel theta power coincided with the period of DBS activation. In

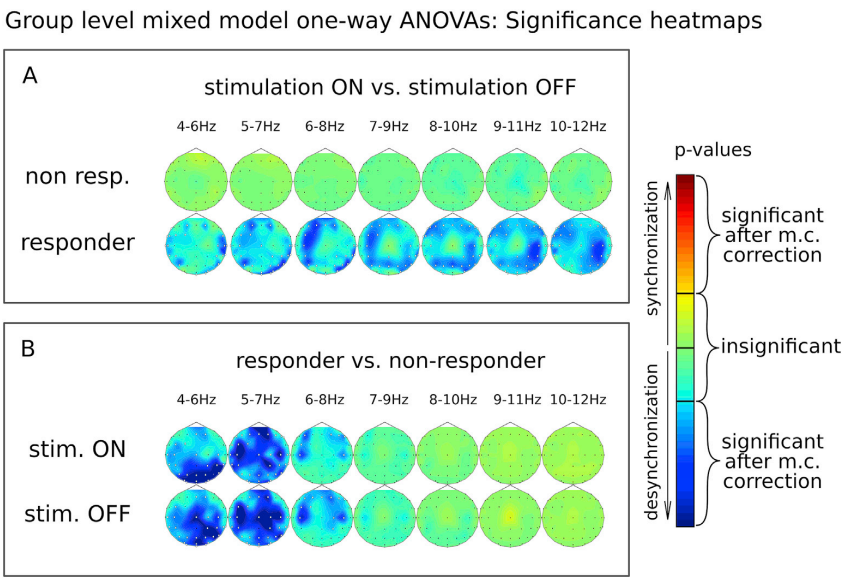

Fig. 2. Mixed model one-way ANOVA results with narrower frequency bands. In order to interrogate the reason for the significant interaction effects from the previous two-way ANOVA analyses, subsequent one-way ANOVA analyses were performed. These analyses were done for 2 Hz wide sub-bands of the theta and alpha frequency bands. (A) Significant main effects of stimulation-condition were found for the responder sub-group only, and were present in both the theta and alpha frequency bands. The negative gradient is suggestive of a desynchronization of activity in these frequency bands (i.e. cortical theta and alpha-band activity were desynchronized when stimulation was changed from OFF to ON in responders). Significant main effects of stimulation-condition in the non-responder sub-group were not found (i.e. cortical activity did not change when stimulation was changed from OFF to ON in the non-responders). Taken together, these analyses reveal ANT-DBS desynchronized theta and alpha-band activity in responders, but had no effect on cortical activity in non-responders; these differential effects were the reason for the interaction effect in the previous two-way ANOVA analyses. (B) Significant main effects of response-type were found both when stimulation was ON and when it was OFF, localized to the theta-frequency band. Taken together, these analyses suggest that there was an overall lower level the theta-band activity in responders compared to non-responders; which validates the significant main effect of response-type in the previous two-way ANOVA analyses. Note: EEG channels are marked by black dots, white dots represent channels which were significant ($p < 0.05$) after multiple comparison corrections.

Fig. 6, stimulation ramping is highlighted in yellow, whereas fully activated DBS is highlighted in green. These analyses were done at the single-subject level for all patients, and revealed a rapid theta power decrease with DBS activation in responders. Non-responders and responders showed temporary and lasting reduction of ANT-DBS related theta power, respectively. The effects of ANT-DBS on theta activity were always present in the two patients with bitemporal lobe epilepsy, but were less pronounced in the single patient with left temporal lobe epilepsy.

3.5. Classification of responders and non-responders

In this study, we grouped patients based on a maximum likelihood approach into responders and non-responders (see methods section). However, when reanalyzing the stimulation-induced theta band reduction and considering the patient with a 42% seizure reduction as a non-responder instead of a responder (following the community standards of a 50% threshold), the results remained unchanged. To investigate the robustness of our findings independent of these grouping issues (see supplementary fig. 3). Importantly, neither correlations nor individual subject level theta-band findings were affected by the classification approach, since the seizure reduction rate was used as a continuous metric.

3.6. Electrode locations of responders and non-responders

The position of the active DBS-lead contacts was compared between the responder and non-responder groups. Relative positions were calculated as the 1) lateral distance from the midline, 2) distance superior to the AC/DC line and 3) distance posterior to the AC normalized with respect to the AC/PC length. Hemispheres were averaged within patients prior to averaging patients. No systematic difference was found between the two groups ($p < 0.42$ – lateral; $p < 0.98$ – superior; $p < 0.83$ – posterior).

4. Discussion

This study revealed marked differences in cortical activity between ANT-DBS responders and non-responders. Non-responders presented with greater overall oscillatory power in the theta frequency band compared to responders and healthy controls. Furthermore, cortical activity depended both on stimulation-condition (ON/OFF) and response-type (responders/non-responders). Specifically, there was a significant ANT-DBS effect in the responder (but not the non-responder) sub-group with a desynchronization of cortical theta and alpha activity during StimOn (but not StimOff). Taken together, these findings suggest that non-responders had higher overall levels of theta-band activity compared to responders and healthy controls. However, non-responders and responders showed a different response to ANT-DBS with temporary and lasting reduction of theta power, respectively.

Due to the anatomical variability of DBS targets in stereotactic space from subject to subject, and the importance of lead positioning with respect to clinical outcomes, we analyzed the electrode lead localization on the basis of postoperative imaging. This analysis revealed, that the

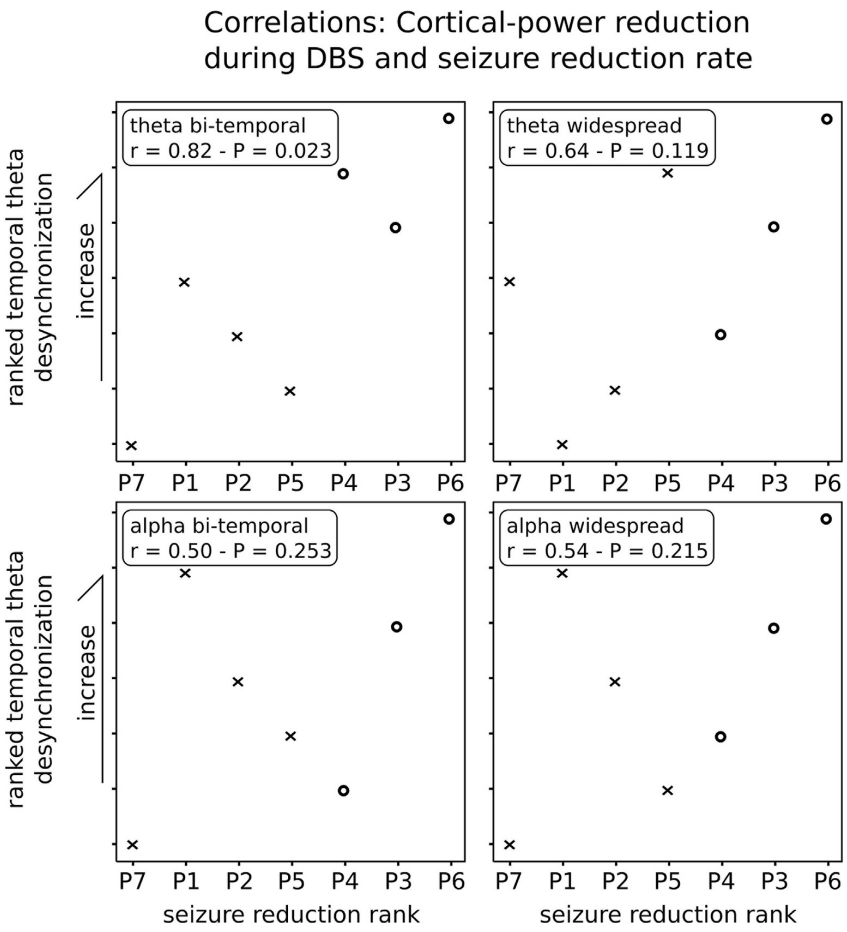

Fig. 3. Stimulation and seizure reduction. Spearman correlations were performed in order to compare seizure reduction with desynchronization of theta and alpha band activity in particular regions of interest (the seizure onset zones of the patient population; temporal lobe channels and multifocal/ widespread). A significant correlation was found between seizure reduction and reduction of 4–6 Hz theta-band activity for the temporal lobe channels ($r = 0.82$; $p = 0.023$), whereas the three other correlations were not significant. Responders correspond to o's whereas non-responder correspond to x's.

active contact locations were not significantly different between responders and non-responders in our study. This underlines the necessity to identify physiological biomarkers for refined targeting during DBS surgery.

Along these lines, when investigating regions of interest of modulated oscillatory activity, it was found that ANT-DBS, when effective in reducing seizure counts, was linked to a reduction of cortical theta-band activity in the temporal lobe channels. Furthermore, the level of theta desynchronization was found to be correlated with seizure reduction. At both the group level and the single-subject level, cortical theta-activity was significantly reduced in all responders, and only in one non-responder. Notably, this non-responder showed a larger seizure reduction rate (25%) compared to the other non-responders in this study (8%, 5.5%, and −3.5%). Finally, time-domain analysis revealed that the stimulation-induced theta desynchronization effects were rapid, immediate, sustained for the entirety of the stimulation period, but reverted equally fast following stimulation cessation, which matches previous findings in subcortical brain areas (Stypulkowski et al., 2013; Yu et al., 2018).

Early studies have described epilepsy as a disorder of hypersynchonization, at least during periods of epileptiform activity (Penfield and Jasper, 1954). Ictogenic regions are expected to show increased correlated activity with other brain areas, which is interpreted as a form of hypersynchonization (Kramer and Cash, 2012). Recent evidence suggests abnormal connectivity and network topology, especially for the delta and theta bands, in patients with focal epilepsy (Horstmann et al., 2010; Wilke et al., 2010). Previous studies have shown that patients with various forms of epilepsy had increased cortical theta-band activity compared to healthy controls (Adebimpe et al., 2015; Miyauchi et al., 1991; Quraan et al., 2013). This was corroborated by our findings when comparing non-responders to healthy controls, but not when comparing responders to healthy controls. Moreover, a recent study in humans not only demonstrated ictal recruitment of the ANT in focal epilepsy, but also found that the emergence of the theta rhythm maximally discriminated the endogenous ictal state from other interictal states (Toth et al., 2019). In humans, high frequency stimulation of the ANT has been shown to reduce broadband (Yu et al., 2018) and theta-specific (Zumsteg et al., 2006) activity in the hippocampus/mesial temporal lobe, and has been suggested to work by desynchronizing epileptic networks. As such, when efficacious, the cycling stimulation protocol of ANT-DBS may work by periodically suppressing or resetting epileptic networks and limiting the buildup of hypersynchronous activity.

A transcranial magnetic stimulation study demonstrated that continuous ANT-DBS led to increased short-interval intracortical inhibition, suggesting that ANT-DBS might drive cortical inhibitory circuits (Molnar et al., 2006). Here, we not only found a potential pathophysiological role of cortical theta-band activity (albeit phenotype-specific, i.e. in temporal lobe epilepsy), but also found that desynchronization of temporal theta-band activity may be therapeutically relevant. To the best of our knowledge, this is the first study which has shown a physiological

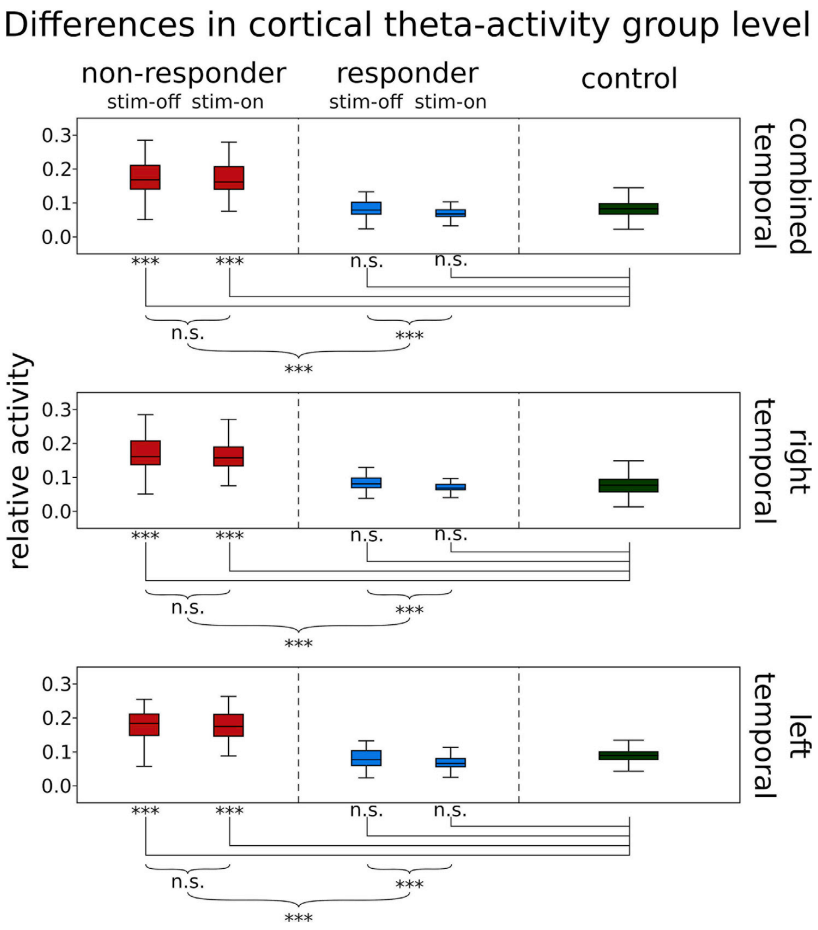

Fig. 4. Group level differences in temporal theta activity between non-responders, responders, and healthy control subjects. These evaluations revealed significantly greater levels of theta-band activity in non-responders (during stimulation ON and OFF) compared to both responders and healthy controls (i.e. temporal theta activity was greater for non-responders compared to responders and healthy controls). Temporal lobe channels theta activity did not differ between responders and healthy controls. Furthermore, the difference in temporal lobe channels theta band activity between stimulation ON and stimulation OFF was significant for responders, whereas this difference was not significant for non-responders. Notes: Each box portrays the lower and upper quartiles and median; whiskers end at 1.5-times the values of the interquartile range before/after the first/third quartile. ***($p < 0.001$).

correlative link between ANT-DBS induced changes of cortical activity and seizure reduction rates, while highlighting differences in ANT-DBS effects between responders and non-responders. These findings not only shed light on different nodes of pathological network activity, but also demonstrate the feasibility of non-invasively interrogating them in relation to the effectiveness of ANT-DBS.

Studies in rats and non-human primates have shown that the ANT has numerous projections, among which also various structures of the limbic system, including the hippocampus (Shibata, 1993; Shibata and Kato, 1993; van Groen et al., 1999; van Groen and Wyss, 1990a, 1990b). The hippocampal formation projects via the subiculum and entorhinal cortex to the perirhinal cortex, and from there to temporal cortical areas (Amaral and Cowan, 1980; Wyss et al., 1979). As such, the responder-specific desynchronization of temporal theta-activity reported here may be the result of a propagated suppression of activity via this pathway. While both responders and non-responders would be expected to have structural/functional connectivity between the ANT and temporal lobe areas, the possible influence of the ANT on ictogenic networks may vary between patients with temporal- and extratemporal epilepsies. Or, it could be that the increased levels of theta hypersynchronization in non-responders as compared to responders were less amenable by ANT-DBS. However, it could also be that variability in lead placement may have differentially affected these networks between the responder and non-responder sub-groups.

4.1. Clinical implications

Converging evidence (Fisher et al., 2010; Hodaie et al., 2002; Kerrigan et al., 2004) supports the hypothesis (Middlebrooks et al., 2018; Osorio et al., 2007) that ANT-DBS may have a more efficacious response in patients with temporal lobe epilepsy, compared to patients with multifocal or extratemporal epilepsy. This was reflected in our findings as well as during the double-blinded phase of the SANTE study where significant effects were found for temporal lobe epilepsy patients only. Therefore, patients with temporal lobe epilepsy may be preferred candidates for ANT-DBS procedures. Furthermore, the presented study not only discerned a physiological hallmark of clinically effective stimulation (i.e. desynchronization of theta-band activity), but also found that cortical signatures differed between patients with temporal lobe epilepsy (responder) and patients with extratemporal or multifocal epilepsy (non-responder) in that the latter presented with greater theta synchronization at rest (and during stimulation). This finding may represent a potential predictor of responsiveness (i.e. a potential patient selection criterion). One might have expected that the theta activity of responders during the OFF condition would be different from controls, which was not the case. This might be related to the fact that we most likely recorded from lateral temporal and not mesial temporal structures with scalp EEG electrodes.

However, since the seizure onset zone (temporal vs. extratemporal/multifocal) and level of theta synchronization were coupled in this study,

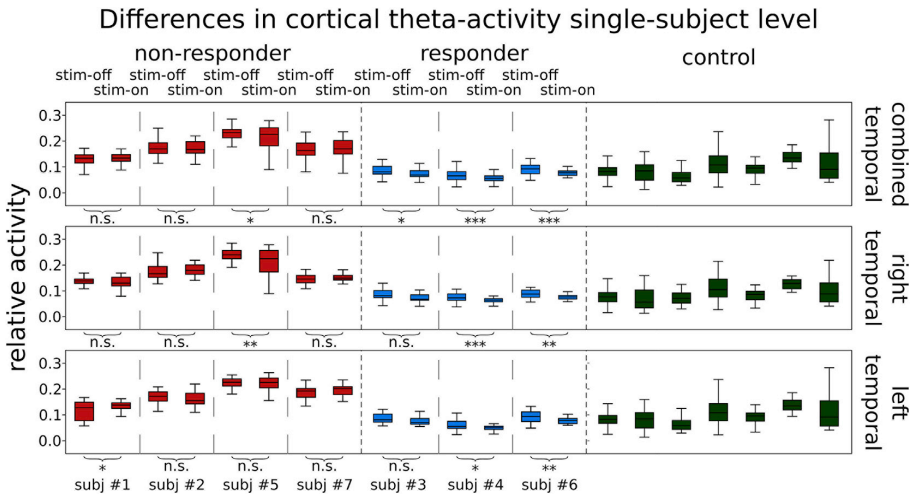

Fig. 5. Group level differences in temporal theta activity between non-responders, responders, and healthy controls. In line with the group results, the individual level results confirm the ANT-DBS modulation of theta-activity in responders. The ANT-DBS effect was somewhat weaker in subject #3 who presented with unilateral temporal lobe seizures, whereas subjects #4 and #6 presented with bi-temporal lobe seizures. Notably, the non-responder (subject #5) who showed an ANT-DBS effect as well had a relevantly higher seizure reduction (i.e., 25%) than the other non-responders. Notes: Each box portrays the lower and upper quartiles and median; whiskers end at 1.5-times the values of the interquartile range before/after the first/third quartile. ***($p < 0.001$).

further data are required to determine whether a predictive factor of ANT-DBS responsiveness may have been dependent upon (i) seizure onset zone/epilepsy type, (ii) the level of theta synchronization, or (iii) indeed a combination of these two phenomena.

Moreover, the findings of this study may increase the efficiency of stimulation programming. Currently, an unambiguous definition of the most optimal stimulation has not been defined (Kulju et al., 2018; Lehtimäki et al., 2016; Möttönen et al., 2015). Evaluation of clinical efficacy is done over the course of several months and the use of a seizure diary. This time-consuming process limits the evaluation of a variety of stimulation paradigms, and generally only a few are actually evaluated in each patient. While other studies have demonstrated that ANT-DBS may be linked to reductions of subcortical (hippocampal) activity (Stypulkowski et al., 2013; Yu et al., 2018; Zumsteg et al., 2006), we have shown that efficacious stimulation was linked to suppression of cortical (temporal lobe channels) activity, which could be measured non-invasively. Thus, this physiological hallmark (i.e. ANT-DBS induced reductions of cortical theta-band activity) may be used as a potential candidate biomarker for selection of clinically effective stimulation parameters/contacts. As the theta suppressing effects were immediate, only few seconds may be required when evaluating candidate stimulation paradigms based on functional physiological read-outs (temporal lobe channels desynchronization), compared to months when using the established approach of using seizure diaries. Furthermore, considering that the next generation of DBS-leads may have increased numbers of stimulation contacts, development of a simple to use and quickly assessable physiological biomarkers for evaluating treatment response is important for optimizing clinical efficacy. For stimulation programming, we propose an assessment to initially scan the available contacts using the proposed candidate biomarker, and subsequent evaluation using the traditional long-term assessment of applying the seizure diary approach.

This candidate biomarker may not only represent a practical method of selecting optimal stimulation parameters/contacts for patients who have already been implanted, but may also serve as an intraoperative physiological hallmark for lead implantations. Currently, robust structural radiological methods to specifically delineate the ANT from other thalamic sub-structures have not been defined, nor have functional intraoperative physiological hallmarks (Liu et al., 2012; Stypulkowski et al., 2014; Van Hoesen, 1995). This may lead to misplaced electrode leads (Lehtimäki et al., 2018). While it is common to guide the implantation of the DBS-leads via imaging procedures only (Cukiert and Lehtimäki, 2017), we propose to investigate the theta-modulating effects of ANT-DBS as a potential biomarker for verification of the implantation site in order to improve lead positioning. This can be done intraoperatively through the use of scalp electrodes on the temporal lobe areas, and monitoring changes of cortical theta-activity during stimulation, which may be indicative of a clinically efficacious lead placement.

4.2. Limitations

We acknowledge that this study was limited by a low number of patients; however, phenotype-specific differences (i.e. temporal vs. extratemporal or multifocal seizure onset zones) in response rate were also reported in the blinded phase of the SANTE trial. Moreover, in the eyes-closed waking condition, the patients might fall asleep. Even though we took measures to avoid this and do not have any indication that this happened in our study, future work might consider investigating these patients in the eyes-open condition.

Due to the explorative nature of this study, we enforced strict steps to reduce the family-wise error rate. We initially investigated the effects of ANT-DBS in epilepsy patients without limiting our investigation to areas which have previously been identified as regions of interest or frequency bands of interest. This was done in order not to bias this study towards previously established findings, and to give room to the discovery of new effects. However, in order to limit the number of hypotheses (and thereby reduce the family-wise error rate), we reduced the number of frequency bands of interest in a step-wise manner. During the initial ANOVA analyses (which were corrected for multiple comparisons), the theta and the alpha bands were selected as frequency bands of interest due to significant main and interactions effects. The regions of interest were selected based on the seizure onset zones of the patient population. As only the temporal lobe channel areas in the theta-band correlated with seizure reduction, other regions and frequency bands of interest were discarded from further analyses in order to limit the number of hypotheses. Moreover, analyses were performed at the single-subject level in order to ensure consistency within sub-groups, and to ensure that no individual

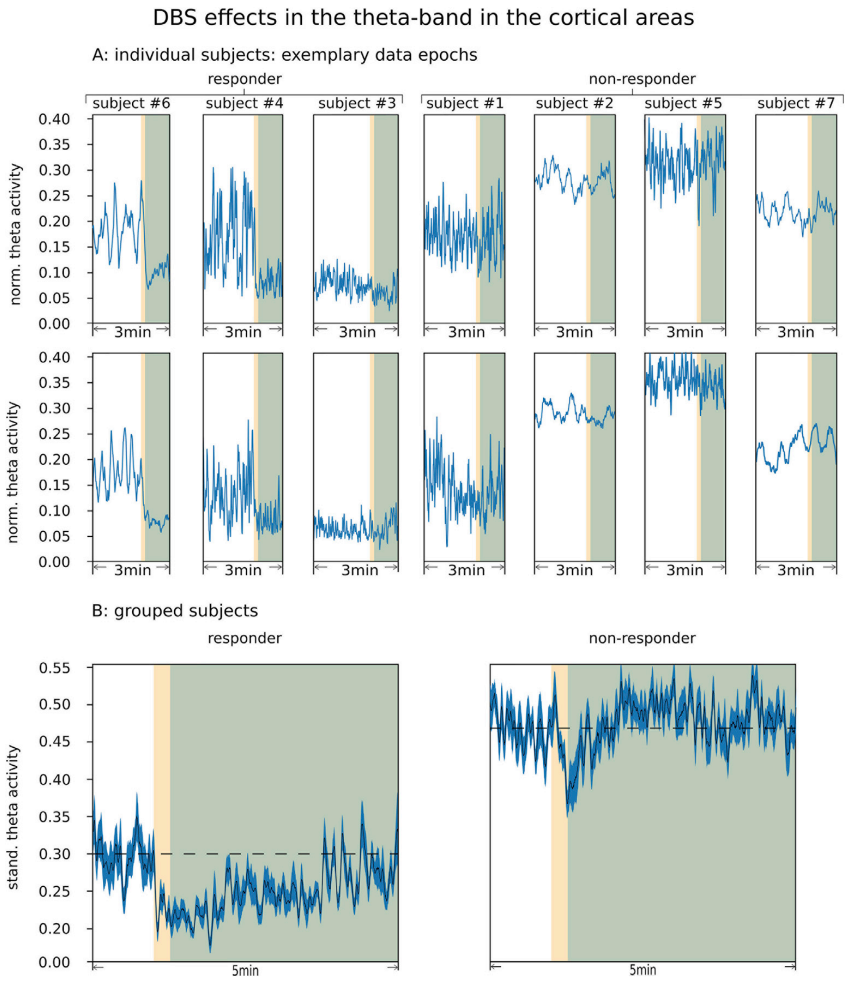

Fig. 6. Time-domain analysis of theta desynchronization effects. Individual epochs extracted from the time domain theta-band filtered signal (averaged for temporal lobe channels) of all patients are portrayed (A). Standardized group data averaged across all trials for all subjects confirms the effect that was observed in individual subjects (B). Variance is indicated by the blue shaded region. This figure demonstrates that stimulation activation coincided with rapid reduction in theta-power in responder. Non-responders did not show a sustained ANT-DBS related reduction in cortical theta-activity. Furthermore, responders had an overall lower level of theta activity. Note: Stimulation ramping is highlighted yellow, fully activated DBS is highlighted green.

patient disproportionately skewed the group results. While, to the best of our knowledge, this is the first study to assess cortical physiological hallmarks of ANT-DBS and clinical responsiveness, further studies regarding the stimulation-induced changes of neurophysiological activity are warranted in order to better understand the mechanisms of ANT-DBS, aid in patient selection, and optimize treatment success.

Study funding

M.S. was supported by the Graduate Training Centre of Neuroscience & International Max Planck Research School, Graduate School of Neural Information Processing, Tuebingen, Germany. Y.G.W. was supported by the German Research Foundation [WE4896/3-1; not related to this work]. S.R. was supported by a research grant (not related to this work) from Medtronic. A.G. was supported by research grants (not related to this work) from Medtronic, Boston Scientific, Abbott, the Baden-Wuerttemberg Foundation and the German Federal Ministry of Education and Research.

Declaration of competing interest

None.

CRediT authorship contribution statement

Maximillian Scherer: Conceptualization, Investigation, Data curation, Formal analysis, Validation, Software, Writing - original draft, Writing - review & editing. **Luka Milosevic:** Conceptualization, Writing - original draft, Writing - review & editing, Project administration, Supervision. **Robert Guggenberger:** Data curation, Supervision, Writing - review & editing. **Volker Maus:** Investigation, Project administration, Writing - review & editing. **Georgios Naros:** Investigation, Writing - review & editing. **Florian Grimm:** Investigation, Writing - review & editing. **Iancu Bucurenciu:** Investigation, Writing - review & editing. **Bernhard J. Steinhoff:** Supervision, Writing - review & editing. **Yvonne G. Weber:** Investigation, Writing - review & editing. **Holger Lerche:** Supervision, Writing - review & editing. **Daniel Weiss:** Supervision, Writing - review & editing. **Sabine Rona:** Investigation, Project administration, Writing - review & editing. **Alireza Gharabaghi:** Conceptualization, Investigation, Supervision, Writing - original draft, Writing - review & editing, Project administration, Resources, Funding acquisition.

Acknowledgements

V.M.'s current affiliation is the Institute of Neuroradiology, University Hospital Göttingen. The authors declare no competing financial interests.

Data and code will be shared upon reasonable request.

Appendix A. Supplementary data

Supplementary data to this article can be found online at https://doi.org/10.1016/j.neuroimage.2020.116967.

References

Adebimpe, A., Aarabi, A., Bourel-Ponchel, E., Mahmoudzadeh, M., Wallois, F., 2015. EEG resting state analysis of cortical sources in patients with benign epilepsy with centrotemporal spikes. NeuroImage Clin. 9, 275–282. https://doi.org/10.1016/j.nicl.2015.08.014.

Amaral, D.G., Cowan, W.M., 1980. Subcortical afferents to the hippocampal formation in the monkey. J. Comp. Neurol. 189, 573–591. https://doi.org/10.1002/cne.901890402.

Child, N.D., Benarroch, E.E., 2013. Anterior nucleus of the thalamus: functional organization and clinical implications. Neurology 81, 1869–1876. https://doi.org/10.1212/01.wnl.0000436078.95856.56.

Cukiert, A., Lehtimäki, K., 2017. Deep brain stimulation targeting in refractory epilepsy. Epilepsia 58, 80–84. https://doi.org/10.1111/epi.13686.

Fisher, R., Salanova, V., Witt, T., Worth, R., Henry, T., Gross, R., Oommen, K., Osorio, I., Nazzaro, J., Labar, D., Kaplitt, M., Sperling, M., Sandok, E., Neal, J., Handforth, A., Stern, J., DeSalles, A., Chung, S., Shetter, A., Bergen, D., Bakay, R., Henderson, J., French, J., Baltuch, G., Rosenfeld, W., Youkilis, A., Marks, W., Garcia, P., Barbaro, N., Fountain, N., Bazil, C., Goodman, R., McKhann, G., Babu Krishnamurthy, K., Papavassiliou, S., Epstein, C., Pollard, J., Tonder, L., Grebin, J., Coffey, R., Graves, N., the SANTE Study Group, 2010. Electrical stimulation of the anterior nucleus of thalamus for treatment of refractory epilepsy: deep Brain Stimulation of Anterior Thalamus for Epilepsy. Epilepsia 51, 899–908. https://doi.org/10.1111/j.1528-1167.2010.02536.x.

Fisher, R.S., Velasco, A.L., 2014. Electrical brain stimulation for epilepsy. Nat. Rev. Neurol. 10, 261–270. https://doi.org/10.1038/nrneurol.2014.59.

Halpern, C.H., Samadani, U., Litt, B., Jaggi, J.L., Baltuch, G.H., 2008. Deep brain stimulation for epilepsy. Neurotherapeutics 5, 59–67. https://doi.org/10.1016/j.nurt.2007.10.065.

Hamani, C., Ewerton, F.I.S., Bonilha, S.M., Ballester, G., Mello, L.E.A.M., Lozano, A.M., 2004. Bilateral anterior thalamic nucleus lesions and high-frequency stimulation are protective against pilocarpine-induced seizures and status epilepticus. Neurosurgery 54, 191–197. https://doi.org/10.1227/01.NEU.0000097552.31763.AE.

Hodaie, M., Wennberg, R.A., Dostrovsky, J.O., Lozano, A.M., 2002. Chronic anterior thalamus stimulation for intractable epilepsy. Epilepsia 43, 603–608. https://doi.org/10.1046/j.1528-1157.2002.26001.x.

Horstmann, M.-T., Bialonski, S., Noennig, N., Mai, H., Prusseit, J., Wellmer, J., Hinrichs, H., Lehnertz, K., 2010. State dependent properties of epileptic brain networks: comparative graph–theoretical analyses of simultaneously recorded EEG and MEG. Clin. Neurophysiol. 121, 172–185. https://doi.org/10.1016/j.clinph.2009.10.013.

Kerrigan, J.F., Litt, B., Fisher, R.S., Cranstoun, S., French, J.A., Blum, D.E., Dichter, M., Shetter, A., Baltuch, G., Jaggi, J., Krone, S., Brodie, M., Rise, M., Graves, N., 2004. Electrical stimulation of the anterior nucleus of the thalamus for the treatment of intractable epilepsy. Epilepsia 45, 346–354. https://doi.org/10.1111/j.0013-9580.2004.01304.x.

Kramer, M.A., Cash, S.S., 2012. Epilepsy as a disorder of cortical network organization. Neurosci. Rev. J. Bringing Neurobiol. Neurol. Psychiatry 18, 360–372. https://doi.org/10.1177/1073858411422754.

Kulju, T., Haapasalo, J., Lehtimäki, K., Rainesalo, S., Peltola, J., 2018. Similarities between the responses to ANT-DBS and prior VNS in refractory epilepsy. Brain Behav. 8, e00983 https://doi.org/10.1002/brb3.983.

Kwan, P., Brodie, M.J., 2000. Early identification of refractory epilepsy. N. Engl. J. Med. 342, 314–319. https://doi.org/10.1056/NEJM200002033420503.

Lane, M.A., Kahlenberg, C.A., Li, Z., Kulandaival, K., Secore, K.L., Thadani, V.M., Bujarski, K.A., Kobylarz, E.J., Roberts, D.W., Tosteson, T.D., Jobst, B.C., 2017. The implantation effect: delay in seizure occurrence with implantation of intracranial electrodes. Acta Neurol. Scand. 135, 115–121. https://doi.org/10.1111/ane.12662.

Laxpati, N.G., Kasoff, W.S., Gross, R.E., 2014. Deep brain stimulation for the treatment of epilepsy: circuits, targets, and trials. Neurotherapeutics 11, 508–526. https://doi.org/10.1007/s13311-014-0279-9.

Lehtimäki, K., Gielen, F., Abouihia, A., Beth, G., Brionne, T.C., Coenen, V.A., Gonçalves Ferreira, A., Boon, P., Elger, C., Taylor, R.S., Ryvlin, P., Gil-Nagel, A., 2018. The surgical approach to the anterior nucleus of thalamus in patients with refractory epilepsy: experience from the international multicenter registry (MORE). Neurosurgery 84, 141–150. https://doi.org/10.1093/neuros/nyy023.

Lehtimäki, K., Möttönen, T., Järventausta, K., Katisko, J., Tähtinen, T., Haapasalo, J., Niskakangas, T., Kiekara, T., Öhman, J., Peltola, J., 2016. Outcome based definition of the anterior thalamic deep brain stimulation target in refractory epilepsy. Brain Stimulat. 9, 268–275. https://doi.org/10.1016/j.brs.2015.09.014.

Lim, S.-N., Lee, S.-T., Tsai, Y.-T., Chen, I.-A., Tu, P.-H., Chen, J.-L., Chang, H.-W., Su, Y.-C., Wu, T., 2007. Electrical stimulation of the anterior nucleus of the thalamus for intractable epilepsy: a long-term follow-up study. Epilepsia 48, 342–347. https://doi.org/10.1111/j.1528-1167.2006.00898.x.

Liu, H.G., Yang, A.C., Meng, D.W., Chen, N., Zhang, J.G., 2012. Stimulation of the anterior nucleus of the thalamus induces changes in amino acids in the hippocampi of epileptic rats. Brain Res. 1477, 37–44. https://doi.org/10.1016/j.brainres.2012.08.007.

Löscher, W., Klitgaard, H., Twyman, R.E., Schmidt, D., 2013. New avenues for anti-epileptic drug discovery and development. Nat. Rev. Drug Discov. 12, 757.

Middlebrooks, E.H., Grewal, S.S., Stead, M., Lundstrom, B.N., Worrell, G.A., Gompel, J.J.V., 2018. Differences in functional connectivity profiles as a predictor of response to anterior thalamic nucleus deep brain stimulation for epilepsy: a hypothesis for the mechanism of action and a potential biomarker for outcomes. Neurosurg. Focus FOC 45, E7.

Mirski, M.A., Rossell, L.A., Terry, J.B., Fisher, R.S., 1997. Anticonvulsant effect of anterior thalamic high frequency electrical stimulation in the rat. Epilepsy Res. 28, 89–100. https://doi.org/10.1016/S0920-1211(97)00034-X.

Miyauchi, T., Endo, K., Yamaguchi, T., Hagimoto, H., 1991. Computerized analysis of EEG background activity in epileptic patients. Epilepsia 32, 870–881. https://doi.org/10.1111/j.1528-1157.1991.tb05544.x.

Molnar, G.F., Sailer, A., Gunraj, C.A., Cunic, D.I., Wennberg, R.A., Lozano, A.M., Chen, R., 2006. Changes in motor cortex excitability with stimulation of anterior thalamus in epilepsy. Neurology 66, 566–571. https://doi.org/10.1212/01.wnl.0000198254.08581.6b.

Möttönen, T., Katisko, J., Haapasalo, J., Tähtinen, T., Kiekara, T., Kähärä, V., Peltola, J., Öhman, J., Lehtimäki, K., 2015. Defining the anterior nucleus of the thalamus (ANT) as a deep brain stimulation target in refractory epilepsy: delineation using 3 T MRI and intraoperative microelectrode recording. NeuroImage Clin. 7, 823–829. https://doi.org/10.1016/j.nicl.2015.03.001.

Osorio, I., Overman, J., Giftakis, J., Wilkinson, S.B., 2007. High frequency thalamic stimulation for inoperable mesial temporal epilepsy. Epilepsia 48, 1561–1571. https://doi.org/10.1111/j.1528-1167.2007.01044.x.

Penfield, W., Jasper, H., 1954. Epilepsy and the Functional Anatomy of the Human Brain, Epilepsy and the Functional Anatomy of the Human Brain. Little, Brown & Co., Oxford, England.

Quraan, M.A., McCormick, C., Cohn, M., Valiante, T.A., McAndrews, M.P., 2013. Altered resting state brain dynamics in temporal lobe epilepsy can Be observed in spectral power, functional connectivity and graph theory metrics. PloS One 8, e68609. https://doi.org/10.1371/journal.pone.0068609.

Salanova, V., Witt, T., Worth, R., Henry, T.R., Gross, R.E., Nazzaro, J.M., Labar, D., Sperling, M.R., Sharan, A., Sandok, E., Handforth, A., Stern, J.M., Chung, S., Henderson, J.M., French, J., Baltuch, G., Rosenfeld, W.E., Garcia, P., Barbaro, N.M., Fountain, N.B., Elias, W.J., Goodman, R.R., Pollard, J.R., Tröster, A.I., Irwin, C.P., Lambrecht, K., Graves, N., Fisher, R., 2015. Long-term efficacy and safety of thalamic stimulation for drug-resistant partial epilepsy. Neurology 84, 1017–1025. https://doi.org/10.1212/WNL.0000000000001334.

Shi, L., Yang, A.C., Li, J.J., Meng, D.W., Jiang, B., Zhang, J.G., 2015. Favorable modulation in neurotransmitters: effects of chronic anterior thalamic nuclei stimulation observed in epileptic monkeys. Exp. Neurol. 265, 94–101. https://doi.org/10.1016/j.expneurol.2015.01.003.

Shibata, H., 1993. Direct projections from the anterior thalamic nuclei to the retrohippocampal region in the rat. J. Comp. Neurol. 337, 431–445. https://doi.org/10.1002/cne.903370307.

Shibata, H., Kato, A., 1993. Topographic relationship between anteromedial thalamic nucleus neurons and their cortical terminal fields in the rat. Neurosci. Res. 17, 63–69. https://doi.org/10.1016/0168-0102(93)90030-T.

Sitnikov, A.R., Grigoryan, Y.A., Mishnyakova, L.P., 2018. Bilateral stereotactic lesions and chronic stimulation of the anterior thalamic nuclei for treatment of pharmacoresistant epilepsy. Surg. Neurol. Int. 9 https://doi.org/10.4103/sni.sni_25_18.

Son, B., Shon, Y.M., Kim, S., Choi, J., Kim, J., 2016. Relationship between postoperative EEG driving response and lead location in deep brain stimulation of the anterior nucleus of the thalamus for refractory epilepsy. Stereotact. Funct. Neurosurg. 94, 336–341. https://doi.org/10.1159/000449012.

Stypulkowski, P.H., Stanslaski, S.R., Denison, T.J., Giftakis, J.E., 2013. Chronic evaluation of a clinical system for deep brain stimulation and recording of neural network activity. Stereotact. Funct. Neurosurg. 91, 220–232. https://doi.org/10.1159/000345493.

Stypulkowski, P.H., Stanslaski, S.R., Jensen, R.M., Denison, T.J., Giftakis, J.E., 2014. Brain stimulation for epilepsy – local and remote modulation of network excitability. Brain Stimulat. 7, 350–358. https://doi.org/10.1016/j.brs.2014.02.002.

Sweeney-Reed, C.M., Lee, H., Rampp, S., Zaehle, T., Buentjen, L., Voges, J., Holtkamp, M., Hinrichs, H., Heinze, H.-J., Schmitt, F.C., 2016. Thalamic interictal epileptiform discharges in deep brain stimulated epilepsy patients. J. Neurol. 263, 2120–2126. https://doi.org/10.1007/s00415-016-8246-5.

Takebayashi, S., Hashizume, K., Tanaka, T., Hodozuka, A., 2007. The effect of electrical stimulation and lesioning of the anterior thalamic nucleus on kainic acid–induced focal cortical seizure status in rats. Epilepsia 48, 348–358. https://doi.org/10.1111/j.1528-1167.2006.00948.x.

Téllez-Zenteno, J.F., Hernández-Ronquillo, L., 2012. A review of the epidemiology of temporal lobe epilepsy. Epilepsy Res. Treat. https://doi.org/10.1155/2012/630853, 2012.

Toth, E., Chaitanya, G., Pizarro, D., Kumar, S.S., Ilyas, A., Romeo, A., Riley, K., Vlachos, I., David, O., Balasubramanian, K., Pati, S., 2019. Ictal Recruitment of Anterior Nucleus of Thalamus in Human Focal Epilepsy. bioRxiv, 788422. https://doi.org/10.1101/788422.

Vajda, F.J.E., Eadie, M.J., 2014. The clinical pharmacology of traditional antiepileptic drugs. Epileptic Disord. 16, 395–408. https://doi.org/10.1684/epd.2014.0704.

van Groen, T., Kadish, I., Wyss, J.M., 1999. Efferent connections of the anteromedial nucleus of the thalamus of the rat. Brain Res. Rev. 30, 1–26. https://doi.org/10.1016/S0165-0173(99)00006-5.

van Groen, T., Wyss, J.M., 1990a. The connections of presubiculum and parasubiculum in the rat. Brain Res. 518, 227–243. https://doi.org/10.1016/0006-8993(90)90976-I.

van Groen, T., Wyss, J.M., 1990b. The postsubicular cortex in the rat: characterization of the fourth region of the subicular cortex and its connections. Brain Res. 529, 165–177. https://doi.org/10.1016/0006-8993(90)90824-U.

Van Hoesen, G.W., 1995. Anatomy of the medial temporal lobe. In: Magn. Reson. Imaging, Workshop on Magnetic Resonance Techniques and Epilepsy Research, 13, pp. 1047–1055. https://doi.org/10.1016/0730-725X(95)02012-I.

Wilke, C., van Drongelen, W., Kohrman, M., He, B., 2010. Neocortical seizure foci localization by means of a directed transfer function method. Epilepsia 51, 564–572. https://doi.org/10.1111/j.1528-1167.2009.02329.x.

Wyckhuys, T., Geerts, P.J., Raedt, R., Vonck, K., Wadman, W., Boon, P., 2009. Deep brain stimulation for epilepsy: knowledge gained from experimental animal models. Acta Neurol. Belg. 109, 63–80.

Wyss, J.M., Swanson, L.W., Cowan, W.M., 1979. A study of subcortical afferents to the hippocampal formation in the rat. Neuroscience 4, 463–476. https://doi.org/10.1016/0306-4522(79)90124-6.

Yu, T., Wang, X., Li, Y., Zhang, G., Worrell, G., Chauvel, P., Ni, D., Qiao, L., Liu, C., Li, L., Ren, L., Wang, Y., 2018. High-frequency stimulation of anterior nucleus of thalamus desynchronizes epileptic network in humans. Brain 141, 2631–2643. https://doi.org/10.1093/brain/awy187.

Zumsteg, D., Lozano, A.M., Wennberg, R.A., 2006. Mesial temporal inhibition in a patient with deep brain stimulation of the anterior thalamus for epilepsy. Epilepsia 47, 1958–1962. https://doi.org/10.1111/j.1528-1167.2006.00824.x.

RESEARCH ARTICLE

Online Mapping With the Deep Brain Stimulation Lead: A Novel Targeting Tool in Parkinson's Disease

Luka Milosevic, PhD,[1] Maximilian Scherer, MSc,[1] Idil Cebi, MD,[1,2] Robert Guggenberger, PhD,[1] Kathrin Machetanz, MD,[1] Georgios Naros, MD,[1] Daniel Weiss, MD,[2] and Alireza Gharabaghi, MD[1*]

[1]*Division of Functional and Restorative Neurosurgery, Department of Neurosurgery, and Tübingen NeuroCampus, University of Tübingen, Tübingen, Germany*
[2]*Centre for Neurology, Department for Neurodegenerative Diseases, and Hertie Institute for Clinical Brain Research, University Tübingen, Tübingen, Germany*

ABSTRACT: **Background:** Beta-frequency oscillations (13–30 Hz) are a subthalamic hallmark in patients with Parkinson's disease, and there is increased interest in their utility as an intraoperative marker.
Objectives: The objectives of this study were to assess whether beta activity measured directly from macrocontacts of deep brain stimulation leads could be used (a) as an intraoperative electrophysiological approach for guiding lead placements and (b) for physiologically informed stimulation delivery.
Methods: Every millimeter along the surgical trajectory, local field-potential data were collected from each macrocontact, and power spectral densities were calculated and visualized (n = 39 patients). This was done for online intraoperative functional mapping and post hoc statistical analyses using 2 methods: generating distributions of spectral activity along surgical trajectories and direct delineation (presence versus lack) of beta peaks. In a subset of patients, this approach was corroborated by microelectrode recordings. Furthermore, the match rate between beta peaks at the final target position and the clinically determined best stimulation site were assessed.
Results: Subthalamic recording sites were delineated by both methods of reconstructing functional topographies of spectral activity along surgical trajectories at the group level ($P < 0.0001$). Beta peaks were detected when any portion of the 1.5 mm macrocontact was within the microelectrode-defined subthalamic border. The highest beta peak at the final implantation site corresponded to the site of active stimulation in 73.3% of hemispheres ($P < 0.0001$). In 93.3% of hemispheres, active stimulation corresponded to the first-highest or second-highest beta peak.
Conclusions: Online measures of beta activity with the deep brain stimulation macroelectrode can be used to inform surgical lead placement and contribute to optimization of stimulation programming procedures.

Key Words: beta oscillations; deep brain stimulation; Parkinson's disease; subthalamic nucleus

Deep brain stimulation (DBS) of the subthalamic nucleus (STN) is a well-established and efficacious therapy for the management of the motor symptoms of Parkinson's disease.[1,2] Many factors contribute to the clinical benefit of STN-DBS, including patient selection, stimulation programming, medication adjustments, and disease progression.[3,4] However, one important factor that may preclude other clinically controllable factors is the proper placement of the DBS lead.[5-7] A study that assessed lead placements in more than 28,000 cases (from 2 large North American databases) identified staggeringly high rates of revision and removal, between 15.2% and 34.0%, with up to 48.5% being attributed to improper targeting or lack of therapeutic efficacy.[8] In another study that investigated 41 consecutive patients who complained about suboptimal results from their DBS devices, 46% were identified as having misplaced leads.[9] Misplaced leads not only limit therapeutic efficacy but also can give

*Correspondence to: Dr. Alireza Gharabaghi, Division of Functional and Restorative Neurosurgery, Eberhard Karls University Tuebingen, Otfried-Mueller-Str.45, 72076 Tuebingen, Germany; E-mail: alireza.gharabaghi@uni-tuebingen.de

Relevant conflicts of interests/financial disclosures: Nothing to report.

Funding agency: This work was supported by grants from the University of Tübingen and Abbott.

Received: 12 December 2019; **Revised:** 16 April 2020; **Accepted:** 17 April 2020

Published online 18 May 2020 in Wiley Online Library (wileyonlinelibrary.com). DOI: 10.1002/mds.28093

rise to intolerable motor and/or nonmotor side effects.[10,11] As such, maximized efforts toward proper lead positioning prior to and during STN-DBS surgeries are warranted.

The traditional approach for determining the implantation site of the DBS macroelectrode is a multistep process. The position is tentatively determined based on a fusion of preoperative magnetic resonance imaging (MRI) and computed tomography images used in conjunction with stereotactic atlases to determine the stereotactic coordinates of the tentative target location.[12] The radiologically defined anatomical target is then corroborated by an intraoperative electrophysiological mapping procedure in combination with test stimulation prior to the final DBS macroelectrode implantation. Microelectrode recording (MER) of single unit activity is the gold-standard electrophysiological approach used for identification of the implantation target. This procedure involves delineation of anatomical structures along the surgical trajectory based on characteristic neuronal firing properties,[13] propensity for oscillatory behavior in the spike train,[14] and responsiveness to active or passive movements of the contralateral limbs.[15]

Although electrophysiological confirmation of the target location is considered a crucial and arguably necessary step,[5,16] some centers choose to forego MER mapping procedures in favor of reducing surgical time and increasing tolerance, due to a lack of dedicated personnel or resources, and/or the risk of hemorrhage. Image-guided-only surgeries have the additional benefit of being able to be performed while the patient is under general anesthesia, whereas in electrophysiology-driven approaches the patient is most often awake. The consequence of foregoing electrophysiological mapping, however, is an increased risk of suboptimal lead placement.[17-19] In this study, we sought to demonstrate a novel, automated method of electrophysiologically informed STN-DBS implantation that does not require the use of microelectrodes.

There is an increased interest in the use of oscillatory activity as a functional readout of STN entry and exit,[20] and previous studies of local field potential (LFP) activity derived from low-pass filtered MERs have demonstrated that the spatial extent of the STN could be characterized by increased oscillatory activity in the beta (13–30 Hz) frequency band[14,21-26] and/or high-frequency (>500 Hz) neuronal "noise."[27-29] The hypothesis of this study was that entry into and progression through the STN could be characterized by increased beta oscillatory activity measured from the DBS macroelectrodes directly. Dynamic (millimeter by millimeter) DBS macroelectrode recordings allow for the creation of a clinically relevant, LFP-based functional topology of the STN based on an established subthalamic neurophysiological marker. As such, the first objective of this study was to investigate whether DBS macrocontact recordings of beta-frequency activity could be used to intraoperatively guide lead placement. Moreover, because excessive beta-synchrony is suggested to be of pathophysiological relevance,[30] the second objective was to investigate whether this marker could be used for physiologically informed stimulation programming.

The benefits of an LFP-driven mapping approach are that the procedure can be automated and that the interpretation of the electrophysiological results may be more intuitive. Although such an approach may also be possible using MERs, the use of only the DBS macroelectrode may reduce the risk of hemorrhage and may also have time-savings and cost-saving benefits. A disadvantage of this approach compared with MER-guided procedures is that MERs can offer multiple simultaneous recording trajectories, thus increased information in the x and y planes. A disadvantage of electrophysiology guided approaches in general (LFP or MER) compared with image-guided only procedures is that the patient is usually awake; however, awake electrophysiology guided surgeries enable robust scrutiny of side effect thresholds during perioperative test stimulation and allow for the ability to make targeted implantations of stimulation contacts into different regions along the dorsal-ventral axis, such as placement of a stimulating contact into the zona incerta[31] or substantia nigra pars reticulata (SNr).[32] Thus, we suggest that the presented LFP-based DBS macroelectrode mapping procedure may be used as an alternative to or in conjunction with MER-guided procedures, with notable advantages compared with procedures that rely on image guidance only.

Methods

Patients and Lead Types

A total of 39 patients with Parkinson's disease were included in this study; 13 patients ($n_{hemispheres}$ = 26) received bilateral omnidirectional DBS leads (3389, Medtronic Inc, Minneapolis, MN) and 26 patients ($n_{hemispheres}$ = 52) received bilateral segmented DBS leads (6170, Abbott Laboratories, Lake Bluff, IL). The dorsal-most and ventral-most levels of the segmented leads contained omnidirectional contacts, whereas the 2 middle levels contained 3 segments each (frontal, medial, lateral). Each patient underwent DBS implantation after overnight withdrawal from antiparkinsonian medication, and there were no surgical complications to report. The study was approved by the ethics committee of the University Hospital Tübingen. Patient demographics are available in the Supplementary Material.

Surgical Procedures

In each patient, the tentative location of the STN was first determined radiologically.[33] The desired electrode depth in the STN region was determined by phenotype-specific clinical symptoms. In tremor-dominant patients, the tentative location of the dorsal-most contacts was at the upper border of the STN to stimulate the zona

incerta.[31] In patients with dominant gait and postural symptoms, the tentative location of the ventral-most contact was at the lower border of the STN to stimulate the SNr region.[32] Patients with segmented leads who did not fit either of the aforementioned criteria were implanted such that the levels with segmented contacts were within the STN to allow for the maximized potential of directional stimulation titration. Planning of the surgical trajectory/approach did not differ based on these distinct targets; rather, only the implantation depth was considered based on electrophysiological mapping.

In all 39 patients ($n_{hemispheres}$ = 78), recordings of the LFPs were obtained simultaneously from 4 to 8 monopolar macroelectrode recordings of omnidirectional or segmented lead contacts at every millimeter along the surgical trajectory. Measurements began with the bottom of ventral-most contact at 8 to 10 mm above the tentative target, and each subsequently dorsal contact level simultaneously recorded at +2 mm, +4 mm, and + 6 mm above, respectively.[34] At each depth, 30-second LFP recordings were simultaneously acquired from each contact, and the power spectral density (PSD) functions were obtained (details in section "Online LFP-based mapping: DBS macroelectrode recordings") and visualized online (as seen in Fig. 1). In 8 ($n_{hemispheres}$ = 16) of the 26 patients with segmented leads, MERs were performed (details in section "MER-based mapping: Microelectrode recordings") prior to DBS macroelectrode recordings.

Online LFP-Based Mapping: DBS Macroelectrode Recordings

Monopolar LFP recordings from each of the DBS contacts were sampled at ≥1200 Hz (hardware filter: 0.075 Hz–3.5 kHz) using an intraoperative recording device (NeuroOmega, Alpha Omega Engineering, Nof HaGalil, Israel). For online calculations of PSDs, 30-second LFP recordings were streamed from the NeuroOmega device (the streaming function is available via the NeuroOmega application programming interface) to an external personal computer. The LFP data were then transformed into the frequency domain using a multitaper approach (1 Hz frequency resolution) in Python 3.6 (Python Software Foundation, Fredericksburg, Virginia, USA; code available in the Supplementary Material). At each depth, PSDs were plotted and displayed immediately after calculation (as in Fig. 1). In cases where microelectrode recordings were not performed, the final position of the DBS lead was determined based on the presence and spatial extent of beta activity (with different depths used for the different desired functional outcomes, as explained previously). In the case of a complete lack of beta activity along the surgical trajectory, lead positioning relied on the results of perioperative test stimulation (eg, symptom reduction and adverse effects elicited by stimulation of nearby fiber pathways). If side effect thresholds were acceptable, the lead was positioned according to the radiologically defined target. If side effect thresholds were unacceptable, the DBS lead was repositioned and a second DBS LFP mapping trajectory was performed.

Post hoc statistical analyses of LFP data were also carried out using 2 separate methods (outlined in sections "Omnidirectional leads: Beta-peak depth spectrograms" and "Segmented leads: Beta-peak discretization"). One method involved reconstructing the distributions of spectral activity along surgical trajectories (done for patients with segmented leads), and the other method involved direct discretization (presence vs. lack) of beta activity (done for patients with segmented leads). The reason for using 2 separate data sets for the 2 different, although complementary, analyses was that this prevents overinflation of statistical power and prevents redundancy (ie, analyzing the same data set twice in 2 different ways). Moreover, the inclusion of patients with 2 different lead types was meant to demonstrate that the LFP-based DBS macroelectrode mapping approach could be applied regardless of electrode type/model.

Omnidirectional Leads: Beta-Peak Depth Spectrograms

For the 13 patients ($n_{hemispheres}$ = 26) with omnidirectional leads, 3-dimensional "depth spectrograms" (depth, frequency, power) were generated for each contact and for each hemisphere by normalizing beta-peak amplitudes with respect to the highest beta-peak amplitude recorded across all depths ($n_{hemispheres}$ = 21; we excluded 2 patients and a total of 5 hemispheres because of excessive noise or lack of beta peaks). This was done to generate a distribution of the spectral information across the surgical trajectory. This enables the visualization of the estimated spatial extent of the STN and demonstrates the reproducibility of measurements across successive contacts. A group depth spectrogram was generated by averaging the depth spectrograms of the ventral-most (or second-most ventral in case of strong artifacts) contact from each hemisphere ($n_{hemispheres}$ = 21) aligned at (1) the depth of the highest beta peak (y axis) and (2) the frequency of the highest beta peak (x axis). For each individual hemisphere, the mean squared error was calculated between the depth spectrogram of the ventral-most (or second-most ventral in case of strong artifacts) contact and a 3-dimensional Gaussian distribution, followed by a permutation test (100,000 permutations) to determine the significance of the mean squared error. This permutation test was also performed for the group depth spectrogram, except the peak voxel of each permutation was also centered. Postoperative imaging was performed with MRI and computed tomography in omnidirectional and segmented leads, respectively (further methodological details are available in Supplementary Material).[35] The MRI-

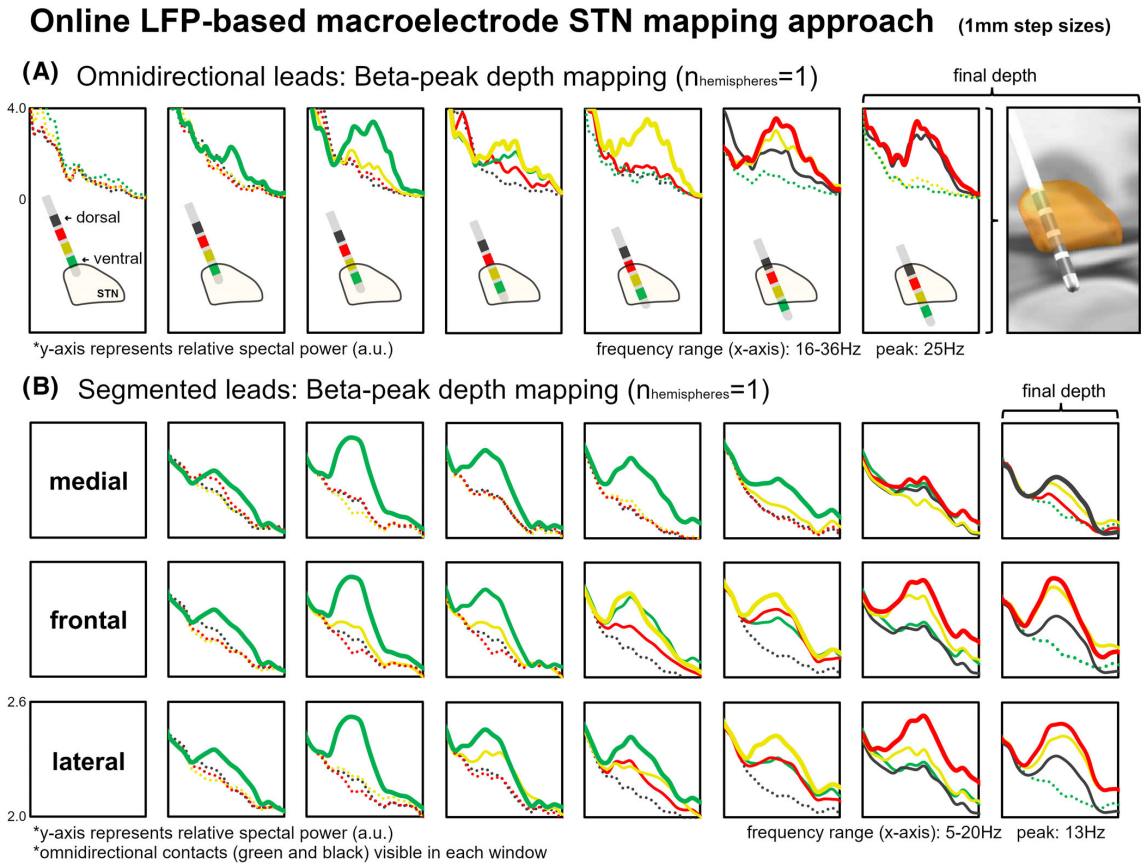

FIG. 1. Online local field potential–based macroelectrode STN mapping approach. Entry of each successive macrocontact into the STN was determined by sequential increases in beta power. (**A**) Sample recording trajectory from 1 hemisphere using an omnidirectional lead. Power spectral densitys at the final depth are corroborated by postoperative lead localization. (**B**) Sample recording trajectory from 1 hemisphere using a segmented lead. The power spectral density at the 2 omnidirectional contact levels (green ventral-most and black dorsal-most contacts) are displayed as duplicates in each of the directional windows (medial, frontal, lateral; which correspond to the 3 segmented contacts at the yellow second-most ventral and red second-most dorsal contact levels). STN, subthalamic nucleus. [Color figure can be viewed at wileyonlinelibrary.com]

based postoperative lead localizations could indeed corroborate intraoperative results (further examples are available in the Supplementary Material).

Segmented Leads: Beta-Peak Discretization

Of the 26 patients ($n_{hemispheres}$ = 52) with segmented leads, data from 8 patients ($n_{hemispheres}$ = 16) were used for corroboration with MER (discussed in the next section). For the other 18 patients ($n_{hemispheres}$ = 36), PSD measurements were used for LFP-based beta-peak discretization. For each hemisphere ($n_{hemispheres}$ = 27; we excluded 1 patient and a total of 9 hemispheres because of excessive noise or lack of beta peaks), the depth-normalized (subsequently subtracting 2 mm, 4 mm, and 6 mm from contacts dorsal to the ventral-most, respectively) beta-peak amplitudes at each contact were plotted along with the PSD amplitudes of nonpeaks (ie, background activity within the patient-specific beta-peak frequency range). To obtain a visualization of the group data, all individual hemispheres ($n_{hemispheres}$ = 27) were normalized (by dividing by the interdecile of the local nonpeak activity; data that come from the recording sites assumed to be outside, not within, the STN) and plotted together after alignment to the depth of the LFP-defined STN entry (ie, first depth at which a user-defined beta peak was detected by a deviation/increase with respect to "background" nonpeak activity). This method for analyzing data from segmented electrodes, which carries more information (ie, directional information), allows for the ability to discern both the depth and direction of the highest beta peak across the entire recording trajectory on a per-hemisphere basis in a condensed manner. For each hemisphere individually, as well as for the group data,

2-tailed *t* tests (unpaired) were used to differentiate the amplitudes of beta peaks from the amplitudes of nonpeak background activity.

MER-Based Mapping: Microelectrode Recordings

In 8 patients ($n_{hemispheres}$ = 16), LFP beta-peak mapping was corroborated by the MER of single-unit activity. Electrophysiological mapping of the STN and SNr using single-unit activity has been previously reported.[13,36] Briefly, STN neurons were identified by firing rates of ~20 to 60 Hz and irregular firing patterns, periods of beta activity, and responsiveness to passive movements of the contralateral extremities. After 4-mm to 6-mm advancement through the STN, exit from ventral border was identified by a reduction in background noise. After a brief quiescent period, SNr neurons were identified by faster firing rates of 80 to 120 Hz and regular firing patterns.

To corroborate the LFP-based beta-peak mapping approach, we compared the spatial characteristics of beta-peak appearance/disappearance ($n_{hemispheres}$ = 13; we excluded 3 hemispheres because of excessive noise or lack of beta peaks) along the surgical trajectories (1 mm step sizes) using the ventral-most contact with respect to the MER-defined STN entry and exit (submillimeter spatial resolution; ~0.1 mm step sizes). We defined the average depth of the first beta peak and the average depth of the highest beta peak with respect to the MER-defined STN entry. We also defined the average depth of the last beta

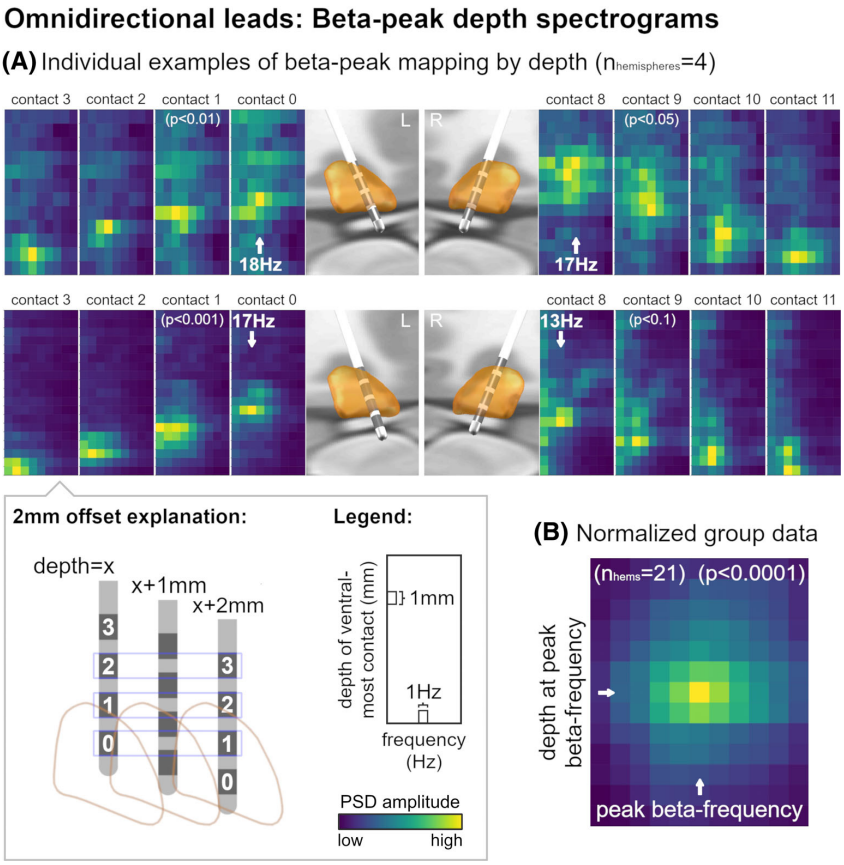

FIG. 2. Omnidirectional leads: beta-peak depth spectrograms. This approach allows for the visualization of the spatial-specificity of subthalamic nucleus beta-frequency activity across the surgical trajectory. (**A**) Individual examples (2 patients; $n_{hemispheres}$ = 4) of depth spectrograms and postoperative leads localizations. The 2-mm offsets are demonstrated in successive contact depth spectrograms from ventral to dorsal (ie, each successive contact records the same as the ventral-most contact after a 2 mm, 4 mm, and 6 mm advancements, respectively). The legend in the bottom left of this figure shows the depth (1 mm) and frequency (1 Hz) resolutions of the respective axes and also demonstrates the reason for the 2-mm offsets. In each of the 11 patients, the mean squared error of the beta-frequency depth spectrogram was significantly smaller compared with its permutations in 19 of 21 hemispheres (2 were P = 0.1–0.05, 6 were P = 0.05–0.01; 3 were P = 0.01–0.001; 8 were P < 0.001). (**B**) This was also confirmed at the group level ($n_{hemispheres}$ = 21; P < 0.0001). This group spectrogram was generated by normalizing with respect to the depth of the highest beta peak (*y*-axis) and the frequency of the beta peak (*x*-axis). PSD, power spectral density. [Color figure can be viewed at wileyonlinelibrary.com]

peak and the average depth of the first recording site at which the beta peak disappeared with respect to the MER-defined STN exit.

Clinical Relevance of Beta-Peak Amplitudes at Final Implantation Site

To determine if beta-peak amplitudes measured at the final implantation site had clinical relevance, we calculated how often the lead was programmed to stimulate at the same level at which the highest beta-peak amplitude was measured (26 patients; $n_{hemispheres}$ = 45; the total number of hemispheres with viable electrophysiological data and who were not tremor dominant). Tremor-dominant patients (9 patients; $n_{hemispheres}$ = 18) were excluded as these patients were most often programmed on the dorsal-most contacts to stimulate the zona incerta (outside of the STN). For segmented leads, the contacts at each segmented level were averaged together to get the average beta-peak amplitude for that level. Lead programming was done using a standard monopolar review ≥8 weeks after surgery, and the clinician was blinded with respect to the LFP results. If bipolar stimulation was programmed ($n_{hemispheres}$ = 11), a match was considered if 1 of the bipolar contacts was the contact with highest beta peak.

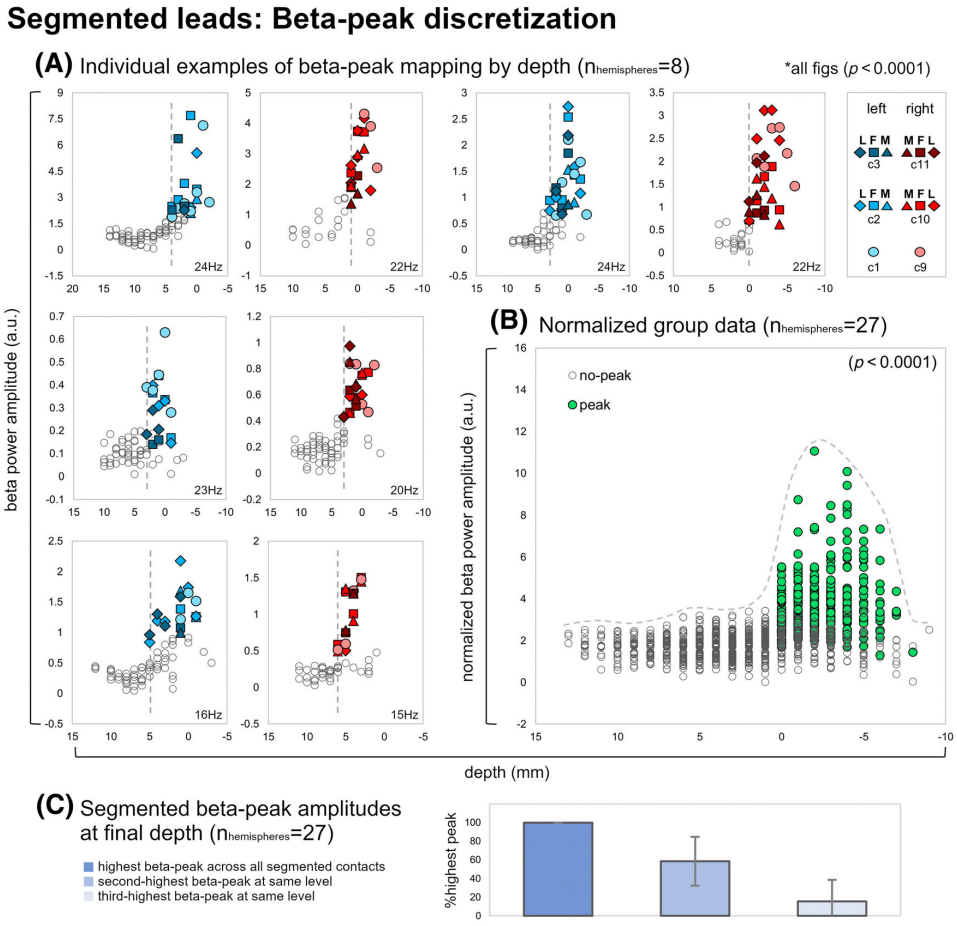

FIG. 3. Segmented leads: beta-peak discretization. Beta-peak amplitudes at recording sites presumed to be within the subthalamic nucleus were significantly greater than at sites not within the subthalamic nucleus. (**A**) Individual examples (4 patients; $n_{hemispheres}$ = 8) of beta-peak amplitudes plotted by depth. The depth of each contact was normalized with respect to the ventral-most contact (by subtracting 2 mm, 4 mm, and 6 mm from the second-most ventral, second-most dorsal, and dorsal-most contact levels, respectively). In each of 17 patients, when considering hemispheres individually ($n_{hemispheres}$ = 27), subthalamic nucleus beta peaks could be robustly differentiated from nonpeaks ($P < 0.0001$). The beta-peak frequency is displayed in the bottom right corner of each plot. (**B**) The same was true for the normalized group ($n_{hemispheres}$ = 27) data ($P < 0.0001$). Beta-peak amplitude normalization was done by dividing by the range of the background noise (ie, nonpeak activity), and depth normalization was done by assigning depth 0 to the recording site of the first beta peak. (**C**) At the final implantation sites, the highest beta-peak amplitude across all segmented contacts was considered as 100%. The average amplitudes (± standard deviation) of the second-highest and third-highest beta peaks at the same level are shown, normalized to the highest peak. F, frontal; L, lateral; M, medial. [Color figure can be viewed at wileyonlinelibrary.com]

Results

Online LFP-Based Mapping: DBS Macroelectrode Recordings

We applied the LFP-based mapping approach in 78 hemispheres; in 16 of these hemispheres, microelectrode recordings were performed beforehand and used to determine the final trajectories of the DBS leads. In 47 of the remaining 62 hemispheres, the LFP physiology decided the final lead positioning. In the remainder, intraoperative test stimulation (symptom suppression, reasonable side effect thresholds) determined the final trajectories. In most of these cases, lead repositioning was not required, and electrodes were implanted at the radiologically defined target sites. In 2 hemispheres (outlined in the patient demographics table in the Supplementary Material), a second macroelectrode trajectory was performed, which each time yielded desirable electrophysiological results. From patients in whom postoperative MRI imaging was available, 2 examples of comparisons between LFP physiology and postoperative lead reconstruction are presented in Figure 2, and additional examples are available in the Supplementary Material.

Omnidirectional Leads: Beta-Peak Depth Spectrograms

Using PSD amplitudes in the beta-frequency band, 2 unique methods were employed to visualize and statistically differentiate STN recording sites from non-STN recording sites. The first method was to generate a spectral distribution of the patient-specific beta peak along the surgical trajectory; this was done for patients with omnidirectional leads. In 19 of 21 hemispheres (11 patients), the mean squared error of the beta-frequency depth spectrogram was significantly smaller compared with its permutations (2 were P = 0.1–0.5, 6 were P < 0.05–0.01, 3 were P = 0.01–0.001, 8 were P < 0.001; Fig. 2A). This indicates that, for most hemispheres, the depth spectrogram resembled a Gaussian

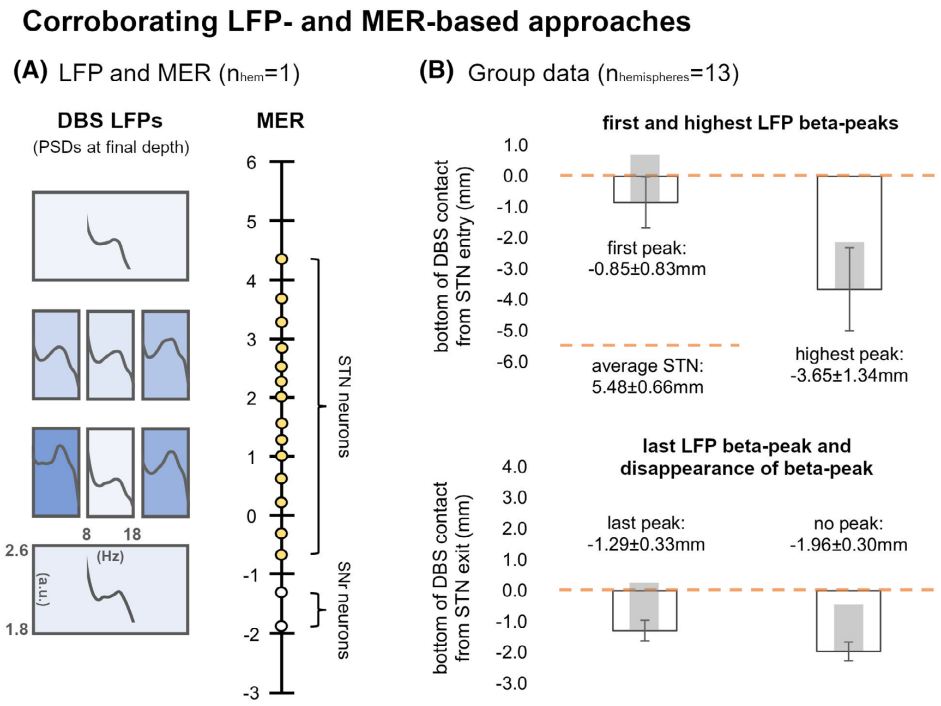

FIG. 4. Corroborating LFP-based and MER-based approaches. The macroelectrode LFP-based mapping approach was corroborated by the conventional MER-based mapping approach in 8 patients. (**A**) Displayed are the PSD amplitudes for each contact at the final implantation site (left) and the results from MER mapping of single unit activity along the surgical trajectory (right) from 1 representative hemisphere. Color gradient on DBS electrode contacts represents the relative beta-peak amplitude across contacts (ie, darkest blue being the highest peak and white being the lowest peak or no peak). (**B**) Group data ($n_{hemispheres}$ = 13) demonstrates the average locations (± standard deviation) of the first detected beta peak and the highest beta peak with respect to the MER-defined STN entry (orange dashed line; top) as well as the locations of the last detected beta peak and the first location of the disappearance of the beta peak with respect to the MER-defined STN exit (orange dashed line; bottom). The depth at which each LFP measurement was obtained corresponds to the position of the bottom of the DBS macrocontact. The translucent gray rectangle in each bar represents the spatial extent of the DBS contact (1.5 mm). The group data suggest that a beta peak could be detected as long as a portion of the DBS macrocontact was within the MER-defined STN boundaries. DSB, deep brain stimulation; LFP, local field potential; MER, microelectrode recording; PSD, power spectral density; SNr, substantia nigra pars reticulata; STN, subthalamic nucleus. [Color figure can be viewed at wileyonlinelibrary.com]

distribution. This was confirmed at the group level ($n_{hemispheres}$ = 21; $P < 0.0001$; Fig. 2B).

Segmented Leads: Beta-Peak Discretization

The second method was to discretize the amplitudes of beta peaks at depths assumed to be within the STN from PSD amplitudes of background noise; this was done for patients with segmented leads. Beta-peak amplitudes at recording sites presumed to be within the STN were significantly greater than PSD amplitudes at recording sites not within the STN. This method provided additional direction-specific information (ie, which segmented contacts contained the highest amplitude beta peaks). When considering each hemisphere individually ($n_{hemispheres}$ = 27; 17 patients), STN beta peaks could be robustly differentiated from nonpeaks ($P < 0.0001$; Fig. 3A), and the same was true for the normalized group data ($P < 0.0001$;

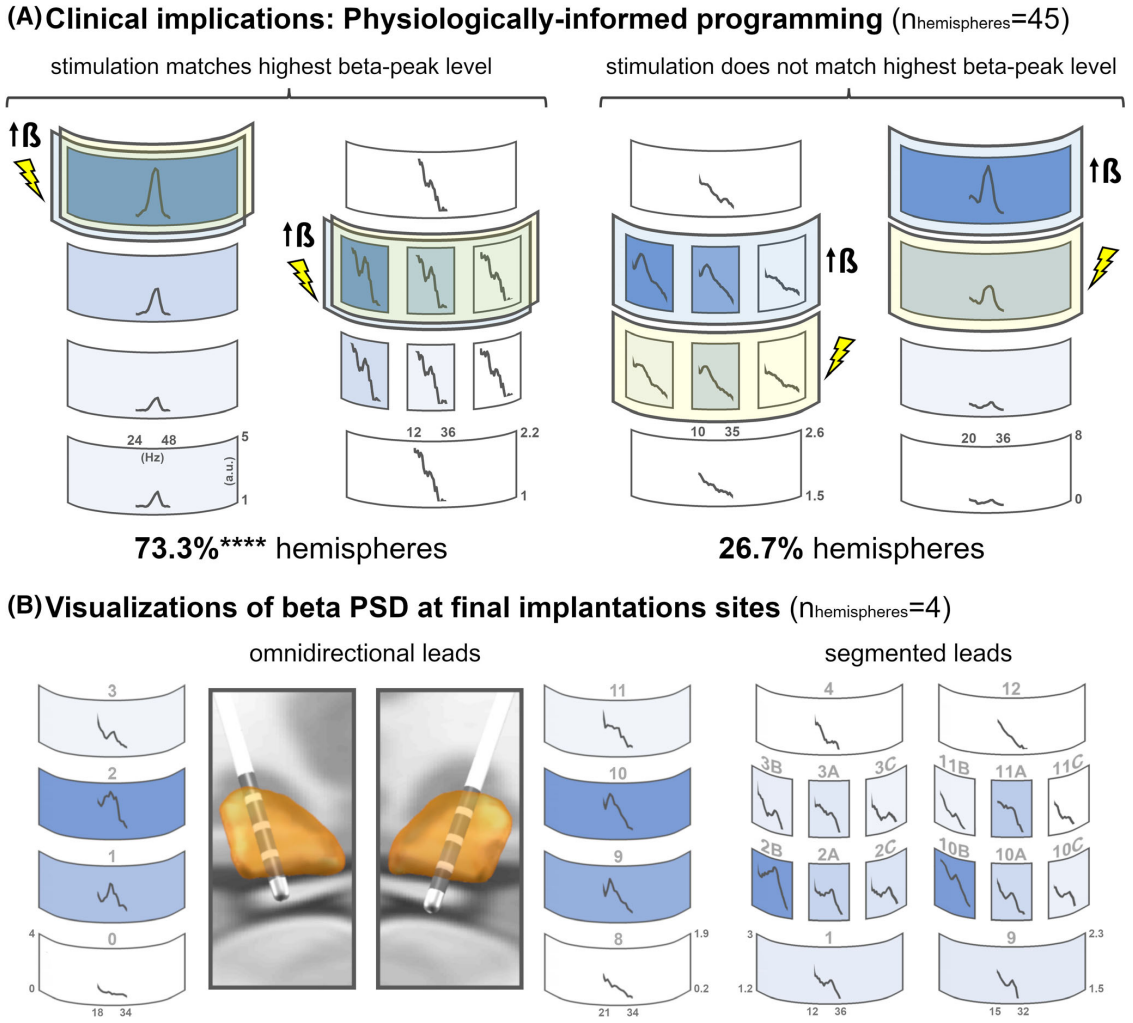

FIG. 5. Clinical implications: physiologically informed programming. (**A**) The macrocontact level with the highest beta-peak amplitude corresponded to the site of active stimulation (results of blinded monopolar reviews) 73.3% (33/45) of the time (26 patients; $n_{hemispheres}$ = 45). Of the remaining 26.7% (12/45), 75.0% (9/12) were programmed at the level of the second highest beta peak. Thus, the site of active stimulation was at either the highest or second-highest beta-peak level 93.3% (42/45) of the time. Tremor-dominant patients were excluded from this analysis. The displayed data are representative examples from 4 separate patients (4 hemispheres). (**B**) Additional representative examples of beta PSDs plotted on each of the deep brain stimulation macrocontacts at the final implantation sites for 1 patient with omnidirectional leads and another patient with segmented leads. Color gradients on DBS electrode contacts represent the relative beta-peak amplitudes across contacts per hemisphere (ie, darkest blue being the highest peak and white being the lowest peak or no peak). PSD, power spectral density. ****$P < 0.0001$. [Color figure can be viewed at wileyonlinelibrary.com]

Fig. 3B). Of the 62 hemispheres from 31 patients originally included in these analyses, statistically significant LFP-based electrophysiological STN delineation was achieved in 46 hemispheres (74.2%).

Corroborating LFP-Mapping and MER-Based Mapping Approaches

In the 8 patients in whom MER ($n_{hemispheres}$ = 16) and PSD measurements ($n_{hemispheres}$ = 13) were obtained, our results suggest that a detectable peak was measured when some portion of the DBS macrocontact was within the STN. Specifically, beta peaks first appeared when the bottom of the DBS contact was on average 0.85 ± 0.83 mm (mean ± standard deviation) beyond the MER-defined dorsal border (ie, when slightly more than half of the macrocontact had entered the STN). The largest peak was found when the bottom of the DBS contact was on average 3.65 ± 1.34 mm beyond the MER-defined border. Beta peaks were still visible when the bottom of the DBS macrocontact was an average of 1.29 ± 0.33 mm beyond the MER-defined ventral STN border (ie, when the majority of the DBS macrocontact had exited the STN but a small portion remained within). Beta peaks were no longer visible once the bottom of the DBS macrocontact was an average of 1.96 ± 0.30 mm beyond the ventral STN border. The average MER-defined spatial extent of STN was 5.48 ± 0.66 mm. These results are summarized in Figure 4.

Using data from all LFP-based mapping procedures ($n_{hemispheres}$ = 61), it was determined that the highest beta-peak amplitude was located 2.31 ± 1.6 mm beyond the area of first detectable beta peak (LFP-defined approach). Adjusting this value to account for the difference between MER-defined and LFP-defined dorsal border entry (ie, 0.85 ± 0.83 mm) confirms that the highest macroeletrode-defined beta peak was found when the bottom of the DBS contact was ~3.16 mm beyond the MER-defined STN border, which corroborates the aforementioned result of the highest beta-peak location.

Clinical Relevance of Beta-Peak Amplitudes at Final Implantation Site

The contact level with the highest beta-peak amplitude matched the clinically applied stimulation contact in 73.3% (33/45) of eligible hemispheres (Fig. 5A). Of the remaining 26.7% (12/45), 75% (9/12) were programmed at the level of the second-highest beta peak, whereas the remainder (3/12) were programmed at the dorsal-most contact level (which was neither the highest nor second-highest beta peak). This means that the site of active stimulation was at either the highest or second-highest beta-peak level 93.3% (42/45) of the time. Of the hemispheres, 2/3 that where neither at the highest nor second highest belonged to a single bilaterally mismatched patient who happened to be an equivalence-type patient who was programmed at the dorsal-most contacts on both sides for tremor benefit; contacts that were likely mostly outside of the STN as determined by a lack of beta peaks. If we exclude this patient, the active site of stimulation was at the highest beta-peak level 76.7% (33/43) of the time and at the level of the highest or second-highest peak 97.7% (42/43) of the time. If we consider that the maximum number of contacts that can simultaneously be in the STN is 3 (which covers a span of 5.5 mm), the match rate (73.3–76.7%) was more than 2-fold greater than chance (33.3%) and was statistically significant ($P < 0.0001$; binomial test).

Discussion

This study sought to demonstrate the instantaneous surgical and subsequent clinical relevance of subthalamic beta oscillations by applying a novel technique of functional mapping during DBS implantation procedures. The presented LFP-based method of electrophysiologically informed STN-DBS implantation required little time and fewer components (ie, use of the DBS macroelectrode only) and offered the possibility for semi-automation. We presented an online method (Fig. 1) for the intraoperative visualization and detection of the physiological STN topography based on PSD amplitudes in the beta-frequency band and presented 2 approaches for summary and statistical analysis of the results. One approach was to generate a distribution of beta-specific spectral information across the entire recording trajectory (Fig. 2), whereas the other approach was to discretize STN beta peaks from background activity (Fig. 3). In addition to describing the surgical functional utility of a beta-driven mapping approach, we also described a potentially promising technique for pathophysiologically informed stimulation programming (Fig. 5A). We suggest that delivering electrical stimulation from the macroelectrode contacts with the highest beta power at the final implantation site may yield the most favourable therapeutic results, which is corroborated by studies that suggest a relationship between subthalamic beta oscillations and clinical features of Parkinson's disease.

Surgical Utility: Electrophysiological Mapping

Improved imaging capabilities have led to the reconsideration of the use of electrophysiological mapping procedures.[37] Other arguments in support of omitting electrophysiological mapping procedures include reduced surgical time (thus, increased surgical tolerability) and reduced perioperative complications such as hemorrhage (although the risk rate is quite low at 3.3% for hematoma of any type, and 0.6% for symptomatic hematoma[38]).

However, neither high-resolution[39] nor conventional[40] imaging can account for perioperative deviations from preoperative anatomical targeting such as brain-shift,[41] which often contribute to suboptimal DBS lead placements.[42] Such deviations can only be accounted for when electrophysiological mapping procedures are correctly employed. Thus, we aimed to provide a novel methodology that can account for the majority of the aforementioned microelectrode contraindications while still providing a means of performing essential electrophysiologically informed implantations.

Given the unexpectedly high rate of DBS surgeries requiring lead revision or removal,[8] it can be argued that awake electrophysiology-guided implantations may be in the best interest of patients in the long term if corrective procedures can be avoided. Electrophysiological mapping procedures can reduce the likelihood of subsequent corrective surgeries, reduce the risk of surgical complications from subsequent procedures, and maximize therapeutic potential through optimized lead placement.[6] The approach described here furthermore reduces the necessity of expertise required for interpretation of MERs, can be performed rather quickly (barring technical or procedural obstacles, a 15-mm surgical trajectory takes only ~11 minutes; 30-second recordings at each depth and 15 seconds between depths) and eliminates time consumption associated with performing MERs. In addition, the risk of perioperative surgical complications (such as hemorrhage) from multipass microelectrode trajectories may be reduced. The described method furthermore allows for permutation of contact positions in accordance with patients' individual functional goals, such as placing the dorsal-most contact into the zona incerta to maximize effects on tremor,[31] placing the ventral-most contact into the SNr to potentially modulate gait dysfunction,[32] and/or placing segmented contacts into the STN to maximize the therapeutic window of STN-DBS.[43] Although z-direction titration is also possible with MERs, a particular advantage of the DBS macroelectrode approach is that once the optimal spot is determined based on electrophysiological results, the electrode stays in that spot chronically, whereas with MERs, the microwires must be removed and subsequently replaced by the chronic lead, which might introduce additional inaccuracies. As such, the DBS macrocontact approach may even serve as a final check to confirm that the DBS electrode is in place after replacing the microwire (ie, performing a DBS macroelectrode recording at the final position), thus the approach may also be used in conjunction with the traditional MER approach.

Two studies have previously applied a similar but distinct DBS macroelectrode mapping approach in smaller patient cohorts (n = 9[44] and n = 6[45]). The major difference is that both of these studies applied bipolar derivations of LFP recordings for offline spectral analyses. When 2 macrocontacts are both within the STN, bipolar recordings may lead to partial signal cancellation. Thus, for this application, bipolar recordings suffer from a nonstationary reference that leads to an inherent bias that shifts the location of the areas with highest beta activity to border regions where 1 contact is within the STN while another is outside of the STN. Conventional MER systems may also be configured such that the tip of the microelectrode is referenced to the macrotip located 3 mm dorsally, and each of these components are advanced together along the surgical trajectory (ie, a nonstationary reference). Monopolar recordings, as employed here, have a fixed reference and have the ability to create a functional topography of beta activity both within and outside of the STN without the bias of a moving reference. Although bipolar recordings may limit the effects of volume conduction,[46] our results nevertheless demonstrate the viability of using monopolar recordings for electrophysiological mapping and moreover suggest that the region of highest beta activity may not necessarily be at the immediate border region (although monopolar LFP recordings using microelectrodes would provide greater spatial acuity for assessing this).

Surgical Utility: Considerations and Limitations

Based on the results of corroboration with conventional MER-based mapping, offsets between LFP-defined and MER-defined borders should be taken into consideration, namely, that a beta peak may be visible if any portion of the DBS macrocontact is within the STN. Other considerations while performing these online recordings include that the patient should keep voluntary movements (which can desynchronize beta activity and/or induce movement artifacts) to a minimum, should not be speaking, and should be awake/alert. Because these behaviors are sometimes unavoidable, measurements at a particular depth may need to be repeated. Patients should be *off* medication, as antiparkinsonian medications have been shown to attenuate beta oscillations.[47] Furthermore, this method has not yet been confirmed in patients operated on under general anesthesia (which has effects on neuronal activity[48]). In this study, we could visualize and delineate STN from non-STN recording sites in 76.7% of hemispheres. However, a particularly important limitation of this approach is that some patients may lack beta activity[49] (also described in parkinsonian primate models[50]). In such cases, lead placements must rely on preoperative imaging and planning as well as results from perioperative test stimulation. However, in the event that both electrophysiological and perioperative test stimulation results are not favorable, an additional macroelectrode trajectory may have to be performed. Although this circumstance is not ideal, it still enables the ability to perform an electrophysiologically informed corrective trajectory on the spot, whereas an asleep image-guided-only procedure may result in a chronic lead misplacement that would necessitate a subsequent corrective procedure at a later date. In this regard,

the advantage of MERs is that they can enable performing multiple simultaneous recording trajectories, thus generating more information in the anterior–posterior and medial–lateral planes prior to macroelectrode implantation. Segmented leads may be able to provide some additional directional information in these planes as well in the fact that the distance between centroids of the directional contacts is 1.22 mm (compared with the 2 mm between MER trajectories adjacent to the central track). Thus, if perioperative test stimulation returns suboptimal side effect thresholds, but 1 of the directional contacts may have a small beta peak in 1 particular direction (and no peaks at all in the other directions), this may inform the direction for a potential revised trajectory. Finally, a notable limitation of electrophysiologically informed surgeries altogether is that they usually require that the patient be awake, unlike image-guided-only surgeries; however, awake surgeries allow for the ability to test for sensory-related adverse effects (ie, stimulation of lemniscus fibers) or behavioral-related adverse effects (ie, speech effects from stimulation of cortico-bulbar fibers).

Clinical Utility: Stimulation Programming

Subthalamic hypersynchrony in the beta-frequency band has been suggested to be associated with clinical features of Parkinson's disease.[30,51-54] In addition, both levodopa therapy[14,47,55] and STN-DBS,[56-58] the conventional therapeutic interventions for Parkinson's disease, have been suggested to disrupt/desynchronize these purportedly pathological oscillations. As such, we postulated that targeted stimulation delivery to the area of highest beta-peak amplitude may be most therapeutically favorable. We investigated this by comparing the macrocontact level with the highest intraoperatively obtained beta-peak amplitude at the final implantation site to the eventual programmed stimulation site determined during conventional postoperative monopolar review that was blinded to the intraoperative LFP results and found a high degree of correspondence (Fig. 5A). A previous study (n = 128) demonstrated that the spatial extent of the subthalamic beta oscillatory region was a predictor of favorable therapeutic response.[21] Furthermore, a study in patients (n = 4) programmed with bipolar stimulation found that the contact pair that provided optimal efficacy was associated with the highest energy in the beta and gamma frequency bands.[59] Another study applied this approach of beta-targeted stimulation in patients (n = 12) implanted with directional leads.[49] The authors found that the beta power at each contact was correlated with the individual contact's clinical efficacy and that 1 of the 2 contacts with the highest beta power was the most clinically efficient stimulation contact up to 92% of the time, which corresponds with our findings.

Previous studies as well as our own suggest that stimulation programming can be optimized not only to reduce time consumption associated with conducting a complete monopolar review but also to be performed in a physiologically informed manner. As such, we suggest that novel implantable pulse generator software and hardware should include the capability for the clinician to quickly record (eg, for 30 seconds) from each of the macrocontacts of the embedded DBS leads, calculate and display the PSDs (as shown in Fig. 5B), and give the option to the clinician to select stimulation contacts based on the amplitude of PSDs (as shown in Fig. 5A). This is additionally important considering the emergence of segmented DBS leads with many contacts and considering the variability in beta-peak amplitude across directional contacts (Fig. 3C). Although suggested to be able to widen the therapeutic window,[43,60] stimulation programming will become much more cumbersome and time consuming. We foresee that physiologically informed stimulation programming will be feasible in the near future considering the emergence of DBS technologies with chronic sensing capabilities. Thus, studies of macroelectrode LFP signals have the potential for direct technological and clinical translation.

Clinical Utility: Considerations and Limitations

Consistent with previous findings,[29] beta oscillations could still be measured in the subgroup of tremor-dominant patients. For these patients, however, the clinically applied contact was usually not the one with the highest beta activity because of the intended stimulation in the zona incerta, that is, above the dorsal STN border. In nontremor dominant patients, the potential reasons for mismatches between the contact with the highest beta-peak amplitude and the clinically applied stimulation contact level are (1) a narrow therapeutic window at the contact with the highest beta peak because of proximity to the nearby fibers or (2) selection of therapeutically suboptimal active stimulation contacts.[61] Nevertheless, the active contacts corresponded to the level of the first-highest or second-highest beta-peak amplitude in 93.3% of hemispheres, thereby emphasizing the clinical functional utility of this physiological marker. Although it would be valuable to assess the relevance of beta activity recorded with individual segmented contacts for informing directional stimulation, systematic clinical assessments (monopolar review) of directional stimulation titration were not performed in this patient cohort. As such, further clinical research is warranted to determine if beta-peak amplitude could inform directional stimulation programming.

Conclusion

We demonstrated the feasibility of performing an online LFP-based, beta-driven electrophysiological mapping procedure using DBS macroelectrodes. Furthermore, our results suggest that the PSD in the beta-frequency band at

the final implantation site may be used for physiologically informed stimulation delivery. As such, our results demonstrate both surgical and clinical functional utilities of beta oscillations measured from DBS macroelectrodes. These findings may be used to improve both surgical implantation and stimulation programming procedures.

Acknowledgments: We thank Dr. Ramin Azodi-Avval for his contributions to data collection and the patients for their participation in the study.

References

1. Limousin P, Krack P, Pollak P, et al. Electrical stimulation of the subthalamic nucleus in advanced Parkinson's disease. N Engl J Med 1998;339:1105–1111. https://doi.org/10.1056/NEJM199810153391603
2. Benabid AL, Pollak P, Gross C, et al. Acute and long-term effects of subthalamic nucleus stimulation in Parkinson's disease. Stereotact Funct Neurosurg 1994;62:76–84. https://doi.org/10.1159/000098600
3. Vitek JL. Deep brain stimulation for Parkinson's disease. Stereotact Funct Neurosurg 2002;78:119–131. https://doi.org/10.1159/000068959
4. Farris S, Giroux M. Retrospective review of factors leading to dissatisfaction with subthalamic nucleus deep brain stimulation during long-term management. Surg Neurol Int 2013;4:69. https://doi.org/10.4103/2152-7806.112612
5. Hariz MI. Complications of deep brain stimulation surgery. Mov Disord 2002;17:S162–S166. https://doi.org/10.1002/mds.10159
6. Lozano AM, Snyder BJ, Hamani C, et al. Basal ganglia physiology and deep brain stimulation. Mov Disord 2010;25:S71–S75. https://doi.org/10.1002/mds.22714
7. Nickl RC, Reich MM, Pozzi NG, et al. Rescuing suboptimal outcomes of subthalamic deep brain stimulation in Parkinson disease by surgical lead revision. Neurosurgery 2019;85:E314–E321. https://doi.org/10.1093/neuros/nyz018
8. Rolston JD, Englot DJ, Starr PA, et al. An unexpectedly high rate of revisions and removals in deep brain stimulation surgery: analysis of multiple databases. Parkinsonism Relat Disord 2016;33:72–77. https://doi.org/10.1016/j.parkreldis.2016.09.014
9. Okun MS, Tagliati M, Pourfar M, et al. Management of referred deep brain stimulation failures: a retrospective analysis from 2 movement disorders centers. Arch Neurol 2005;62:1250–1255. https://doi.org/10.1001/archneur.62.8.noc40425
10. Moro E, Esselink RJA, Xie J, et al. The impact on Parkinson's disease of electrical parameter settings in STN stimulation. Neurology 2002;59:706–713. https://doi.org/10.1212/wnl.59.5.706
11. Witt K, Daniels C, Volkmann J. Factors associated with neuropsychiatric side effects after STN-DBS in Parkinson's disease. Parkinsonism Relat Disord 2012;18:S168–S170. https://doi.org/10.1016/S1353-8020(11)70052-9
12. Brunenberg EJL, Platel B, Hofman PAM, et al. Magnetic resonance imaging techniques for visualization of the subthalamic nucleus: a review. J Neurosurg 2011;115:971–84. https://doi.org/10.3171/2011.6.JNS101571
13. Hutchison WD, Allan RJ, Opitz H, et al. Neurophysiological identification of the subthalamic nucleus in surgery for Parkinson's disease. Ann Neurol 1998;44:622–628. https://doi.org/10.1002/ana.410440407
14. Weinberger M, Mahant N, Hutchison WD, et al. Beta oscillatory activity in the subthalamic nucleus and its relation to dopaminergic response in Parkinson's disease. J Neurophysiol 2006;96:3248–3256. https://doi.org/10.1152/jn.00697.2006
15. Abosch A, Hutchison WD, Saint-Cyr JA, et al. Movement-related neurons of the subthalamic nucleus in patients with Parkinson disease. J Neurosurg 2002;97:1167–1172. https://doi.org/10.3171/jns.2002.97.5.1167
16. Lee PS, Crammond DJ, Richardson RM. Deep brain stimulation of the subthalamic nucleus and globus pallidus for Parkinson's disease. Curr Concepts Mov Disord Manag 2018;33:207–221. https://doi.org/10.1159/000481105
17. Montgomery EB. Microelectrode targeting of the subthalamic nucleus for deep brain stimulation surgery. Mov Disord 2012;27:1387–1391. https://doi.org/10.1002/mds.25000
18. Lozano CS, Ranjan M, Boutet A, et al. Imaging alone versus microelectrode recording–guided targeting of the STN in patients with Parkinson's disease. J Neurosurg 2018;130:1847–1852. https://doi.org/10.3171/2018.2.JNS172186
19. Bour LJ, Contarino MF, Foncke EMJ, et al. Long-term experience with intraoperative microrecording during DBS neurosurgery in STN and GPi. Acta Neurochir (Wien) 2010;152:2069–2077. https://doi.org/10.1007/s00701-010-0835-y
20. Valsky D, Marmor-Levin O, Deffains M, et al. Stop! border ahead: automatic detection of subthalamic exit during deep brain stimulation surgery. Mov Disord 2017;32:70–79. https://doi.org/10.1002/mds.26806
21. Zaidel A, Spivak A, Grieb B, et al. Subthalamic span of β oscillations predicts deep brain stimulation efficacy for patients with Parkinson's disease. Brain 2010;133:2007–2021. https://doi.org/10.1093/brain/awq144
22. Shamir RR, Zaidel A, Joskowicz L, et al. Microelectrode recording duration and spatial density constraints for automatic targeting of the subthalamic nucleus. Stereotact Funct Neurosurg 2012;90:325–334. https://doi.org/10.1159/000338252
23. Alavi M, Dostrovsky JO, Hodaie M, et al. Spatial extent of beta oscillatory activity in and between the subthalamic nucleus and substantia nigra pars reticulata of Parkinson's disease patients. Exp Neurol 2013;245:60–71. https://doi.org/10.1016/j.expneurol.2012.09.021
24. Kolb R, Abosch A, Felsen G, et al. Use of intraoperative local field potential spectral analysis to differentiate basal ganglia structures in Parkinson's disease patients. Physiol Rep 2017;5:e13322. https://doi.org/10.14814/phy2.13322
25. Thompson JA, Oukal S, Bergman H, et al. Semi-automated application for estimating subthalamic nucleus boundaries and optimal target selection for deep brain stimulation implantation surgery. J Neurosurg 2018;1:1–10. https://doi.org/10.3171/2017.12.JNS171964
26. Kühn AA, Trottenberg T, Kivi A, et al. The relationship between local field potential and neuronal discharge in the subthalamic nucleus of patients with Parkinson's disease. Exp Neurol 2005;194:212–220. https://doi.org/10.1016/j.expneurol.2005.02.010
27. Novak P, Daniluk S, Ellias SA, et al. Detection of the subthalamic nucleus in microelectrographic recordings in Parkinson disease using the high-frequency (> 500 Hz) neuronal background: technical note. J Neurosurg 2007;106:175–179. https://doi.org/10.3171/jns.2007.106.1.175
28. Telkes I, Jimenez-Shahed J, Viswanathan A, et al. Prediction of STN-DBS electrode implantation track in Parkinson's disease by using local field potentials. Front Neurosci 2016;10:198. https://doi.org/10.3389/fnins.2016.00198
29. Telkes I, Viswanathan A, Jimenez-Shahed J, et al. Local field potentials of subthalamic nucleus contain electrophysiological footprints of motor subtypes of Parkinson's disease. Proc Natl Acad Sci 2018;115:E8567–E8576. https://doi.org/10.1073/pnas.1810589115
30. Brown P. Oscillatory nature of human basal ganglia activity: relationship to the pathophysiology of Parkinson's disease. Mov Disord 2003;18:357–63. https://doi.org/10.1002/mds.10358
31. Plaha P, Khan S, Gill SS. Bilateral stimulation of the caudal zona incerta nucleus for tremor control. J Neurol Neurosurg Psychiatry 2008;79:504–513. https://doi.org/10.1136/jnnp.2006.112334
32. Weiss D, Walach M, Meisner C, et al. Nigral stimulation for resistant axial motor impairment in Parkinson's disease? A randomized controlled trial. Brain 2013;136:2098–2108. https://doi.org/10.1093/brain/awt122
33. Bejjani B-P, Dormont D, Pidoux B, et al. Bilateral subthalamic stimulation for Parkinson's disease by using three-dimensional stereotactic magnetic resonance imaging and electrophysiological guidance.

J Neurosurg 2000;92:615–25. https://doi.org/10.3171/jns.2000.92.4.0615

34. Azodi-Avval R, Gharabaghi A. Spatial specificity of beta oscillations and cortico-subthalamic connectivity in Parkinson's disease [doctoral thesis]. Tuebingen, Germany: University of Tuebingen; 2018.
35. Horn A, Li N, Dembek TA, et al. Lead-DBS v2: towards a comprehensive pipeline for deep brain stimulation imaging. NeuroImage 2019;184:293–316. https://doi.org/10.1016/j.neuroimage.2018.08.068
36. Milosevic L, Kalia SK, Hodaie M, et al. Neuronal inhibition and synaptic plasticity of basal ganglia neurons in Parkinson's disease. Brain 2018;141:177–190. https://doi.org/10.1093/brain/awx296
37. Foltynie T, Zrinzo L, Martinez-Torres I, et al. MRI-guided STN DBS in Parkinson's disease without microelectrode recording: efficacy and safety. J Neurol Neurosurg Psychiatry 2011;82:358–363. https://doi.org/10.1136/jnnp.2010.205542
38. Binder DK, Rau GM, Starr PA. Risk factors for hemorrhage during microelectrode-guided deep brain stimulator implantation for movement disorders. Neurosurgery 2005;56:722–732. https://doi.org/10.1227/01.NEU.0000156473.57196.7E
39. Cho Z-H, Min H-K, Oh S-H, et al. Direct visualization of deep brain stimulation targets in Parkinson disease with the use of 7-tesla magnetic resonance imaging: clinical article. J Neurosurg 2010;113:639–647. https://doi.org/10.3171/2010.3.JNS091385
40. Ranjan M, Boutet A, Xu DS, et al. Subthalamic nucleus visualization on routine clinical preoperative MRI scans: a retrospective study of clinical and image characteristics predicting its visualization. Stereotact Funct Neurosurg 2018;96:120–126. https://doi.org/10.1159/000488397
41. Halpern CH, Danish SF, Baltuch GH, et al. Brain shift during deep brain stimulation surgery for Parkinson's disease. Stereotact Funct Neurosurg 2008;86:37–43. https://doi.org/10.1159/000108587
42. Sammartino F, Krishna V, King NKK, et al. Sequence of electrode implantation and outcome of deep brain stimulation for Parkinson's disease. J Neurol Neurosurg Psychiatry 2016;87:859–863. https://doi.org/10.1136/jnnp-2015-311426
43. Pollo C, Kaelin-Lang A, Oertel MF, et al. Directional deep brain stimulation: an intraoperative double-blind pilot study. Brain 2014;137:2015–2026. https://doi.org/10.1093/brain/awu102
44. Chen CC, Pogosyan A, Zrinzo LU, et al. Intra-operative recordings of local field potentials can help localize the subthalamic nucleus in Parkinson's disease surgery. Exp Neurol 2006;198:214–221. https://doi.org/10.1016/j.expneurol.2005.11.019
45. Telkes I, Ince NF, Onaran I, et al. Localization of subthalamic nucleus borders using macroelectrode local field potential recordings. Paper presented at: 36th Annual International Conference of the IEEE Engineering in Medicine and Biology Society; 2014; Chicago, IL. https://doi.org/10.1109/EMBC.2014.6944160
46. Marmor O, Valsky D, Joshua M, et al. Local vs. volume conductance activity of field potentials in the human subthalamic nucleus. J Neurophysiol 2017;117:2140–2151. https://doi.org/10.1152/jn.00756.2016
47. Levy R, Ashby P, Hutchison WD, et al. Dependence of subthalamic nucleus oscillations on movement and dopamine in Parkinson's disease. Brain 2002;125:1196–1209. https://doi.org/10.1093/brain/awf128
48. Raz A, Eimerl D, Zaidel A, et al. Propofol decreases neuronal population spiking activity in the subthalamic nucleus of Parkinsonian patients. Anesth Analg 2010;111:1285–1289. https://doi.org/10.1213/ANE.0b013e3181f565f2
49. Tinkhauser G, Pogosyan A, Debove I, et al. Directional local field potentials: a tool to optimize deep brain stimulation. Mov Disord 2018;33:159–164. https://doi.org/10.1002/mds.27215
50. Connolly AT, Jensen AL, Bello EM, et al. Modulations in oscillatory frequency and coupling in globus pallidus with increasing parkinsonian severity. J Neurosci 2015;35:6231–6240. https://doi.org/10.1523/JNEUROSCI.4137-14.2015
51. Hammond C, Bergman H, Brown P. Pathological synchronization in Parkinson's disease: networks, models and treatments. Trends Neurosci 2007;30:357–364. https://doi.org/10.1016/j.tins.2007.05.004
52. Neumann W-J, Degen K, Schneider G-H, et al. Subthalamic synchronized oscillatory activity correlates with motor impairment in patients with Parkinson's disease. Mov Disord 2016;31:1748–1751. https://doi.org/10.1002/mds.26759
53. Steiner LA, Neumann W-J, Staub-Bartelt F, et al. Subthalamic beta dynamics mirror Parkinsonian bradykinesia months after neurostimulator implantation. Mov Disord 2017;32:1183–1190. https://doi.org/10.1002/mds.27068
54. Kühn AA, Tsui A, Aziz T, et al. Pathological synchronisation in the subthalamic nucleus of patients with Parkinson's disease relates to both bradykinesia and rigidity. Exp Neurol 2009;215:38038–7. https://doi.org/10.1016/j.expneurol.2008.11.008
55. Brown P, Oliviero A, Mazzone P, et al. Dopamine dependency of oscillations between subthalamic nucleus and pallidum in Parkinson's disease. J Neurosci 2001;21:1033–1038. https://doi.org/10.1523/JNEUROSCI.21-03-01033.2001
56. Kühn AA, Kempf F, Brücke C, et al. High-frequency stimulation of the subthalamic nucleus suppresses oscillatory β activity in patients with Parkinson's disease in parallel with improvement in motor performance. J Neurosci 2008;28:6165–73. https://doi.org/10.1523/JNEUROSCI.0282-08.2008
57. Bronte-Stewart H, Barberini C, Koop MM, et al. The STN beta-band profile in Parkinson's disease is stationary and shows prolonged attenuation after deep brain stimulation. Exp Neurol 2009;215:20–28. https://doi.org/10.1016/j.expneurol.2008.09.008
58. Rosa M, Giannicola G, Servello D, et al. Subthalamic local field beta oscillations during ongoing deep brain stimulation in Parkinson's disease in hyperacute and chronic phases. Neurosignals 2011;19:151–162. https://doi.org/10.1159/000328508
59. Ince NF, Gupte A, Wichmann T, et al. Selection of optimal programming contacts based on local field potential recordings from subthalamic nucleus in patients with Parkinson's disease. Neurosurgery 2010;67:390–397. https://doi.org/10.1227/01.NEU.0000372091.64824.63
60. Chase A. Neurosurgery: directional electrodes widen the therapeutic window for deep brain stimulation in movement disorders. Nat Rev Neurol 2014;10:364–364. https://doi.org/10.1038/nrneurol.2014.101
61. Okun MS, Rodriguez RL, Foote KD, et al. A case-based review of troubleshooting deep brain stimulator issues in movement and neuropsychiatric disorders. Parkinsonism Relat Disord 2008;14:532–538. https://doi.org/10.1016/j.parkreldis.2008.01.001

Supporting Data

Additional Supporting Information may be found in the online version of this article at the publisher's web-site.

Comparing the therapeutic window of omnidirectional and directional subthalamic deep brain stimulation in Parkinsons disease

Maximilian Scherer*, Luka Milosevic*, Patrick Bookjans*, Bastian Brunett[1], Idil Hanci*†, Robert Guggenberger*, Daniel Weiss† and Alireza Gharabaghi*
Institute for Neuromodulation and Neurotechnology, Department of Neurosurgery and Neurotechnology, University Hospital Tübingen, University of Tübingen, Tübingen, Germany *
Hertie Institute for Clinical Brain Research, Department of Neurodegenerative Diseases, and German Center of Neurodegenerative Diseases (DZNE), University of Tübingen, Tübingen, Germany †

***Abstract*—Deep brain stimulation (DBS) is an effective treatment for the motor symptoms of patients with Parkinsons disease (PD). A new generation of segmented DBS leads allows the electrical field to be directionally steered orthogonal to the implantation trajectory alternatively to the omnidirectional stimulation in the conventional ring mode. In this study, the therapeutic window of subthalamic DBS was systematically compared between omnidirectional and directional stimulation. In seventeen akinetic-rigid PD patients, the rigidity of the right biceps brachii muscle was evaluated during DBS of the left subthalamic nucleus in the dopaminergic medication-off state. Ten weeks after implantation, a monopolar review of the three upper ring contacts and the three contacts of the upper segmented level was performed. For each contact, we determined the impedance and estimated the therapeutic window by increasing the stimulation intensity in steps of 0.2mA. The therapeutic window of the best ring contact was significantly larger than the two other ring contacts. Stimulating via segmented contacts doubled the impedance, but did not improve the therapeutic window in comparison to the ring mode. Specifically, when stimulating at 1.1mA with the best ring contact, complete suppression of rigidity was achieved in 90% of the patients; this therapeutic threshold was 50% better than the best segmented contact. The best therapeutic threshold for suppression of rigidity can be determined by selection of the optimal ring level. Directional stimulation does not improve the response and threshold, and would necessitate higher power consumption than the ring mode, when applied chronically.**

INTRODUCTION

Deep brain stimulation (DBS) is commonly used in patients with Parkinsons disease (PD) either partially or fully refractory to medical treatment (Benabid et al. 1994; Limousin et al. 1995). Correct configuration of DBS parameters in PD patients is crucial for an effective treatment (Hell et al. 2019; Kuncel and Grill 2004). DBS can be applied through any of the usually four, equally spaced contacts of the DBS lead. The choice of the DBS contact for stimulation crucially affects the clinical efficacy (Hilliard, Frysinger, and Elias 2011). In order to increase efficacy, the electrical field generated from DBS can be steered along the implantation trajectory by contact selection. The latest generation of electrode leads offers additional stimulation options. It allows the electrical field to be directionally steered orthogonal to the implantation trajectory (Martens et al. 2011). This is achieved by segmenting the two middle of the four ring contacts into three segments. This advancement may potentially improve clinical benefit and reduce side-effects of DBS. It has previously been reported that stimulation via segmented contacts is associated with a larger therapeutic window compared to stimulation via ring contacts (Contarino et al. 2014; Pollo et al. 2014; Dembek et al. 2017; Bruno et al. 2020), either related to an increased side effect threshold (Contarino et al. 2014; Dembek et al.

2017) or a decreased therapeutic threshold (Pollo et al. 2014; Bruno et al. 2020). However, not all studies observed a significantly different therapeutic window when comparing omnidirectional (ring) and directional (steered) stimulation (Steigerwald et al. 2016). This may at least in part be related to different stimulation titration step sizes (which were often rather large, e.g., 0.5 mA) and different time periods allocated for the examination in the respective settings (e.g., intraoperative vs. extraoperative evaluation).

In the present study, the treatment-relevant thresholds of subthalamic DBS were compared between ring and segmented stimulation. Specifically, ten weeks after DBS implantation, a monopolar review of the three upper ring contacts and the three contacts of the upper segmented level was performed. For each contact, the therapeutic window was estimated while increasing the stimulation intensity in steps of 0.2 mA, and systematically evaluating the rigidity of the upper extremity. Each stimulation setting was evaluated for 90 s to provide a reliable basis for clinical evaluation. For each contact, the impedance was also determined to relate potential clinical benefits with the respective power consumption and battery life.

METHODS

Patients

The akinetic-rigid PD patients of this study were part of the SANTOP study (*Subthalamic Steering for Therapy Optimization in Parkinson's Disease* 2020; ClinicalTrials.gov: NCT03548506) that evaluated the long-term effects of omnidirectional vs. directional deep brain stimulation in a randomized, cross-over protocol six months after surgery; the respective results will be reported elsewhere. Here, we report the findings of a monopolar review conducted ten weeks after surgery on two consecutive days, i.e., evaluating the three upper ring contacts (day 1) and the three segments of the upper segmented level (day 2). This evaluation could be completed in seventeen PD patients, in whom the rigidity of the right biceps brachii muscle was assessed during DBS of the left subthalamic nucleus in the dopaminergic medication-off state. Furthermore, impedances were measured for all contacts in every patient.

Each patient underwent bilateral implantation of STN-DBS leads (6170, Abbott laboratories, Lake Bluff, Illinois, U.S.) on average 69 days prior to the evaluation. The implantation target was preoperatively identified via magnetic resonance imaging (MRI) and computer tomography (CT) images. Intraoperatively, successful implantation was validated by local field potential beta-peaks (Milosevic et al. 2020) or microelectrode recordings (Hutchison et al. 1998). Postoperative CT images were co-registered with preoperative MRI to confirm accurate electrode implantation. Patients were examined several weeks after the DBS lead implantation to avoid microlesion effects (Granziera et al. 2008), and after overnight withdrawal from dopaminergic medications. Written informed consent was provided by all patients and the study was approved by the ethics committee of the Medical Faculty Tübingen. Detailed information on patient demographics is available in Table 1.

ID	Sex	Age (during surgery; years)	Time between surgery and examination (days)
0	m	65	88
1	f	61	61
2	m	58	78
3	m	71	71
5	f	53	62
6	f	58	63
9	m	68	62
15	f	75	61
16	m	59	67
20	m	73	64
21	m	71	64
22	m	66	75
23	m	67	64
25	m	61	87
26	f	52	57
27	m	50	64
28	m	67	79

Table 1: Patient information.

Stimulation configuration

In all seventeen patients, the three upper ring contacts were evaluated. In addition, three segments of the upper and lower segmented level were investigated in sixteen patients and one patient, respectively. Stimulation was always applied at 130 Hz and 60 ţs, while stepwise increasing the stimulation intensity (see experimental protocol). Stimulation was applied unilateral to the left hemisphere, while rigidity was assessed on the right arm.

Data acquisition and experimental protocol

The patients were instructed to relax their arms and stay awake. Each run lasted 90 seconds and was compromised of two phases: A non-movement phase (30 s) and a continuous passive movement

phase (60 s). During the continuous passive movement phase, an examiner moved the subjects arm with a frequency of 0.5 Hz (acoustically communicated to the examiner via headphones). At the end of each run, the examiner provided an estimate of the patients rigidity according to the MDS-UPDRS assessment. For later analyses, these scores were binarized to represent either a lack (UPDRS score of zero) or the presence of rigidity. In the first run, patients were evaluated OFF stimulation. In the consecutive runs, stimulation was increased from 0.5 mA to 2.5 mA in 0.2 mA increments on one stimulation contact before switching to another contact. The contacts were evaluated in randomized order. Before switching contacts, the paradigm was paused for two minutes to avoid stimulation related carry-over effects (Levin et al. 2009). Above 2.5 mA, the evaluation was continued in 0.2 mA increments; however, the evaluation was focused on side effects only, i.e., without concurrent arm movements. The patient and the examiner did not know which stimulation contact was evaluated at which intensity, since the programming was performed by a third person.

Statistical evaluations

For statistical evaluation, the contacts were grouped on the basis of different categories: (i) according to level, i.e., ring 4 (most upper), ring 3 (second most upper), ring 2 (third most upper), frontal segment, medial segment, lateral segment; (ii) therapeutic window size, i.e., best, second best, worst ring/segment; (iii) therapeutic threshold, i.e., best, second best, worst ring/segment; (iv) side-effect threshold, i.e., best, second best, worst ring/segment. The stimulation effect was estimated using a linear mixed model. The measured clinical efficacy was modeled as the dependent variable. The other variables were modeled as independent variables: Stimulation intensity was included as a categorical fixed factor in order to estimate the effect of stimulation OFF versus a specific stimulation intensity; the patient ID was included as a categorical random factor to compensate for repeated measurements over individual patients.

Patient-wise paired t-tests were applied to investigate the differences between the therapeutic window sizes of ring and segmented contacts. Multiple comparison correction (MCC) was applied using the Bonferroni method and an alpha value of 0.05. The results are presented with a marker indicating either significance or non-significance after MCC.

Determining the therapeutic threshold

The ring/segmented contact which completely suppressed rigidity at the lowest intensity in each patient was considered the best ring/segmented contact, followed by the second best and the worst contact. Specifically, only consistent suppression of rigidity was considered as the therapeutic threshold. For example, if rigidity was present at intensities of 0.5 mA, 0.7 mA and 1.1 mA, but was completely suppressed at 0.9 mA and 1.3 mA, and all higher intensities; the therapeutic threshold was determined at 1.3 mA.

Determining therapeutic window size

Therapeutic windows were determined on the basis of the lower and upper boarder of clinical efficacy. The lowest amplitude necessary for complete suppression of rigidity, the therapeutic threshold, was identified as the lower boarder of the therapeutic window. The highest intensity, which did not cause side effects (e.g., muscle cramps or double vision) was identified as the upper boarder of the therapeutic window. The window size was calculated as the difference between the upper and lower boarder.

Determining contact impedance

The impedance values were measured via the integrated functionality of the programming device by attaching an external pulse generator at the end of the surgery. Low intensity bipolar stimulation was utilized to measure the impedance between individual contacts. The impedance of a specific contact was calculated as the average impedance between this and the other contacts.

Code and data accessibility

Data and evaluation code will be shared upon request. The custom toolbox used to analyze the data will be made publicly available on GitHub (Scherer et al. n.d., in preparation).

RESULTS

The ratio of rigid trials decreased consistently with increasing stimulation intensity. This finding was independent of grouping of the contacts on the basis of different categories, i.e., according to level (Figure 1A), therapeutic window size (Figure 1B, C), therapeutic threshold (Figure 2A, B), and side-effect threshold (Figure 2C, D).

When stimulating at an intensity of 0.7 mA, the ration of rigid trials was significantly reduced in comparison to baseline (i.e., without stimulation); at this intensity 40% of patients had complete suppression of rigidity, when being stimulated via a segmented contact that was laterally steering (Figure 1A), that had the best therapeutic window size (Figure 1B, C), best therapeutic threshold (Figure 2A, B), and worst side-effect threshold (Figure 2C, D). This suggests that laterally steering segments may present large therapeutic windows by way of an improved therapeutic threshold at the expense of a decreased side effect threshold. The stimulation effect of the laterally steering contact plateaued from 2.1 mA onwards, and achieved complete suppression of rigidity in 80% of the patients. A comparison of these effects with the other contacts (both segmented and ring) at the same stimulation intensity revealed no significant differences (see respective plots on the right side of Figures 1 and 2).

All contacts (both ring and segmented ones) showed a significant reduction of rigid trials in comparison to baseline, when stimulating at 1.3 mA; the second highest ring contact (i.e., level 3) led to the largest reduction of rigid trials in comparison to baseline, plateaued from 2.1 mA onwards, and achieved complete suppression of rigidity in 90% of the patients (Figure 1A). However, comparing these effects with the other contacts (both segmented and ring) at the same stimulation intensity revealed no significant differences (see respective plots on the right side of Figures 1 and 2).

Notably, the best ring contact had a therapeutic threshold for complete suppression of rigidity at 1.1 mA (and plateaued onwards) in 90% of the patients (Figure 2A left); this was significantly better (i.e., by 50%) than the best segmented contact (Figure 2A right). However, when further increasing the stimulation intensity, there was no significant difference anymore between the best ring and the other contacts (apart from the worst segmented contact). This suggests an optimal stimulation intensity for complete suppression of rigor for the best ring contact. The best ring contact with the therapeutic threshold at 1.1 mA (Figure 2A), has usually (but not always) the contact with the largest therapeutic window (Figure 1B) and highest side effect threshold (Figure 2C), but could not be attributed to a single electrode level (Figure 1A). With regard to the therapeutic threshold, comparing the segmented contacts and the corresponding ring mode (Figure 2A) revealed no significant differences, and thus indicated that the selection of the optimal ring along the implantation trajectory had a larger influence on rigidity that directional steering (Figure 2A). This observation is supported by the comparison of the therapeutic windows of ring and segmented electrodes:

Specifically, the therapeutic window of the best ring contact was significantly larger (Figure 3A) than the second best ($p < 0.05$) and worst ring contact ($p < 0.01$). When comparing the segments to the corresponding ring mode (Figure 3B), there was only a significant difference for the clinically worst segmented contact ($p < 0.05$). The therapeutic window sizes were 2.3 mA (1.4 mA - 3.7 mA), 2.3 mA (1.3 mA - 3.6 mA), 1.6 mA (1.8 mA - 3.4 mA) and 1.2 mA (2.0 mA - 3.2 mA), for the ring mode, best, second best and worst segmented contacts, respectively. Stimulating via segmented contacts did not improve the therapeutic window in comparison to the respective ring mode (Figure 3B), but doubled the impedance ($p < 0.001$; Figure 4). This indicates that directional stimulation did not improve the treatment-relevant stimulation thresholds and would -due to increased impedances- necessitate higher power consumption than ring mode, when applied chronically.

DISCUSSION

This study showed that the therapeutic window of the best ring contact was significantly larger than the two other ring contacts, whereas stimulating via segmented contacts doubled the impedance, but did not improve the therapeutic window in comparison to the ring mode. Furthermore, complete suppression of rigidity was achieved in 90% of the patients, when stimulating at 1.1mA with the best ring contact; this therapeutic threshold was 50% better than

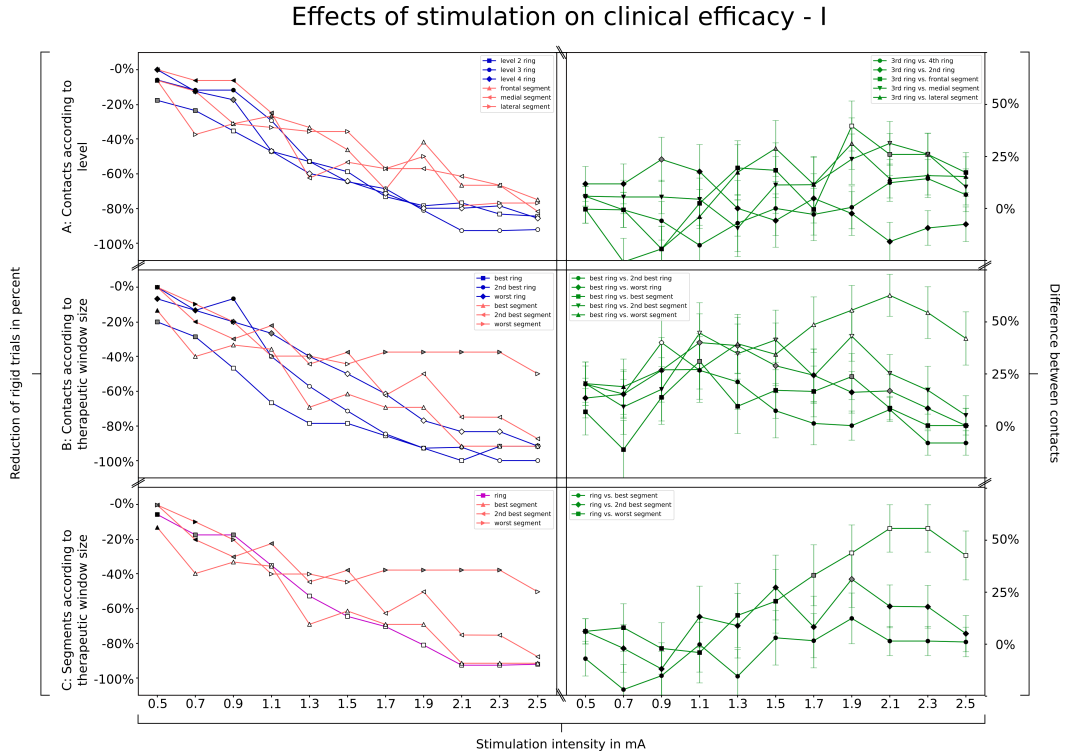

Fig. 1. Effects of stimulation on clinical efficacy - I. Subfigure A shows the findings for contacts grouped by level, subfigure B for contacts grouped by therapeutic window size and subfigures C for segmented contacts ranked by therapeutic window size in comparison to the corresponding ring mode of the same segments. White, gray and black colors of the symbols indicate significant (after MCC), significant (before MCC) and non-significant (i) reduction of rigid trials across all patients (plots on the left side), and (ii) differences between contacts (plots on the right side in green color), respectively. Specifically, 40% reduction of rigid trials at 0.7 mA with the best segmented contact indicated that 40% of patients had complete suppression of rigidity at this specific contact and intensity, a finding that was significant after MCC in comparison to baseline without stimulation. However, when comparing this effect to the effects of the other contacts at the same stimulation intensity (see plots on the right side), there was no significant difference.

the best segmented contact. These observations were unexpected in the light of previous research and technological developments in the field of DBS.

The clinical efficacy of DBS is highly dependent on the programming and contact selection during chronic stimulation (Hell et al. 2019; Kuncel and Grill 2004). To increase the clinical efficacy, the newest generation of DBS leads allows the stimulation to be directionally steered via individual segments of a ring, thereby, increasing the customizability of the stimulation. Specifically, limiting the surface of a contact shifts the electrical field that is generated by the DBS lead (Rebelo et al. 2018). This allows for more focal stimulation orientations and may thereby improve the clinical specificity. Yet, applying stimulation via a segmented lead contact may also increases the power consumption, when the stimulation intensity is not simultaneously decreased, since the smaller surface causes the impedance to increase (Eleopra et al. 2019). Therefore, for the establishment of directional steering in clinical practice, at least one of the following goals need to be achieved: Better clinical response, e.g., more patients with complete suppression of rigidity; same clinical response with less stimulation intensity, i.e., lower therapeutic threshold; larger therapeutic window, i.e., side effects at a higher stimulation threshold.

Therapeutic window sizes

The main goal of steered stimulation is to increase the size of the therapeutic window. This goal may be achieved by either decreasing the therapeutic threshold or increasing the side effect threshold. Accordingly, an increased therapeutic window size has been reported for the best segmented contact

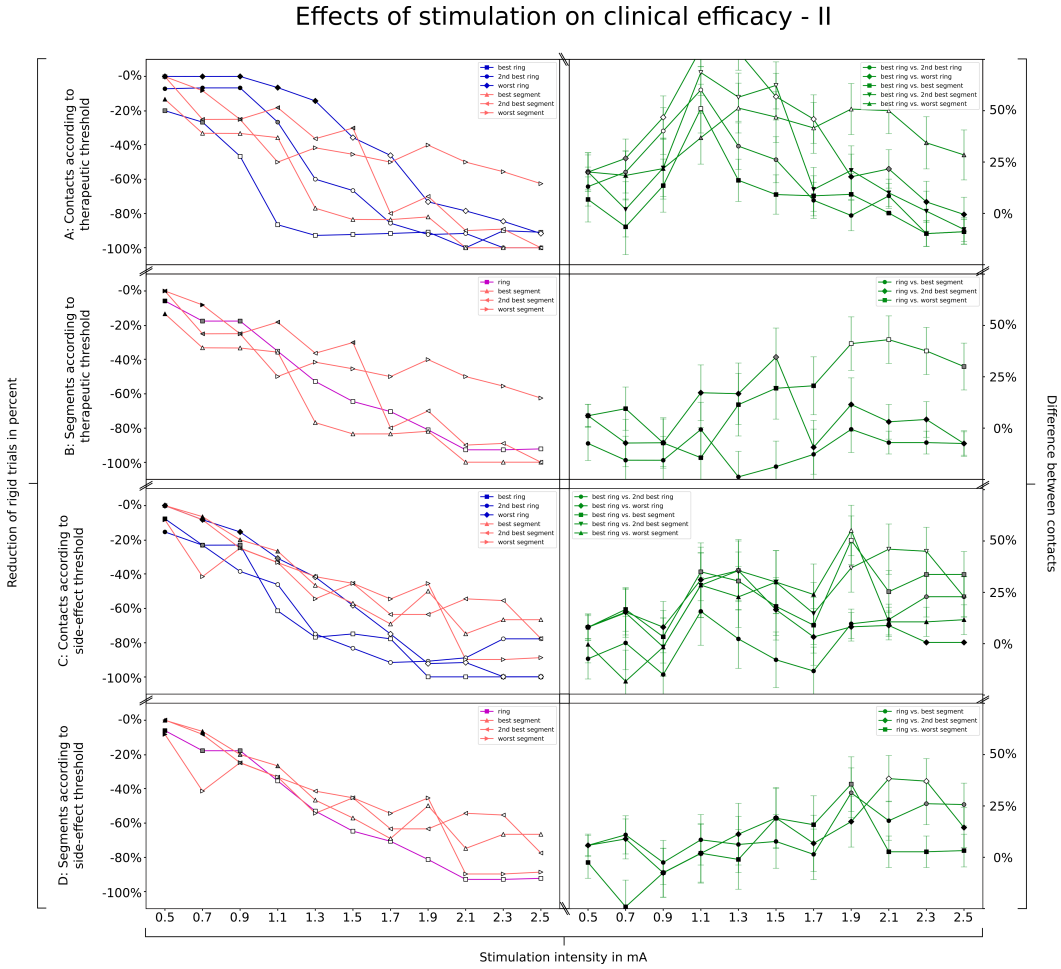

Fig. 2. Effects of stimulation on clinical efficacy - II. Same as figure 1 but for contacts grouped by therapeutic threshold (subfigure A and B), and side-effect threshold (subfigure C and D).

in comparison to ring stimulation. A significantly increased therapeutic window size was reported in (Pollo et al. 2014; Dembek et al. 2017; Bruno et al. 2020). Furthermore, a similar trend was reported in (Steigerwald et al. 2016), yet without being significant on a group level, likely due large variability across patients. This mirrors the results presented by (Contarino et al. 2014) which also indicated an increase of the therapeutic windows size in 3 of 8 patients. The findings of the present study are similar to the findings of these two latter studies. We did not observe an increased size of the therapeutic window when comparing ring and segmented contacts. Yet, steering DBS into the worst direction was associated with a significantly smaller therapeutic window compared to omnidirectional stimulation. This is mirrored in the findings of (Pollo et al. 2014) and (Bruno et al. 2020) which both report the same findings when comparing ring stimulation and steering into the worst direction.

Therapeutic thresholds

As previously mentioned, increases in therapeutic windows size may be the effect of decreased therapeutic thresholds, which may compensate for the smaller size (and increased impedance) of segmented contacts. The higher impedance in turn causes a higher power consumption as more energy is delivered (Koss et al. 2005), when the same stimulation intensity is applied. (Pollo et al.

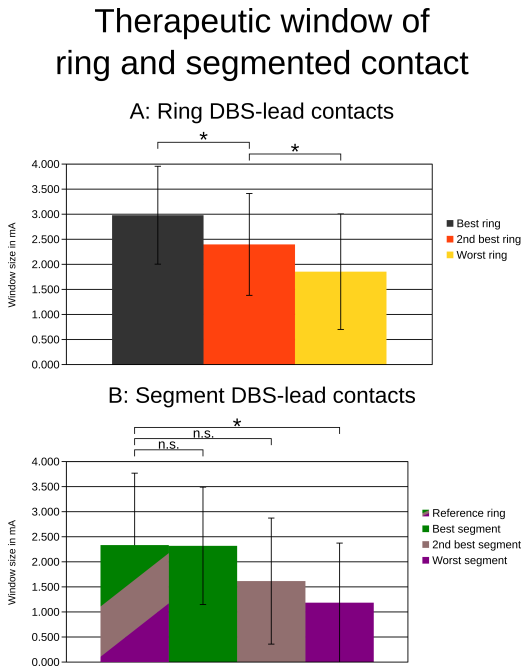

Fig. 3. Therapeutic window of ring and segmented contacts. A:The best ring contact provided a larger therapeutic window than the other two ring contacts. B: The therapeutic window of the segmented contacts and the corresponding ring contact, i.e., the sum of the three segments, was not significantly different, except for the worst segment.

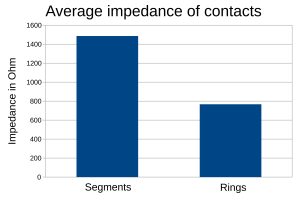

Fig. 4. Average impedance of contacts. The impedance of segmented contacts was twice as high as for ring contacts necessitating a higher energy delivery when the same stimulation parameters are applied.

2014) and (Bruno et al. 2020) reported decreased therapeutic thresholds (by 0.5 mA and 0.7 mA, respectively), when comparing the clinically most effective steering direction with ring stimulation. Yet, (Contarino et al. 2014) and (Dembek et al. 2017) did not observe significantly different therapeutic thresholds between the best segmented versus the ring contact. The results presented in this study mirror the latter findings by showing no significant difference regarding the therapeutic threshold.

Side effect thresholds

Less optimal position of the lead may particularly influence the side effect threshold. (Contarino et al. 2014) observed an increased side effect threshold via steering in 8 out of 15 cases, pushing the side effect threshold by at least 1.0 mA. This observation is further supported by the findings of (Dembek et al. 2017) who reports an increased side effect threshold (1.2 mA) when the stimulation was applied via the best segmented compared to ring contact stimuation. This is in contrast to the findings (no significant difference) of this study and the findings presented by ((Bruno et al. 2020), which also found no significant differences). These different observations are most simply explained by different locations of the electrode lead with the target structure.

Effect of positioning on therapeutic and side effect threshold

(Pollo et al. 2014) observed that the side effect threshold was dependent on the direction of the steering. The reported correlation between the directionality of the steering and the side effect threshold aligns with the physical interpretation of DBS steering: Shifting the electrical field into a certain direction. This observation can likely be extended to the therapeutic and/or side effect threshold when the lead is not optimally placed. In summary, there have been reports of increased side effect thresholds while the therapeutic threshold did not change (Contarino et al. 2014; Steigerwald et al. 2016; Dembek et al. 2017), but also decreased therapeutic thresholds while the side effect threshold remained unchanged (Bruno et al. 2020). Although each investigation used a different paradigm and titration step size (hence increasing variability between studies and decreasing comparability), other factors are most likely caused by the different findings. The most likely explanation for the observed differences is a high inter subject variability regarding the therapeutic window (as already reported by (Steigerwald et al. 2016)) and the lead positioning relative to the target structure and side effect causing close-by structures/areas. Furthermore, all of the previously discussed studies had a patient count of <15 (mostly 10). Therefore, results may potentially be biased by few patients; accordingly, (Pollo et al. 2014) reported their findings for individual patients

and not on the group level. To address this potential variability, we allocated standardized time periods of rigidity evaluation in tandem with small titration steps of the stimulation intensity.

Power consumption

Another major issue was battery lifetime as non-rechargeable impulse generators (IPG) must be replaced when the battery runs low, necessitating an additional surgery (Fakhar et al. 2013; Ondo, Meilak, and Vuong 2007). This increases the morbidity risk for the patient as IPG replacement surgery can cause infection (Themistocleous et al. 2011), with an increased likelihood with increasing number of replacements (Pepper et al. 2013). Therefore, we measured the impedance of ring and segmented contacts, and observed an increase for segmented ones in line with earlier reports (Eleopra et al. 2019). The impedance was on average twice as high for segmented contacts thereby causing the IPG when chronically applied- to consume more power since more electrical energy is delivered (Koss et al. 2005). This observation can easily be explained by the inverse relationship between capacitance (which depends on size) and impedance: The larger the stimulation electrode (higher capacitance), the lower the impedance and the power consumed. As segmented electrode are only approximately 1/3 the size of a regular ring contact, an increase in impedance was to be expected.

Limitations

To reduce the examination time for the patients, several concessions had to be made. In order to decrease the number of potential runs, stimulation intensities were increased in steps of 0.2 mA starting at 0.5 mA (after an initial OFF stimulation run) instead of smaller stimulation titration steps and a regular ramp up starting at 0 mA. The number of potential runs was further decreased by limiting the evaluations of segmented electrodes to one level (i.e., the upper level (lower level in one patient). The number of potential runs was also reduced by limiting the extended evaluation to the intensity of 2.5 mA; since we expected the therapeutic threshold to be reached with this intensity. Furthermore, only the left hemisphere (and the right arm) was investigated. Furthermore, the rigidity was binarized to either being present or being absent, and additional qualitative information on rigidity was removed in order to simplify the analysis. All these adjustments may have reduced the sensitivity of the evaluation. Furthermore, the examinations conduced in the scope of this study focused on the suppression of rigidity and stimulation induced side effects. Other potential benefits from DBS were not investigated.

Conclusion

This study investigated the potential clinical benefit of directional steering of subthalamic deep brain stimulation in patients with Parkinsons disease. Notably, stimulating via segmented contacts doubled the impedance, but did not improve the therapeutic window in comparison to the ring mode. The therapeutic window of the best ring contact was significantly larger than the two other ring contacts. Specifically, when stimulating at 1.1mA with the best ring contact, complete suppression of rigidity was achieved in 90% of the patients; this therapeutic threshold was 50% better than the best segmented contact. Therefore, the best therapeutic threshold for suppression of rigidity can be determined by selection of the optimal ring level. Since directional stimulation does not improve the response (towards rigidity suppression) and side effect threshold, and would necessitate higher power consumption than the ring mode, when applied chronically, caution is advised when choosing this option.

References

Benabid, A. L. et al. (1994). “Acute and Long-Term Effects of Subthalamic Nucleus Stimulation in Parkinson’s Disease”. In: *SFN* 62.1. Publisher: Karger Publishers, pp. 76–84.

Limousin, P. et al. (Jan. 14, 1995). “Effect on parkinsonian signs and symptoms of bilateral subthalamic nucleus stimulation”. In: *The Lancet* 345.8942. Publisher: Elsevier, pp. 91–95.

Hell, Franz et al. (2019). “Deep Brain Stimulation Programming 2.0: Future Perspectives for Target Identification and Adaptive Closed Loop Stimulation”. In: *Front. Neurol.* 10. Publisher: Frontiers.

Kuncel, Alexis M. and Warren M. Grill (Nov. 1, 2004). “Selection of stimulus parameters for deep brain stimulation”. In: *Clinical Neurophysiology* 115.11, pp. 2431–2441.

Hilliard, Justin D., Robert C. Frysinger, and W. Jeff Elias (2011). "Effective Subthalamic Nucleus Deep Brain Stimulation Sites May Differ for Tremor, Bradykinesia and Gait Disturbances in Parkinsons Disease". In: *SFN* 89.6. Publisher: Karger Publishers, pp. 357–364.

Martens, H. C. F. et al. (Mar. 1, 2011). "Spatial steering of deep brain stimulation volumes using a novel lead design". In: *Clinical Neurophysiology* 122.3, pp. 558–566.

Contarino, M. Fiorella et al. (Sept. 23, 2014). "Directional steering". In: *Neurology* 83.13, p. 1163.

Pollo, Claudio et al. (2014). "Directional deep brain stimulation: an intraoperative double-blind pilot study". In: *Brain* 137.7, pp. 2015–2026.

Dembek, Till A. et al. (2017). "Directional DBS increases side-effect thresholdsA prospective, double-blind trial". In: *Movement Disorders* 32.10. _eprint: https://movementdisorders.onlinelibrary.wiley.com/doi/pdf/10.1002/mds.27093, pp. 1380–1388.

Bruno, Sabine et al. (July 15, 2020). "Directional Deep Brain Stimulation of the Thalamic Ventral Intermediate Area for Essential Tremor Increases Therapeutic Window". In: *Neuromodulation: Technology at the Neural Interface* n/a (n/a). _eprint: https://onlinelibrary.wiley.com/doi/pdf/10.1111/ner.13234.

Steigerwald, Frank et al. (2016). "Directional deep brain stimulation of the subthalamic nucleus: A pilot study using a novel neurostimulation device". In: *Movement Disorders* 31.8. _eprint: https://movementdisorders.onlinelibrary.wiley.com/doi/pdf/10.1002/mds.26669, pp. 1240–1243.

Subthalamic Steering for Therapy Optimization in Parkinson's Disease (2020). URL: https://clinicaltrials.gov/ct2/show/NCT03548506 (visited on 09/18/2020).

Milosevic, Luka et al. (2020). "Online Mapping With the Deep Brain Stimulation Lead: A Novel Targeting Tool in Parkinson's Disease". In: *Movement Disorders* 35.9. _eprint: https://movementdisorders.onlinelibrary.wiley.com/doi/pdf/10.1002/mds.28093, pp. 1574–1586.

Hutchison, W. D. et al. (1998). "Neurophysiological identification of the subthalamic nucleus in surgery for Parkinson's disease". In: *Annals of Neurology* 44.4, pp. 622–628.

Granziera, C. et al. (Mar. 1, 2008). "Sub-acute delayed failure of subthalamic DBS in Parkinson's disease: The role of micro-lesion effect". In: *Parkinsonism & Related Disorders* 14.2, pp. 109–113.

Levin, Johannes et al. (2009). "Objective measurement of muscle rigidity in parkinsonian patients treated with subthalamic stimulation". In: *Movement Disorders* 24.1, pp. 57–63.

Scherer, Maximilian et al. (n.d.). "FiNN - A framework for the analysis for neurophysiological networks". In: ().

Rebelo, P. et al. (May 1, 2018). "Thalamic Directional Deep Brain Stimulation for tremor: Spend less, get more". In: *Brain Stimulation* 11.3, pp. 600–606.

Eleopra, Roberto et al. (Sept. 1, 2019). "Brain impedance variation of directional leads implanted in subthalamic nuclei of Parkinsonian patients". In: *Clinical Neurophysiology* 130.9, pp. 1562–1569.

Koss, Adam M. et al. (2005). "Calculating total electrical energy delivered by deep brain stimulation systems". In: *Annals of Neurology* 58.1. _eprint: https://onlinelibrary.wiley.com/doi/pdf/10.1002/ana.20525, pp. 168–168.

Fakhar, Kaihan et al. (Mar. 11, 2013). "Management of Deep Brain Stimulator Battery Failure: Battery Estimators, Charge Density, and Importance of Clinical Symptoms". In: *PLOS ONE* 8.3. Publisher: Public Library of Science, e58665.

Ondo, William G, Catherine Meilak, and Kevin D Vuong (May 1, 2007). "Predictors of battery life for the Activaő Soletra 7426 Neurostimulator". In: *Parkinsonism & Related Disorders* 13.4, pp. 240–242.

Themistocleous, Marios S. et al. (Mar. 23, 2011). "Infected internal pulse generator: Treatment without removal". In: *Surg Neurol Int* 2.

Pepper, Joshua et al. (2013). "The Risk of Hardware Infection in Deep Brain Stimulation Surgery Is Greater at Impulse Generator Replacement than at the Primary Procedure". In: *SFN* 91.1. Publisher: Karger Publishers, pp. 56–65.

ADDITIONAL INFORMATION

Study funding

This was an investigator initiated study that was sponsored by the University Hospital Tübingen and supported by Abbott within the SANTOP clinical trial (NCT03548506).

Competing interests

The authors declare no competing financial interests.

State-dependent decoupling of interhemispheric motor networks with effective deep brain stimulation in Parkinson's disease

Maximilian Scherer*, Luka Milosevic*, Patrick Bookjans*, Bastian Brunett[1], Idil Hanci*†, Robert Guggenberger*, Daniel Weiss† and Alireza Gharabaghi*
Institute for Neuromodulation and Neurotechnology, Department of Neurosurgery and Neurotechnology, University Hospital Tübingen, University of Tübingen, Tübingen, Germany *
Hertie Institute for Clinical Brain Research, Department of Neurodegenerative Diseases, and German Center of Neurodegenerative Diseases (DZNE), University of Tübingen, Tübingen, Germany †

Abstract*—Subthalamic deep brain stimulation (STN-DBS) is an established treatment option for the management of motor symptoms in Parkinsons disease (PD). Knowledge on the physiological underpinnings at the transition from clinically ineffective to effective DBS is, however, scarce. In this study, we intended to differentiate general stimulation-induced changes from therapeutically relevant network effects of DBS during movement and rest. In seventeen akinetic-rigid PD patients, the rigidity of the contralateral biceps brachii muscle was evaluated during unilateral subthalamic stimulation in the dopaminergic medication OFF state. In each patient, the stimulation intensity was increased in 0.2 mA steps during a monopolar review of circular and segmented contacts. Simultaneous electroencephalography (EEG) and electromyography (EMG) captured intensity-dependent changes of spectral power, and of cortico-cortical and cortico-muscular oscillatory synchronization during movement and rest. The data was evaluated using (generalized) linear mixed models. The step-wise increase of stimulation intensity revealed a general broad band power reduction, which was more pronounced in the EEG and EMG spectrum for the rest and movement conditions, respectively. These effects were more apparent and consistent for the circular than the segmented contacts. Therapeutic efficacy was characterized by a more specific pattern regarding cortical topography and spectral changes; effective suppression of rigidity was paralleled by interhemispheric beta band decoupling of motor areas, increased movement related beta modulation range, and movement-related increases of beta band cortico-muscular coherence. Notably, these network changes were stimulation intensity-dependent up until the transition from clinically ineffective to effective DBS. Interhemispheric synchronization may inform the titration of stimulation parameters and provide a physiological marker during both rest and movement - for adaptive DBS.

INTRODUCTION

About 1% of the global population over the age of 60 is affected by Parkinsons disease (Lau and Breteler 2006). Parkinsons disease (PD) is characterized by a degeneration of dopaminergic neurons in the nigrostriatal pathway (Riederer and Wuketich 1976) causing pathological changes of motor (Albin, Young, and Penney 1989) and non-motor functions (Chaudhuri and Schapira 2009). In cases of medically-refractory Parkinsons disease, deep brain stimulation (DBS) of the subthalamic nucleus (STN) is an efficacious surgical option, and has been shown to be particularity effective for the management of antikinetic-rigid symptoms (Benabid et al. 1994; Limousin et al. 1995).

Muscular rigidity is defined as an elevated resistance to passive movement due to increased muscle tone (Fahn 2007). Not surprisingly, parkinsonian rigidity has also been associated with an increase in electromyography (EMG) activity, especially during passive movement (Meara and Cody 1992; Levin et al. 2009).

In healthy subjects, a desynchronization of cortical beta activity is commonly observed during active and passive movements; after the movement

a short time post movement beta synchronization occurs (Cassim et al. 2001; Formaggio et al. 2013). This movement related beta modulation range (between desynchronization and synchronization) is decrease in PD patients (Lim et al. 2006; Degardin et al. 2009; Heinrichs-Graham, Wilson, et al. 2014). Yet, not only the sensorimotor beta band modulation range during movement is altered, but also the beta band power levels at rest. The resting state beta band power measured both in the basal ganglia and the motor cortex is different in untreated PD patients compared to healthy controls (P. Brown 2006; Heinrichs-Graham, Kurz, et al. 2014). However, the cortex is not only locally affected by pathological beta activity, but also on a network level. Increased interhemispheric cortico-cortical coherence (CCC) in the beta band has been reported in PD patients compared to healthy controls (Stoffers, Johannes L. W. Bosboom, et al. 2008). Furthermore, a decrease in cortico-muscular coherence (CMC) compared to healthy controls has also been shown (Salenius et al. 2002). The reported pathological observations in PD patients are likely connected to pathological subcortical activity in the beta band. Increased subthalamic beta activity in the basal ganglia, often considered antikinetic (Jenkinson and Peter Brown 2011), has been associated with antikinetic-rigid features of Parkinsons disease (Peter Brown 2003; Kühn, Tsui, et al. 2009). Yet, this activity is not constant, but rather phases in and out due to its bursty nature (Tinkhauser et al. 2017). Subthalamic beta activity has been extensively studied and is known to be hypersynchronized in most PD patients (Uhlhaas and Singer 2006; Hammond, Bergman, and Peter Brown 2007; Kühn, Tsui, et al. 2009). Both cortical (Silberstein et al. 2005; Devos and Defebvre 2006) and subcortical abnormalities were shown to be correlated with the severity of motor symptoms in PD (Peter Brown 2003; Kühn, Kupsch, et al. 2006; Kühn, Tsui, et al. 2009).

Applying high-frequency DBS to the subthalamic nucleus is hypothesized to create an information lesion (Grill, Snyder, and Miocinovic 2004) between the STN and other structures within the cortico-basal-ganglia loop. On a local level, STN-DBS has been shown to suppress the pathologically high beta activity within the STN (Oswal et al. 2016). On a network level, DBS of the STN has been reported to normalize connectivity throughout the cortico-basal-ganglia loop towards healthy controls (Horn et al. 2019) by modulating the major components of the cortico-basal-ganglia loop (Kahan, Urner, et al. 2014). In particular, the thalamo-cortical pathway has been reported to be strengthened (Kahan, Urner, et al. 2014; Kahan, Mancini, et al. 2019; Horn et al. 2019). Furthermore, STN-DBS has also been reported to reduce the coupling between the STN and premotor areas (Oswal et al. 2016). This is line with reports of STN-DBS not only affecting the STN itself, but also functionally connected structures (H.-M. Chen et al. 2018; Weiss et al. 2015). On the cortical level, STN-DBS has been observed to reduce cortical activity measured above the sensorimotor cortex (Abbasi et al. 2018; Luoma et al. 2018). This is in contrast to the effect from administering levodopa which increases cortical activity in the beta band (Heinrichs-Graham, Kurz, et al. 2014). Dopaminergic medication has also been observed to normalize the sensorimotor-cortical beta modulation range (Degardin et al. 2009; Meissner et al. 2018). Similar observations apply to the effects on cortico-cortical coupling. Both dopaminergic medication (Heinrichs-Graham, Kurz, et al. 2014) and STN-DBS (Silberstein et al. 2005; Weiss et al. 2015) have been shown to decrease cortico-cortical coupling. Yet, the findings on the effects of STN-DBS on cortical coherence are not uncontested as opposing results have been shown with data acquired via magnetoencephalography (MEG) (using another connectivity metric, (Boon, Hillebrand, et al. 2020)) compared to electroencephalography (EEG) based findings. Yet, not only cortico-cortical coupling was affected by levodopa and STN-DBS, increases in cortico-muscular coupling have also been observed (Salenius et al. 2002). As with the findings on cortico-cortical connectivity, these results remain not uncontested as (Hirschmann et al. 2013) reported no normalization due to medication. In a similar fashion did (Airaksinen et al. 2015) not find a consistent effect of STN-DBS on CMC. Furthermore, while (Hirschmann et al. 2013) found a correlation between CMC levels and akinesia/rigidity, these observations could not be replicated in (Airaksinen et al. 2015).

The aforementioned pathophysiological phenomena have been reported to diminish under the influence of levodopa or DBS (Silberstein et al. 2005; Kühn, Kempf, et al. 2008; Levin et al. 2009; Giannicola et al. 2010; Eusebio et al. 2011; Hirschmann et al. 2013; Chung et al. 2018), when

comparing ON and Off conditions. Accordingly, the pathological effects of Parkinsons disease and its treatments (dopaminergic medication/STN-DBS) have a local and network level component (Boon, Geraedts, et al. 2019). However, the mechanisms related the transition from ineffective to effective stimulation for suppression of rigidity are not fully understood (Hess and Hallett 2017).

In this study, we therefore investigated how STN-DBS effects the aforementioned metrics (i.e. EEG power, CCC, EMG power, and CMC) with a particular focus on the electrophysiological differences between stimulation which was effective in completely suppressing rigidity compared to intensities where were ineffective or suboptimal. In particular, we aimed to conceptualize how STN-DBS may be used to shift brain network dynamics from a pathological state towards a state that is more similar to the state observed in healthy subjects.

METHODS

Patients

The patients of this study were part of the SANTOP study (*Subthalamic Steering for Therapy Optimization in Parkinson's Disease* 2020; ClinicalTrials.gov: NCT03548506). The goal of SANTOP was to evaluate the long-term effects of omnidirectional (circular/ring) vs. directional (steered) deep brain stimulation in akinetic-rigid Parkinsons disease (PD) patients in a randomized, cross-over protocol six months after surgery, which will be reported elsewhere. The present work is based on electrophysiological data acquired in the scope of a monopolar review conducted ten weeks after surgery on two consecutive days, i.e., evaluating the three upper ring contacts (day 1) and the three segments of the upper segmented level (day 2). This evaluation could be completed in seventeen PD patients, in whom the rigidity of the right biceps brachii muscle was assessed during DBS of the left subthalamic nucleus in the dopaminergic medication-off state. The detailed clinical findings of this evaluation are reported elsewhere (Scherer, Milosevic, Bookjans, et al. n.d., in preparation). The present work reports the respective electrophysiological findings in these patients, i.e., electroencephalography (EEG) and electromyography (EMG) activity. Each patient underwent bilateral implantation of STN-DBS leads (6170, Abbott laboratories, Lake Bluff, Illinois, U.S.) on average 69 days prior to the evaluation. Preoperative target identification was based on magnetic resonance imaging (MRI) and computer tomography (CT) imaging. This information was intraoperatively supplemented by microelectrode recordings (Hutchison et al. 1998), local field potential recordings (Milosevic, Scherer, et al. 2020), and test stimulation with clinical evaluation. The target position was postoperatively confirmed via CT imaging, which was co-registered with the preoperative MRI. The patients were examined several weeks after the DBS lead implantation to avoid micro-lesion effects (Granziera et al. 2008), and after overnight withdrawal from dopaminergic medications. The electrophysiological stimulation effects could be evaluated in all seventeen patients (Figure 1 and 2); the comparisons between effective vs ineffective stimulation were possible in twelve patients (Figures, 3, 4 and 5), since this analysis required enough data of both condition (effective and ineffective trials) for robust statistical estimation. Written informed consent was provided by all patients and the study was approved by the ethics committee of the Medical Faculty Tübingen. Detailed information on patient demographics is available in table 1.

ID	Full examination	Sex	Age (during surgery; years)	Time between surgery and examination (days)
0	No	m	65	88
1	No	f	61	61
2	Yes	m	58	78
3	Yes	m	71	71
5	Yes	f	53	62
6	No	f	58	63
9	No	m	68	62
15	Yes	f	75	61
16	Yes	m	59	67
20	Yes	m	73	64
21	Yes	m	71	64
22	Yes	m	66	75
23	Yes	m	67	64
25	Yes	m	61	87
26	No	f	52	57
27	Yes	m	50	64
28	Yes	m	67	79

Table 1: Patient information.

Stimulation configuration

In seventeen patients, the three upper ring contacts were evaluated. In addition, three segments of the upper and lower segmented level were investigated in sixteen patients and one patient, respectively. Stimulation was always applied at 130 Hz and 60 µs, while stepwise increasing the stimulation intensity (see experimental protocol). Stimulation

was applied unilateral to the left hemisphere, while rigidity was assessed on the right arm.

Experimental protocol

The patients were instructed to relax their arms and stay awake. Each run lasted 90 seconds and was compromised of two phases: A non-movement phase (30 s) and a continuous passive movement phase (60 s). During the continuous passive movement phase, an examiner moved the subjects arm with a frequency of 0.5 Hz (acoustically communicated to the examiner via headphones). At the end of each run, the examiner provided an estimate of the patients rigidity according to the MDS-UPDRS assessment. For later analyses, these scores were binarized to represent either a lack (UPDRS score of zero) or the presence of rigidity. In the first run, patients were evaluated OFF stimulation. In the consecutive runs, stimulation was increased from 0.5 mA to 2.5 mA in 0.2 mA increments on one stimulation contact before switching to another contact. The contacts were evaluated in randomized order. Before switching contacts, the paradigm was paused for two minutes to avoid stimulation related carry-over effects (Levin et al. 2009). Above 2.5 mA, the evaluation was continued in 0.2 mA increments; however, the evaluation was focused on side effects only, i.e., without concurrent arm movements. The patient and the examiner did not know which stimulation contact was evaluated at which intensity, since the programming was performed by a third person.

Data acquisition

We recorded simultaneously and synchronized 64 channels of electroencephalography (EEG) and two channels of electromyography (EMG) data via BrainAmp DC/EXG amplifiers (Brain Products, Munich, Germany). Data were sampled at 5 kHz. No software filters were applied during data acquisition. The EEG electrode setup was according to the extended 10-20 system, and EMG electrodes were position above the biceps (two channels, for redundancy).

Determining therapeutic window size

The therapeutic window size was defined by the range from onset of continuous rigidity suppression until the appearance of side effects. The first stimulation intensity with side-effects was not considered as part of the therapeutic window.

Classifying contacts

The contacts were grouped on the basis of different categories: (i) according to level, i.e., ring 4 (most upper), ring 3 (second most upper), ring 2 (third most upper), frontal segment, medial segment, lateral segment; (ii) therapeutic window size, i.e., best, second best, worst ring/segment; (iii) therapeutic threshold, i.e., best, second best, worst ring/segment.

Electrophysiological pre-processing

During rest, i.e., non-movement, each 2 s interval was considered an individual trial whereas during movement, trials were defined by a complete flexion and extension cycle (2 s). The movement-related flexion and extension phases were identified via the large-amplitude low-frequency artifact within the EMG signal. This component was extracted by band-pass filtering the EMG signal from 0.25 to 0.75 Hz. Subsequently, peaks and valleys were detected in order to reconstruct the individual trials. Trials shorter than 1 s or longer than 3 s were discarded. In order to balance non-movement and movement, and furthermore remove any movement onset effects, only the last 30 s of the movement phases were evaluated.

Faulty EEG channels were detected using a semi-automated approach. In order not to bias any subsequent analysis, only frequency bands (105-120Hz; 135-145Hz; 155-195Hz) that were not further evaluated within the study, were investigated to determine a channels signal quality. If a channels power in these frequency bands diverged on average more than three standard deviations from the outlier-removed mean power of all 64 EEG channels within these frequency bands, it was considered a faulty channel. The z-distribution of the channels was subsequently plotted and automatic identification was manually verified and optimized. Faulty EEG channels were iteratively substituted by averaging up to four neighboring (non-faulty) EEG channels, and reconstructing the channel with the most available neighbors during each iteration. EMG channels were visually screened to evaluate signal quality.

The raw EEG data were low-pass filtered below 500 Hz and subsequently downsampled to 1 kHz. An adaptive notch filter was applied in the frequency domain to remove line-noise (50 Hz), the stimulation artifact (130 Hz), and artifacts at their respective harmonics. Afterwards, the EEG data were re-referenced using common average re-referencing. The raw EMG data were likewise filtered with the same adaptive notch filter to remove line-noise, the stimulation artifact, and artifacts at their respective harmonics.

Computation of EEG power

The pre-processed EEG data were cut into individual trials using the previously mentioned reconstructed trial markers. Applying Welchs method (Welch 1967), the power spectral density (PSD) of each trial was calculated (1 Hz bins, 50% overlap), and the relative power was defined as the sum of a frequency bands power relative to the overall power between 0 and 300 Hz. The following frequency bands were evaluated: Theta (4-7 Hz), alpha (8-12 Hz), beta (13-32 Hz), and low gamma (33-48 Hz).

Computation of EMG power

After linearly detrending each pre-processed EMG trial individually, an envelope was calculated by taking the absolute value of the EMG signals Hilbert transform. Subsequently, the enveloped data were cut into the aforementioned frequency bands. For each frequency band and each trial, the power was estimated as the mean value of the envelope.

Computation of cortico-cortical connectivity (CCC)

Complex coherency was calculated using the pre-processed EEG data. The strength of the connectivity between channels was calculated as the absolute value of the complex coherency (commonly referred to as magnitude squared coherence), whereas the direction of the connectivity was calculated as the signum of the complex coherencys imaginary part. Furthermore, the imaginary part of the broad band coherence was screened for low absolute values, which would be indicative of either volume conductance or a general low coherence (Scherer, Milosevic, Guggenberger, et al. n.d.(a), in preparation). In order to investigate which cortical regions changed their connectivity level due to, i.e., movement or stimulation, the sum of all absolute connectivity values between a channel within a seed region (left motor cortex) and all possible other target EEG channels outside of this seed region was calculated. The left motor cortex was selected as a seed region due to the prominent role of the left motor cortex in contralateral right movement. Connectivity values of channels within a target region were clustered. The individual regions are described in fig. 5. This connectivity analysis provides information on the strength of the total connectivity of a particular region to the seed region. The connectivity values were thresholded at 0.4 in order to remove the effect of small connectivity values (such as random fluctuations). Connectivity values below the threshold were corrected to 0.

The estimation of connectivity strictly requires multiple time-shifted windows. Furthermore, the reliability of a stationary connectivity estimate increases with a larger number of individual time-shifted windows and a longer total time-frame. In order to maximize the reliability of the connectivity estimates in this study, the full 30s of a runs rest/movement phase were used for a single connectivity estimation (i.e., the data were not epoched, and metrics were derived from complete time courses of the rest/movement trails). The beta band was chosen due to this frequency band's relevance in subcortical pathological electrophysiology (P. Brown 2006) and the importance in movement tasks (Gaetz et al. 2010).

Computation of cortical muscular connectivity (CMC)

This metric was calculated identically to the CCC method described in the previous section, except using the pre-processed EEG data and the pre-processed EMG data. Only connectivity estimates from EEG to EMG were evaluated. CMC was calculated between the EMG recordings and in the individual cortical areas described in the caption of fig. 5. We also focused the CMC analysis to the beta band as the primary frequency band for cortico-muscular communication.

Faulty trial rejection

Individual trials were z-transformed and marked as faulty if their z-score passed a threshold of 3. In order not to bias the results of this study, the trial

rejection was performed on isolated data subsets. A data subset encompassed data from a single patient, either at rest or during movement, with a fixed stimulation configuration. Faulty trial rejection was only performed for EEG and EMG power as this processing step necessitates multiple trials extracted from a single run.

Statistical evaluations

(Generalized) Linear mixed models were employed throughout this study. To assess the effects of movement (termed movement), we contrasted the states rest and movement. The general effect of stimulation intensity (termed stimulation intensity) was assessed as a regression over the effects of the individual stimulation intensities. We furthermore contrasted the states ON- and ON+ in order to examine electrophysiological differences between runs which were clinically effective, i.e., rigidity-free (ON+), and ineffective runs, i.e., those with residual rigidity (ON-); whereas the effect of stimulation alone does not take into account clinical efficacy. We furthermore included an interaction effect between stimulation intensity and movement to investigate whether stimulation had different effects depending upon whether a patient was moving (passively) or at rest. E.g. ON+ may show different effects at rest compared to movement. Furthermore, we assumed a possible interaction between stimulation intensity and ON- vs. ON+ as increasing the stimulation intensity after being clinically effective may have different effects from increases prior to clinical effectiveness. Additionally, we included an interaction effect between movement, ON- vs. ON+, and stimulation intensity. The fixed factor stimulation intensity (continuous), and the random factors patient ID and stimulation contact (nested within patient id) were included in the analysis of all metrics. Furthermore, the following factors were included when a respective contrast was possible: Movement (fixed factor categorical), the contrast between ON- vs. ON+ (fixed factor categorical), trial index (random factor), channel index (random factor) and the respective interaction effects. Inclusion of the trial index and the channel index as random factors corrected for repeated measurements within either the same run or when pooling multiple EEG channels from a distinct area into a region. Differences between patients are modeled by the random factor patient ID. Differences in electrode position and/or orientation are modeled by the random factor stimulation contact which is nested into patient ID, as the electrode positions and orientations vary uniquely from patient to patient. In case of significant interaction effects, subsequent analyses were performed to investigate the discovered dependency between factors. In case DBS OFF was compared to specific stimulation intensities (fig. 2), the analysis was limited to the beta band due to the relevance of this frequency band in movement tasks (Gaetz et al. 2010). The data were corrected for multiple comparisons using the conservative Bonferroni-method and an alpha value of 0.05. All results are presented with a marker indicating either non-significance or significance after MCC.

Code and data accessibility

Data and evaluation code will be shared upon request. The custom toolbox used to analyze the data will be made publicly available on GitHub (Scherer, Milosevic, Guggenberger, et al. n.d.(b), in preparation).

RESULTS

Effects of stepwise increases in stimulation intensity on EEG and EMG activity

EEG activity showed a progressive stepwise decrease in power with increasing stimulation intensity across all frequency bands (fig. 1A). The general effect of stimulation intensity induced by STN-DBS on cortical power was more pronounced during resting state phases compared to movement phases. During movement, also EMG activity showed a progressive stepwise decrease in power with increasing stimulation intensity, whereas there was no slope during rest (fig. 1B).

Effects of ring and segment delivered stimulation on beta band power

Systematic increases of stimulation intensity led to a continuous decrease in beta band power only if DBS was applied via the ring (but not the segmented)contacts (fig. 2; left side). This observation was independent of the grouping of the contacts (level vs. therapeutic window size vs. therapeutic threshold). Consequently, increasing stimulation intensity led to a significant and increasing physiological difference between stimulation with the ring and segmented contacts (fig. 2; right side).

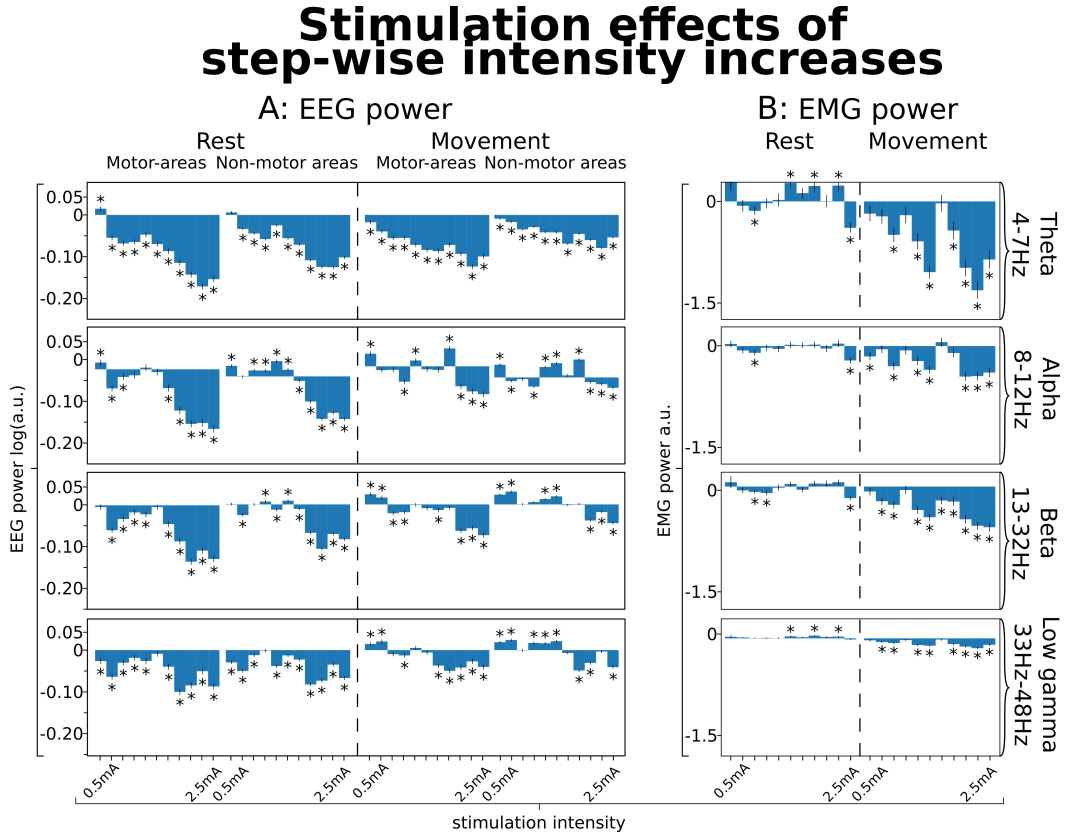

Fig. 1. Stimulation effects of step-wise intensity increases. (A) EEG power was assessed for the left and central motor areas (denoted motor areas) and all remaining areas (denoted remaining areas); generally, stepwise decreases in EEG power were found in most frequency bands (more pronounced in lower frequency bands), both during rest (more pronounced) and with movement. (B). In EMG, no pattern could be observed during rest with increasing stimulation intensity; during movement, increasing stimulation was associated with a decrease in EMG power. Significant changes are marked with a star.

Effects of movement and stimulation on overall cortical power

Movement of the right arm induced a significant desynchronization in the contralateral sensorimotor area in the alpha and beta bands (fig. 3A; ON- & ON+). The movement related desynchronization in the contralateral hemisphere was stronger during ON+ compared to ON- (fig. 3A; ON- & ON+). The contrast of ON- vs. ON+ revealed a significant desynchronization of cortical activity in the beta band (spatially distributed) (fig. 3B). Investigation of the significant interaction between stimulation intensity and ON- vs. ON+ showed that STN-DBS did not decrease cortical activity in the motor areas further after becoming effective (not depicted). The general effect of stimulation intensity was significant and presented as a widespread desynchronization across the cortex (not depicted).

Effects of movement and stimulation on EMG power

Increases in stimulation intensity at rest did not considerably reduce EMG power, neither during ON- nor ON+ (fig. 4). However, increases in stimulation intensity during ON+ and movement led to a large, significant reduction of EMG power; whereas the effect of increases of stimulation intensity during movement and ON- were comparable to the effects observed at rest. Generally, all stimulation dependent effects were strongest in the theta band and declined with increasing frequency.

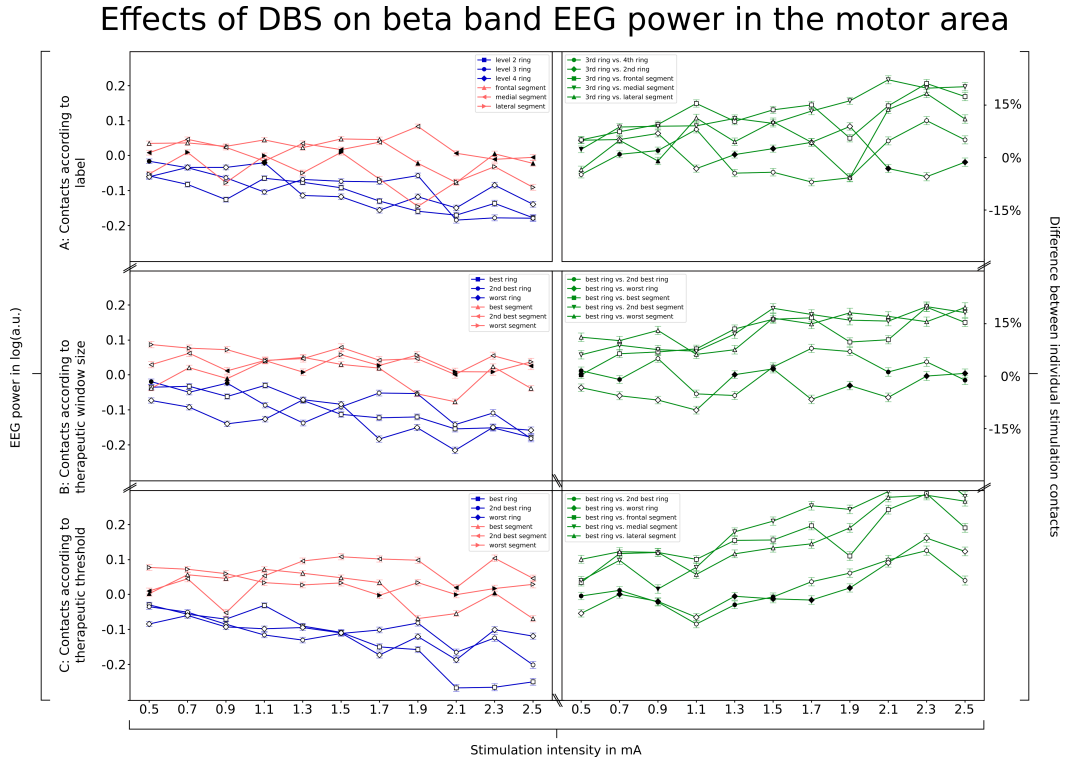

Fig. 2. Effects of DBS on beta band EEG power in the motor area. Increasing stimulation intensity leads to a decrease of cortical beta band activity measured above the motor area. However, this effect was limited to stimulation applied via ring contacts and was not observed for stimulation applied via segmented contacts regardless of contact grouping.

Effects of movement and stimulation on CCC and CMC

We observed a net reduction in interhemispheric sensorimotor beta band CCC when comparing ON- to ON+. Closer investigation showed that increasing the stimulation intensity during ON- reduced CCC until the stimulation was clinically effective (ON+; i.e., absence of any rigidity). After stimulation became clinically effective, CCC was not reduced any further. The same pattern was observed for beta band CMC during movement.

While beta band CCC was not affected by movement (fig. 5A), we observed a significant decrease in interhemispheric CCC during ON+ compared to ON- (fig. 5B). This decrease was more pronounced during the movement phase (higher magnitude) as compared to the resting phase. It was additionally found that stimulation intensity scaled with interhemispheric sensorimotor beta band CCC decrease during ON- (fig. 5C; ON-) both at rest and movement, but not during ON+ (fig. 5C; ON+). Likewise, the effect of stimulation intensity on beta band CMC scaled with stimulation intensity during ON- (fig. 5D). Although a further beta band CMC increase was observed during ON+, this increase was much weaker in amplitude and not significant.

The observed different behavior of beta band CCC and CMC for ON- and ON+, when increasing the intensity, is likely due to an already achieved effective threshold towards the end of ON-. This implies that after reaching this threshold of sensorimotor beta band CCC/CMC reduction, further stimulation intensity increases cause neither additional CCC/CMC decrease, nor increased clinical benefit (which is the discriminative criterion for ON+).

Discussion

In this study, we demonstrated a progressive DBS intensity-dependent reduction of bilateral motor cortex CCC in the beta band. This scaling was only present when the stimulation was clinically still suboptimal (defining criterion of ON-) and vanished

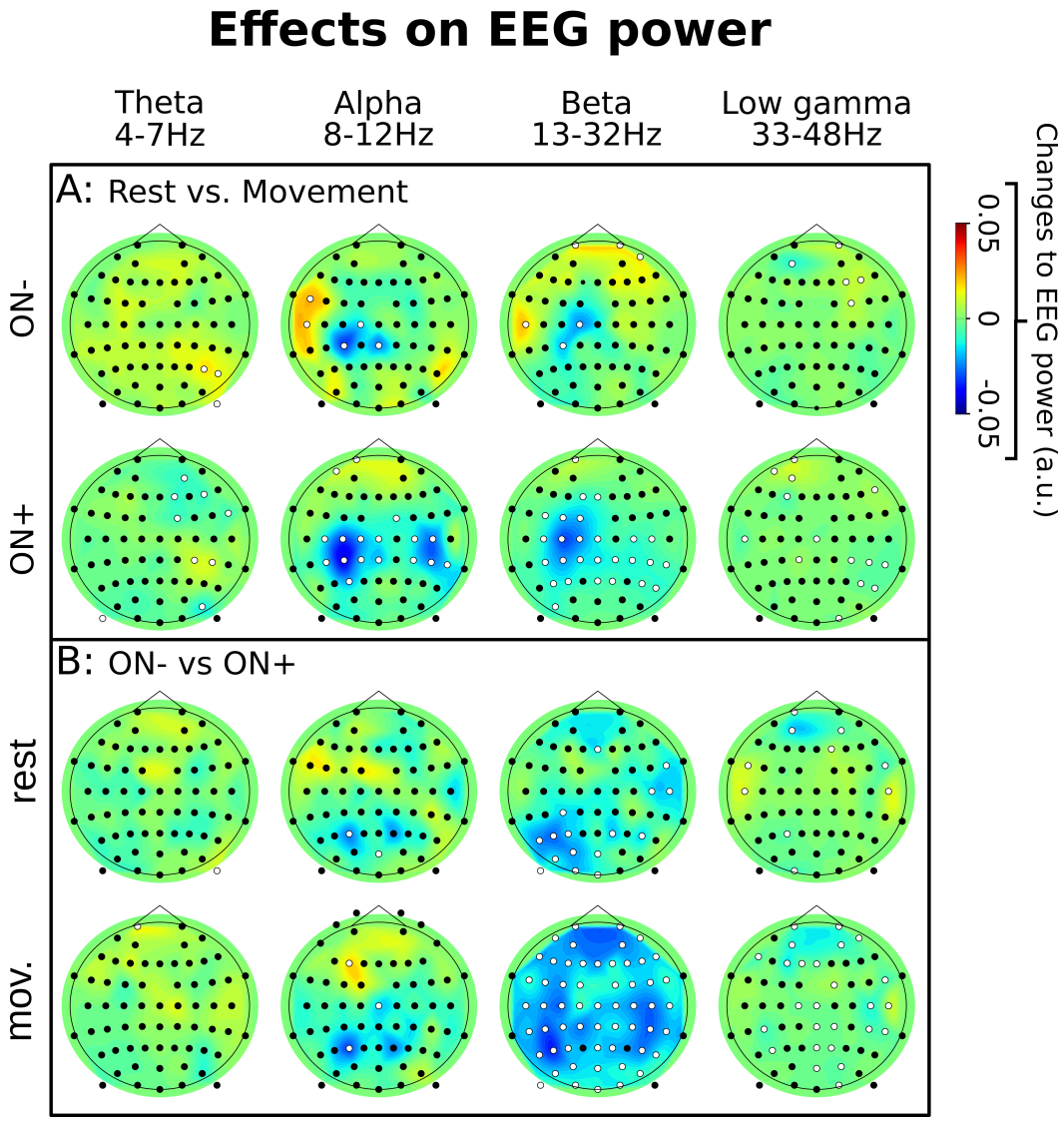

Fig. 3. Effects on EEG power. (A) Movement effects were stronger during ON+ compared to ON- in both the alpha and the beta band. (B) A contrast between ON- vs. ON+ was primarily observed in the beta band, this contrast was stronger during movement compared to rest. Black dots represent non-significant channels, white dots represent significant channels.

once stimulation was clinically fully effective, i.e., complete rigidity suppression (defining criterion of ON+). In line with this observation, we found the average bilateral motor cortex CCC in the beta band to be higher during ON- compared to ON+. Similar observations were made in regards to ipsilateral (towards the passive movement) CMC. We also observed a progressive, DBS intensity-dependent CMC increase during ON- which was much less pronounced during ON+. In tandem with these observations, we observed an increase in movement related beta-modulation range during ON+ compared to ON-. Thus, effective STN-DBS decreases the coupling between motor cortices (during both rest and passive movement), and increases the modulation range and cortico-muscular coherence in the beta band. A connection between the decrease in bilateral sensorimotor beta-band coupling and the reduction of the coupling between the STN and premotor areas (Oswal et al. 2016) is likely. By

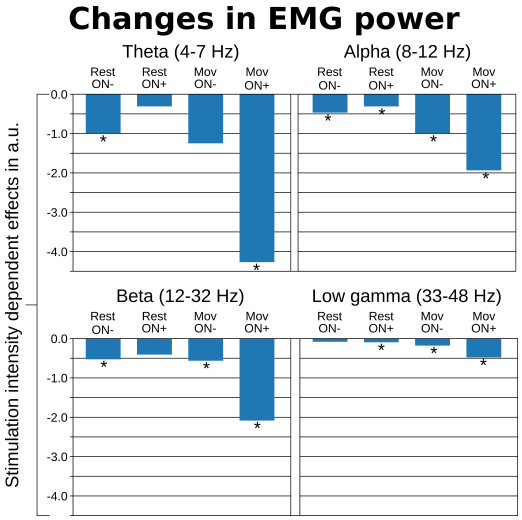

Fig. 4. Changes in EMG power. Increases in stimulation intensity were associated with a decrease in EMG power, albeit with a strong magnitude only during ON+ and movement. Significant changes are marked with a star.

decreasing this coupling, cortical activity is likely less locked to (pathological) subcortical activity, hence increasing the modulation range, which in turn likely enables better motor control. Future systems, which allow for DBS and concurrent, chronic electrocorticography recording my harness these findings for adaptive DBS (Swann et al. 2018; Neumann et al. 2019).

Network coupling in Parkinson's disease

Cortico-cortical coherence (CCC) describes the level of synchrony (inverse to independence) across different cortical areas. Beta band CCC across sensorimotor cortices has been shown to be greater in patients with Parkinsons disease compared to healthy controls (Stoffers, J. L. W. Bosboom, et al. 2008), implicating a lack of independence across cortices. As such, cross-hemispheric CCC may explain the increase in rigidity with activation of contralateral limbs (i.e., activation maneuver; although this phenomenon was not directly studied here) (Powell, Hanson, et al. 2011). Increased cross-hemispheric sensorimotor CCC may also strengthen local beta synchrony, resulting in a reduction of the modulation range of beta power (such as movement-related changes in beta band activity). Heinrichs-Graham and colleagues (Heinrichs-Graham, Wilson, et al. 2014) have demonstrated that the modulation range of beta (and alpha) band power was indeed lower in patients with Parkinsons disease compared to healthy control subjects, while (Silberstein et al. 2005) showed that increased CCC correlated with the severity of parkinsonian features (UPDRS based). Thus, it is conceivable that sensorimotor beta band power cannot be modulated as dynamically during periods of increased cross-hemispheric CCC. Our findings demonstrate that sensorimotor beta band CCC was overall more reduced during ON+ compared to ON- (fig. 5B). This generally greater reduction of CCC with ON+ was indeed associated with greater levels of movement related reductions of beta band power (i.e., increased modulation range; as seen in fig. 2A; Beta). Taken together, these findings support the hypothesis that reduced beta band CCC may allow for greater movement related modulation of beta band power, which is related with the alleviation of rigid symptoms. Indeed, the increased cortico-cortical coupling in Parkinsons disease has been shown to be suppressed both by the administration of levodopa (Silberstein et al. 2005; Stoffers, Johannes L. W. Bosboom, et al. 2008) and through STN-DBS (Silberstein et al. 2005; Weiss et al. 2015). While CCC has been shown to be greater in patients with Parkinsons disease, CMC was shown to be reduced (Salenius et al. 2002; Sridharan et al. 2019), and this reduction is thought to be associated with the presence of rigidity (Mazzoni, Shabbott, and Cortés 2012; Airaksinen et al. 2015). From a mechanistic perspective, greater levels of CMC are thought to be indicative of better motor control (Lattari et al. 2010), i.e., more efficacious communication between the brain and periphery. Accordingly, we found increases in CMC during movement and clinically efficacious stimulation (fig. 5D). Yet, this effect appears to confined to the ispilateral (towards the movement) hemisphere. Although the left (contralateral) hemisphere is mainly responsible for right arm movement (BRINKMAN and KUYPERS 1973), there is a substantial contribution towards right arm movement from the ipsilateral hemisphere on a single neuron (Tanji, Okano, and Sato 1988; Donchin et al. 2002), and a multi-neuron level (R. Chen, Cohen, and Hallett 1997; Verstynen et al. 2005). Noteworthy, post movement hypersynchronization of beta band activity is one of the mechanisms which is not confined to the contralateral hemisphere, but also present in the ispilateral hemisphere (Cassim et al. 2001). This

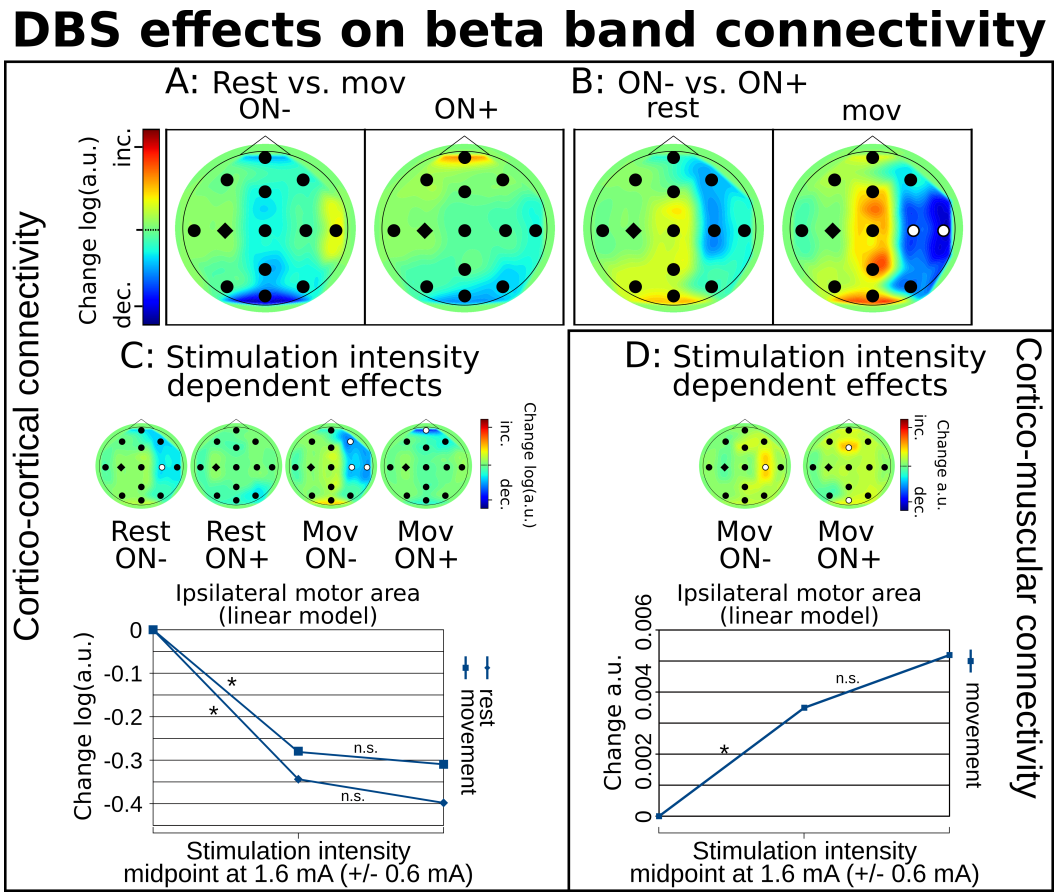

Fig. 5. DBS effects on connectivity in the beta band. Subfigures (A) to (C) describe cortico-cortical coupling effects in the beta band whereas subfigure (D) describes cortico-muscular coupling effects in the beta band. (A) This figure shows the contrast of rest vs. movement for ON- and ON+, separately. Movement did not induce significant (de)coupling, neither during ON- nor ON+; (B) This figure shows the contrast between ON- and ON+ for rest and movement, separately. Effective stimulation led to a decrease in interhemispheric CCC. This effect was more pronounced during movement, but still visible at rest. (C) This figure shows effects correlating with increasing stimulation intensity for rest & ON-, rest & ON+, movement & ON-, and movement & ON+, separately. Increasing stimulation intensity led to a decrease of bilateral sensorimotor CCC during ON-, regardless of rest or movement; this was not observed during ON+ anymore. (D) This figure shows effects correlating with increasing stimulation intensity for movement & ON- and movement & ON+. Increasing stimulation intensity led to a significant increase in ipsilateral CMC during ON-.This pattern was not observed during ON+. Black dots represent non-significant channels, white dots represent significant channels. Significant effects on bar plots are marked with a star. The seed region is markered with a diamond. Cortical regions were defined as follows: Prefrontal (Fp1, Fp2), left frontal (AF7, AF3, F7, F5, F3), frontal central (F1, Fz, F2), frontal right (AF4, AF8, F4, F6, F8), temporal left (FT9, FT7, T7, TP9, TP7), motor left (FC5, FC3, C5, C3, CP5, CP3), motor central (FC1, FC2, C1, Cz, C2, CP1, CPz, CP2), motor right (FC4, FC6, C4, C6, CP4, CP6), temporal right (FT8, FT10, T8, TP8, TP10), parietal left (P7, P5, P3, PO9, PO7, PO3), parietal central (P1, Pz, P2), parietal right (P4, P6, P8, PO4, PO8, PO10), and occipital (POz, O1, Oz, O2).

observation aligns with our observation of a (although substantially lower in amplitude) movement related modulation of beta band activity in the ipsilateral sensorimotor area, exclusively present during ON+. In line with the previously mentioned findings on CMC, we also observed a stronger (passive) movement-related effect on CMC during ON+ compared to ON-. This is reflective of the reduced modulation range of cortical activity in untreated patients with Parkinsons disease, most prominently observed in the beta band. Thus, in the presence of effective STN-DBS, movement-related beta power, cross-cortical coupling, and cortico-muscular coupling phenomena all seem to converge towards less pathological brain network dynamics (Stoffers, J. L. W. Bosboom, et al. 2008; Levin

et al. 2009; Heinrichs-Graham, Wilson, et al. 2014), while simultaneously contributing to symptomatic improvement.

Local STN-DBS changes in Parkinson's disease

In this study, we demonstrated progressive, intensity-dependent physiological changes leading to desynchronization of cortical beta activity, with an intensity-response function that is congruent with subcortical findings (Milosevic, Kalia, et al. 2018). This is in line with previous studies which reported an STN-DBS induced reduction of cortical activity (Abbasi et al. 2018; Luoma et al. 2018). The observed changes of cortical activity are likely the result of antidromic activation of cortico-subthalamic hyperdirect pathway fibers (Miocinovic et al. 2018). This would also explain the reported difference between the effect on cortical physiology from STN-DBS versus the effect observed after administering dopamine replacement drugs (increase in activity (Heinrichs-Graham, Kurz, et al. 2014)). The observed pharmacological effects may also be present in STN-DBS patients, but are likely camouflaged by random antidromic activation completely masking this change. We also observed DBS to reduce EMG activity in the upper limb during passive movement which has been described as pathologically increased in untreated Parkinsons disease (Meara and Cody 1992; Cantello et al. 1995; Levin et al. 2009; Powell, Muthumani, and Xia 2016; Ruonala et al. 2018).

Power and connectivity based electrophysiological markers for STN-DBS

Pathologically high levels of subcortical beta-activity are a common marker used during the DBS-lead implantation procedure (Kühn, Trottenberg, et al. 2005; Zaidel et al. 2010). This information can be acquired using either microelectrodes, macro-electrodes or DBS-leads (Milosevic, Scherer, et al. 2020). Yet, for DBS programming no comparable marker is available since the implantable pulse generator is commonly programmed weeks after the implantation procedure (in order to avoid micro-lesion effects affecting the programming procedure (Granziera et al. 2008)). After a recovery period, a subjective evaluation of, e.g, rigidity and tremor is performed by a trained specialist. In order to further optimize this programming process, it could be supplemented by information acquired from objective evaluation criteria. One candidate for such an objective marker has been subcortical beta band activity. This is also a primary marker under the investigation for use in adaptive DBS systems (Little and Peter Brown 2020). One possible limitation of power-based markers is that they may be confounded by movement (Johnson et al. 2016). In comparison, this study showed that bilateral motor cortical beta band CCC decreased while stimulation effectivity increased and did not decrease further after full clinical effectivity was achieved. Furthermore, beta band CCC was not confounded by movement, neither during ineffective nor during effective stimulation. Therefore, we propose to consider motor cortical beta band CCC as a potential marker for clinical programming and/or adaptive DBS systems, which could be used on its own or in conjunction with other markers.

Limitations

This study analyzed concatenated data acquired from multiple stimulation sites within the same patient in order to increase the amount of available data from each patient as well as increase data granularity for assessment of the differences between ON- and ON+ stimulation intensities. Therefore, appropriate measures were taken to compensate for any statistical error otherwise present in repeated measurement setups. From a statistical perspective, any potential bias from this approach would be accounted for by the fact that stimulation sites, nested within patients, were modeled as a random factor compensating for repeated measurements within the same patient across different stimulation sites. Furthermore, stimulation sites were modeled as nested within patients as identically named stimulation sites (i.e., contact #3 or frontal segment) were expected to differ between patients due to, i.e., rotational shifts or different final lead positions within the STN. Nevertheless, future studies may consider to investigate only one stimulation contact (e.g., the clinically applied one) with more trials.

Another limitation of this study is that although the patients were repeatedly instructed during examinations not to support the movement (i.e., remain relaxed and not to contribute to the passive movements), we cannot completely exclude

the possibility that active movements occasionally occurred. In such cases, the experimenters skipped 1-3 movement cycles while instructing the patient to relax. These cycles were automatically detected during data pre-processing and removed from further evaluation. Furthermore, additional studies are necessary that investigate the respective physiology also during active movements to determine the robustness of the identified markers.

Additionally, we did not assess patients in the presence of antiparkinsonian medications (i.e., compare ON versus OFF medication condition). These analyses were not done as the primary objective of this study was to isolate stimulation-related benefits on muscular rigidity in small stimulation intensity titration steps. Moreover, inclusion of such an analysis would have significantly extended the already long experimental protocol. Future studies may therefore investigate the impact of additional dopaminergic medication of the reported DBS effects to more closely resemble real live conditions.

Furthermore, we evaluated acute and non chronic DBS effects in this study. This was primarily due to the fact that STN-DBS effects on rigidity usually appear within 20 s and disappear (after DBS OFF) within 60 s (Levin et al. 2009). However, future studies may examine whether longer follow-up periods may lead to changes in the physiological response despite consistent clinical effects along the line of adaptation processes. Finally, the interpretation of the results has been focused on the implications of beta activity. The modulation of gamma activity, considered a prokinetic rhythm (Cassidy et al. 2002; Liu et al. 2008), in the sensorimotor cortices has been shown to be exclusive to active movements (Cheyne et al. 2008) and has not been observed during passive movements (Muthukumaraswamy 2010). Therefore, it has been theorized that motor cortical gamma activity may be linked to motor planning rather than motor execution (Nowak, Zich, and Stagg 2018), which would not apply to passive movements of the limb (as investigated here).

Conclusion

Interhemispheric synchronization provides an objective marker that may inform the titration of stimulation parameters in clinical practice. Furthermore, this approach may provide in the long run a physiological marker for adaptive DBS that could be applied during both rest and movement.

References

Lau, Lonneke ML de and Monique MB Breteler (June 1, 2006). “Epidemiology of Parkinson’s disease”. In: *The Lancet Neurology* 5.6. Publisher: Elsevier, pp. 525–535.

Riederer, P. and St. Wuketich (Sept. 1, 1976). “Time course of nigrostriatal degeneration in parkinson’s disease”. In: *J. Neural Transmission* 38.3, pp. 277–301.

Albin, Roger L., Anne B. Young, and John B. Penney (Jan. 1, 1989). “The functional anatomy of basal ganglia disorders”. In: *Trends in Neurosciences* 12.10, pp. 366–375.

Chaudhuri, K Ray and Anthony HV Schapira (May 1, 2009). “Non-motor symptoms of Parkinson’s disease: dopaminergic pathophysiology and treatment”. In: *The Lancet Neurology* 8.5, pp. 464–474.

Benabid, A. L. et al. (1994). “Acute and Long-Term Effects of Subthalamic Nucleus Stimulation in Parkinson’s Disease”. In: *SFN* 62.1. Publisher: Karger Publishers, pp. 76–84.

Limousin, P. et al. (Jan. 14, 1995). “Effect on parkinsonian signs and symptoms of bilateral subthalamic nucleus stimulation”. In: *The Lancet* 345.8942. Publisher: Elsevier, pp. 91–95.

Fahn, Stanley (Jan. 1, 2007). “Chapter 16 - Hypokinesia and Hyperkinesia”. In: *Textbook of Clinical Neurology (Third Edition)*. Ed. by Christopher G. Goetz. Philadelphia: W.B. Saunders, pp. 289–306.

Meara, R. J. and F. W. J. Cody (Aug. 1, 1992). “RELATIONSHIP BETWEEN ELECTROMYOGRAPHIC ACTIVITY AND CLINICALLY ASSESSED RIGIDITY STUDIED AT THE WRIST JOINT IN PARKINSON’S DISEASE”. In: *Brain* 115.4. Publisher: Oxford Academic, pp. 1167–1180.

Levin, Johannes et al. (2009). “Objective measurement of muscle rigidity in parkinsonian patients treated with subthalamic stimulation”. In: *Movement Disorders* 24.1, pp. 57–63.

Cassim, F. et al. (Dec. 4, 2001). “Does post-movement beta synchronization reflect an idling motor cortex?” In: *Neuroreport* 12.17, pp. 3859–3863.

Formaggio, Emanuela et al. (2013). "Modulation of event-related desynchronization in robot-assisted hand performance: brain oscillatory changes in active, passive and imagined movements". In: *J NeuroEngineering Rehabil* 10.1, p. 24.

Lim, Vanessa K. et al. (Dec. 11, 2006). "Decreased desychronisation during self-paced movements in frequency bands involving sensorimotor integration and motor functioning in Parkinson's disease". In: *Brain Research Bulletin* 71.1, pp. 245–251.

Degardin, A. et al. (Mar. 1, 2009). "Deficient sensory beta synchronization in Parkinsons disease". In: *Clinical Neurophysiology* 120.3, pp. 636–642.

Heinrichs-Graham, Elizabeth, Tony W. Wilson, et al. (Oct. 1, 2014). "Neuromagnetic Evidence of Abnormal Movement-Related Beta Desynchronization in Parkinson's Disease". In: *Cereb Cortex* 24.10. Publisher: Oxford Academic, pp. 2669–2678.

Brown, P. (2006). "Bad oscillations in Parkinsons disease". In: *Parkinsons Disease and Related Disorders*. Ed. by P. Riederer et al. Journal of Neural Transmission. Supplementa. Vienna: Springer, pp. 27–30.

Heinrichs-Graham, Elizabeth, Max J. Kurz, et al. (July 9, 2014). "Hypersynchrony despite pathologically reduced beta oscillations in patients with Parkinson's disease: a pharmacomagnetoencephalography study". In: *Journal of Neurophysiology* 112.7. Publisher: American Physiological Society, pp. 1739–1747.

Stoffers, Diederick, Johannes L. W. Bosboom, et al. (Sept. 1, 2008). "Dopaminergic modulation of cortico-cortical functional connectivity in Parkinson's disease: An MEG study". In: *Experimental Neurology* 213.1, pp. 191–195.

Salenius, Stephan et al. (Mar. 1, 2002). "Defective cortical drive to muscle in Parkinsons disease and its improvement with levodopa". In: *Brain* 125.3. Publisher: Oxford Academic, pp. 491–500.

Jenkinson, Ned and Peter Brown (Dec. 1, 2011). "New insights into the relationship between dopamine, beta oscillations and motor function". In: *Trends in Neurosciences* 34.12. Publisher: Elsevier, pp. 611–618.

Brown, Peter (Apr. 2003). "Oscillatory nature of human basal ganglia activity: relationship to the pathophysiology of Parkinson's disease". In: *Mov. Disord.* 18.4, pp. 357–363.

Kühn, Andrea A., Alexander Tsui, et al. (Feb. 2009). "Pathological synchronisation in the subthalamic nucleus of patients with Parkinson's disease relates to both bradykinesia and rigidity". In: *Exp. Neurol.* 215.2, pp. 380–387.

Tinkhauser, Gerd et al. (Apr. 1, 2017). "The modulatory effect of adaptive deep brain stimulation on beta bursts in Parkinsons disease". In: *Brain* 140.4, pp. 1053–1067.

Uhlhaas, Peter J. and Wolf Singer (Oct. 5, 2006). "Neural Synchrony in Brain Disorders: Relevance for Cognitive Dysfunctions and Pathophysiology". In: *Neuron* 52.1. Publisher: Elsevier, pp. 155–168.

Hammond, Constance, Hagai Bergman, and Peter Brown (July 1, 2007). "Pathological synchronization in Parkinson's disease: networks, models and treatments". In: *Trends in Neurosciences* 30.7. Publisher: Elsevier, pp. 357–364.

Silberstein, Paul et al. (June 1, 2005). "Cortico-cortical coupling in Parkinson's disease and its modulation by therapy". In: *Brain* 128.6. Publisher: Oxford Academic, pp. 1277–1291.

Devos, D. and L. Defebvre (Jan. 1, 2006). "Effect of deep brain stimulation and l-Dopa on electrocortical rhythms related to movement in Parkinson's disease". In: *Progress in Brain Research*. Ed. by Christa Neuper and Wolfgang Klimesch. Vol. 159. Event-Related Dynamics of Brain Oscillations. Elsevier, pp. 331–349.

Kühn, Andrea A., Andreas Kupsch, et al. (2006). "Reduction in subthalamic 835 Hz oscillatory activity correlates with clinical improvement in Parkinson's disease". In: *European Journal of Neuroscience* 23.7. _eprint: https://onlinelibrary.wiley.com/doi/pdf/10.1111/j.1460-9568.2006.04717.x, pp. 1956–1960.

Grill, Warren M., Andrea N. Snyder, and Svjetlana Miocinovic (May 19, 2004). "Deep brain stimulation creates an informational lesion of the stimulated nucleus". In: *NeuroReport* 15.7, pp. 1137–1140.

Oswal, Ashwini et al. (May 1, 2016). "Deep brain stimulation modulates synchrony within spatially and spectrally distinct resting state networks in Parkinsons disease". In: *Brain* 139.5, pp. 1482–1496.

Horn, Andreas et al. (Oct. 1, 2019). "Deep brain stimulation induced normalization of the human

functional connectome in Parkinsons disease". In: *Brain* 142.10, pp. 3129–3143.

Kahan, Joshua, Maren Urner, et al. (2014). "Resting state functional MRI in Parkinsons disease: the impact of deep brain stimulation on effective connectivity". In: *Brain* 137.4, p. 1130.

Kahan, Joshua, Laura Mancini, et al. (Aug. 1, 2019). "Deep brain stimulation has state-dependent effects on motor connectivity in Parkinsons disease". In: *Brain* 142.8, pp. 2417–2431.

Chen, Hui-Min et al. (2018). "Effective network of deep brain stimulation of subthalamic nucleus with bimodal positron emission tomography/functional magnetic resonance imaging in Parkinson's disease". In: *CNS Neuroscience & Therapeutics* 24.2. _eprint: https://onlinelibrary.wiley.com/doi/pdf/10.1111/cns.12783, pp. 135–143.

Weiss, Daniel et al. (Mar. 1, 2015). "Subthalamic stimulation modulates cortical motor network activity and synchronization in Parkinsons disease". In: *Brain* 138.3. Publisher: Oxford Academic, pp. 679–693.

Abbasi, Omid et al. (July 1, 2018). "Unilateral deep brain stimulation suppresses alpha and beta oscillations in sensorimotor cortices". In: *NeuroImage* 174, pp. 201–207.

Luoma, Jarkko et al. (Sept. 14, 2018). "Spontaneous sensorimotor cortical activity is suppressed by deep brain stimulation in patients with advanced Parkinsons disease". In: *Neuroscience Letters* 683, pp. 48–53.

Meissner, Sarah Nadine et al. (Jan. 1, 2018). "The significance of brain oscillations in motor sequence learning: Insights from Parkinson's disease". In: *NeuroImage: Clinical* 20, pp. 448–457.

Boon, Lennard I., Arjan Hillebrand, et al. (Jan. 1, 2020). "Motor effects of deep brain stimulation correlate with increased functional connectivity in Parkinson's disease: An MEG study". In: *NeuroImage: Clinical* 26, p. 102225.

Hirschmann, J. et al. (Mar. 1, 2013). "Differential modulation of STN-cortical and cortico-muscular coherence by movement and levodopa in Parkinson's disease". In: *NeuroImage* 68, pp. 203–213.

Airaksinen, Katja et al. (Apr. 1, 2015). "Cortico-muscular coherence in advanced Parkinsons disease with deep brain stimulation". In: *Clinical Neurophysiology* 126.4, pp. 748–755.

Kühn, Andrea A., Florian Kempf, et al. (June 11, 2008). "High-Frequency Stimulation of the Subthalamic Nucleus Suppresses Oscillatory Activity in Patients with Parkinson's Disease in Parallel with Improvement in Motor Performance". In: *J Neurosci* 28.24, pp. 6165–6173.

Giannicola, Gaia et al. (Nov. 1, 2010). "The effects of levodopa and ongoing deep brain stimulation on subthalamic beta oscillations in Parkinson's disease". In: *Experimental Neurology* 226.1, pp. 120–127.

Eusebio, A et al. (May 2011). "Deep brain stimulation can suppress pathological synchronisation in parkinsonian patients". In: *J Neurol Neurosurg Psychiatry* 82.5, pp. 569–573.

Chung, Jae Woo et al. (Jan. 1, 2018). "Beta-band oscillations in the supplementary motor cortex are modulated by levodopa and associated with functional activity in the basal ganglia". In: *NeuroImage: Clinical* 19, pp. 559–571.

Boon, Lennard I., Victor J. Geraedts, et al. (2019). "A systematic review of MEG-based studies in Parkinson's disease: The motor system and beyond". In: *Human Brain Mapping* 40.9. _eprint: https://onlinelibrary.wiley.com/doi/pdf/10.1002/hbm.24562, pp. 2827–2848.

Hess, Christopher W. and Mark Hallett (Apr. 2017). "The Phenomenology of Parkinson's Disease". In: *Semin Neurol* 37.2. Publisher: Thieme Medical Publishers, pp. 109–117.

Subthalamic Steering for Therapy Optimization in Parkinson's Disease (2020). URL: https://clinicaltrials.gov/ct2/show/NCT03548506 (visited on 09/18/2020).

Scherer, Maximilian, Luka Milosevic, Patrick Bookjans, et al. (n.d.). "Comparing the therapeutic window of omnidirectional and directional subthalamic deep brain stimulation in Parkinsons disease". In: ().

Hutchison, W. D. et al. (1998). "Neurophysiological identification of the subthalamic nucleus in surgery for Parkinson's disease". In: *Annals of Neurology* 44.4, pp. 622–628.

Milosevic, Luka, Maximilian Scherer, et al. (2020). "Online Mapping With the Deep Brain Stimulation Lead: A Novel Targeting Tool in Parkinson's Disease". In: *Movement Disorders* 35.9. _eprint: https://movementdisorders.onlineli-

brary.wiley.com/doi/pdf/10.1002/mds.28093, pp. 1574–1586.

Granziera, C. et al. (Mar. 1, 2008). "Sub-acute delayed failure of subthalamic DBS in Parkinson's disease: The role of micro-lesion effect". In: *Parkinsonism & Related Disorders* 14.2, pp. 109–113.

Welch, P. (June 1967). "The use of fast Fourier transform for the estimation of power spectra: A method based on time averaging over short, modified periodograms". In: *IEEE Transactions on Audio and Electroacoustics* 15.2. Conference Name: IEEE Transactions on Audio and Electroacoustics, pp. 70–73.

Scherer, Maximilian, Luka Milosevic, Robert Guggenberger, et al. (n.d.[a]). "Directionalized Absolute Coherence (DAC)". In: ().

Gaetz, W. et al. (June 1, 2010). "Neuromagnetic imaging of movement-related cortical oscillations in children and adults: Age predicts post-movement beta rebound". In: *NeuroImage* 51.2, pp. 792–807.

Scherer, Maximilian, Luka Milosevic, Robert Guggenberger, et al. (n.d.[b]). "FiNN - A framework for the analysis for neurophysiological networks". In: ().

Swann, Nicole C. et al. (Aug. 2018). "Adaptive deep brain stimulation for Parkinsons disease using motor cortex sensing". In: *J Neural Eng* 15.4, p. 046006.

Neumann, Wolf-Julian et al. (2019). "Toward electrophysiology-based intelligent adaptive deep brain stimulation for movement disorders". In: *Neurotherapeutics* 16.1. Publisher: Springer, pp. 105–118.

Stoffers, Diederick, J. L. W. Bosboom, et al. (June 1, 2008). "Increased cortico-cortical functional connectivity in early-stage Parkinson's disease: An MEG study". In: *NeuroImage* 41.2, pp. 212–222.

Powell, Douglas, Nicholas Hanson, et al. (Aug. 2011). "Enhancement of parkinsonian rigidity with contralateral hand activation". In: *Clin Neurophysiol* 122.8, pp. 1595–1601.

Sridharan, Kousik Sarathy et al. (June 3, 2019). "Electromagnetic mapping of the effects of deep brain stimulation and dopaminergic medication on movement-related cortical activity and corticomuscular coherence in Parkinsons disease". In: *bioRxiv*. Publisher: Cold Spring Harbor Laboratory Section: New Results, p. 657882.

Mazzoni, Pietro, Britne Shabbott, and Juan Camilo Cortés (June 2012). "Motor Control Abnormalities in Parkinsons Disease". In: *Cold Spring Harb Perspect Med* 2.6.

Lattari, E et al. (Nov. 16, 2010). "Corticomuscular coherence behavior in fine motor control of force: a critical review". In: *RevNeurol* 10, pp. 610–623.

BRINKMAN, J. and H. G. J. M. KUYPERS (Dec. 1, 1973). "CEREBRAL CONTROL OF CONTRALATERAL AND IPSILATERAL ARM, HAND AND FINGER MOVEMENTS IN THE SPLIT-BRAIN RHESUS MONKEY1". In: *Brain* 96.4, pp. 653–674.

Tanji, J., K. Okano, and K. C. Sato (July 1, 1988). "Neuronal activity in cortical motor areas related to ipsilateral, contralateral, and bilateral digit movements of the monkey". In: *Journal of Neurophysiology* 60.1. Publisher: American Physiological Society, pp. 325–343.

Donchin, O. et al. (Dec. 1, 2002). "Single-Unit Activity Related to Bimanual Arm Movements in the Primary and Supplementary Motor Cortices". In: *Journal of Neurophysiology* 88.6. Publisher: American Physiological Society, pp. 3498–3517.

Chen, Robert, Leonardo G. Cohen, and Mark Hallett (Nov. 1997). "Role of the Ipsilateral Motor Cortex in Voluntary Movement". In: *Canadian Journal of Neurological Sciences* 24.4. Publisher: Cambridge University Press, pp. 284–291.

Verstynen, Timothy et al. (Mar. 1, 2005). "Ipsilateral Motor Cortex Activity During Unimanual Hand Movements Relates to Task Complexity". In: *Journal of Neurophysiology* 93.3. Publisher: American Physiological Society, pp. 1209–1222.

Milosevic, Luka, Suneil K. Kalia, et al. (Jan. 1, 2018). "Neuronal inhibition and synaptic plasticity of basal ganglia neurons in Parkinson's disease". In: *Brain* 141.1. Publisher: Oxford Academic, pp. 177–190.

Miocinovic, Svjetlana et al. (Oct. 24, 2018). "Cortical Potentials Evoked by Subthalamic Stimulation Demonstrate a Short Latency Hyperdirect Pathway in Humans". In: *J Neurosci* 38.43, pp. 9129–9141.

Cantello, Roberto et al. (Oct. 1, 1995). "Parkinson's disease rigidity: EMG in a small hand muscle at rest". In: *Electroencephalography and Clinical Neurophysiology/Electromyography and Motor Control* 97.5, pp. 215–222.

Powell, Douglas, Anburaj Muthumani, and RuiPing Xia (Aug. 28, 2016). "A comparison of the effects of continuous versus discontinuous movement patterns on parkinsonian rigidity and reflex responses to passive stretch and shortening". In: *Journal of Nature and Science (JNSCI)* 2.8. Number: 8, p. 201.

Ruonala, Verneri et al. (2018). "Levodopa-Induced Changes in Electromyographic Patterns in Patients with Advanced Parkinsons Disease". In: *Front. Neurol.* 9. Publisher: Frontiers.

Kühn, Andrea A., Thomas Trottenberg, et al. (July 2005). "The relationship between local field potential and neuronal discharge in the subthalamic nucleus of patients with Parkinson's disease". In: *Exp Neurol* 194.1, pp. 212–220.

Zaidel, Adam et al. (July 1, 2010). "Subthalamic span of oscillations predicts deep brain stimulation efficacy for patients with Parkinsons disease". In: *Brain* 133.7. Publisher: Oxford Academic, pp. 2007–2021.

Little, Simon and Peter Brown (2020). "Debugging Adaptive Deep Brain Stimulation for Parkinson's Disease". In: *Movement Disorders* 35.4. _eprint: https://movementdisorders.onlinelibrary.wiley.com/doi/pdf/10.1002/mds.27996, pp. 555–561.

Johnson, Luke A. et al. (Dec. 2016). "Closed-Loop Deep Brain Stimulation Effects on Parkinsonian Motor Symptoms in a Non-Human Primate - Is Beta Enough?" In: *Brain Stimul* 9.6, pp. 892–896.

Cassidy, Michael et al. (June 1, 2002). "Movementrelated changes in synchronization in the human basal ganglia". In: *Brain* 125.6. Publisher: Oxford Academic, pp. 1235–1246.

Liu, Xuguang et al. (June 1, 2008). "The sensory and motor representation of synchronized oscillations in the globus pallidus in patients with primary dystonia". In: *Brain* 131.6. Publisher: Oxford Academic, pp. 1562–1573.

Cheyne, Douglas et al. (Aug. 1, 2008). "Self-paced movements induce high-frequency gamma oscillations in primary motor cortex". In: *NeuroImage* 42.1, pp. 332–342.

Muthukumaraswamy, Suresh D. (Sept. 8, 2010). "Functional Properties of Human Primary Motor Cortex Gamma Oscillations". In: *Journal of Neurophysiology* 104.5. Publisher: American Physiological Society, pp. 2873–2885.

Nowak, Magdalena, Catharina Zich, and Charlotte J. Stagg (June 1, 2018). "Motor Cortical Gamma Oscillations: What Have We Learnt and Where Are We Headed?" In: *Curr Behav Neurosci Rep* 5.2, pp. 136–142.

Additional information

Study funding

This was an investigator initiated study that was sponsored by the University Hospital Tuebingen and supported by Abbott within the SANTOP clinical trial (NCT03548506).

Competing interests

The authors declare no competing financial interests.

6 Acknowledgment

I would like to thank my supervisor, Prof. Gharabaghi, for his guidance and support throughout the years, especially in regards to the academic freedom I was given to pursue personal research interests. Furthermore, I am grateful for the advice and education I have received from Dr. Guggenberger and Dr. Milosevic, greatly expanding my knowledge in both neuroscientific theory and methodology. Furthermore, I want to thank the members of the advisory board Prof. Braun and Prof. Hertrich for their valuable feedback. Finally, I want to thank any lab member I have collaborated with over the years. It has been a pleasure to work with each and everyone of you.